Sediment transport in pipes and sewers with deposited beds

R W P May

Report SR 320
January 1993

HR Wallingford

Registered Office: **HR Wallingford Ltd.** Howbery Park, Wallingford, Oxfordshire, OX10 8BA, UK
Telephone: 0491 35381 International + 44 491 35381 Telex: 848552 HRSWAL G.
Facsimile: 0491 32233 International + 44 491 32233 Registered in England No. 1622174

Contract

This report describes work funded by the Department of the Environment under Research Contract PECD 7/6/167 for which the DOE nominated officers were Dr R Thorogood and Mr P D Woodhead and the HR nominated officer was Dr W R White. The HR job number was RQS 0070. It is published on behalf of the Department of the Environment, but any opinions expressed in this report are not necessarily those of the funding Department. The project was managed by Mr R W P May.

Prepared by RWP. May (name) Research Manager (job title)

Approved by E.C. Bowers Hydrodynamics Group Manager.

Date 9-2-1993

Summary

Sediment transport in pipes and sewers with deposited beds

R W P May

Report SR 320
January 1993

This report describes the results of laboratory studies carried out at HR on the movement of non-cohesive sediments in sewer pipes. Equations are presented for predicting the flow resistance and the rate of sediment transport with deposited beds and also the flow conditions needed to prevent deposition occurring.

Tests were made using a 21m length of 450mm diameter concrete pipe mounted in a tilting flume with separate recirculation systems for the water and sediment. Four different gradings of sand were used with d_{50} sizes of 0.47mm, 0.58mm, 0.61mm and 0.73mm ; the two intermediate gradings were obtained by mixing the 0.47mm and 0.73mm sands in different proportions.

The main purpose of the experiments was to investigate flow conditions with significant amounts of deposited sediment ; the average depth of deposit was varied between 13% and 27% of the pipe diameter. Tests were made with flow velocities between 0.4m/s and 1.3m/s and with proportional depths (relative to the pipe invert) of y/D = 0.5, 0.75 and 1.0. The scope of the study was also extended to include tests at the limit of deposition and with separated dunes (corresponding to average sediment depths between 0.3% and 1% of the pipe diameter).

A theoretical model of bed-load movement in pipes was developed which applies both to conditions at the limit of deposition and to transport with deposited beds. The model identified certain non-dimensional transport and mobility parameters which proved useful in the analysis of the experimental data.

The results for the limit of deposition in the 450mm diameter concrete pipe were analysed in combination with equivalent data from previous HR studies with 77mm and 158mm diameter smooth pipes and a 299mm diameter concrete pipe. The method used to correlate all the data indicated that limiting transport rates in rough pipes are less than would occur in smooth pipes of the same diameter.

The tests with continuous deposits showed that the flow resistance of the bed varied both with the mobility of the particles and with the Froude number of the flow. Equations were developed for estimating the composite roughness of pipes with deposited beds.

The sediment transport rates with continuous deposits were compared with values predicted by several existing equations. Overall, the Ackers method gave reasonable results but it did consistently over-estimate transport rates for the finer sands. The theoretical model of bed-load movement was used to

develop a new transport equation for pipes that fitted the experimental data more closely.

The resistance and transport equations for continuous deposits can be applied to the case of separated dunes provided proper allowance is made for the dimensions and spacing of the dunes.

Notation

A	Cross-sectional area of flow
A_a	Cross-sectional area of sediment corresponding to active depth
A_s	Cross-sectional area of sediment bed
A_t	Total cross-sectional area of sediment and flow
B	Surface width of flow
b	Coefficient in Laursen's Equation (10)
C_v	Volumetric sediment concentration (= Q_s/Q)
C_{vd}	Value of C_v for separated dunes
D	Internal diameter of pipe
D_{gr}	Non-dimensional grain size, Equation (7)
d	Sediment size
d_{50}	Mean sediment size (50% finer by weight)
E	Specific energy of flow
e	Voids ratio of sediment bed (volume of voids/volume of particles)
F_b	Mobility parameter based on total bed shear stress, Equation (41)
$F_{b,o}$	Value of F_b for zero Froude number
F_g	Mobility parameter based on grain shear stress, Equation (40)
F_r	Froude number of flow
F_s	Mobility parameter based on effective shear stress, Equation (51)
f	Coefficient of friction between sediment and pipe
G_s	Mobility parameter based on effective shear stress and particle/pipe friction, Equation (28)
g	Acceleration due to gravity
h	Depth of flow above sediment bed
i	Hydraulic gradient of flow
J	Parameter in Ackers' Equations (17) and (A.11)
K	Parameter in Ackers' Equations (17) and (A.15)
k	Roughness coefficient in Colebrook-White equation
k_b	Value of k for total bed resistance
k_c	Composite value of k for pipe and sediment bed
k_g	Value of k for grain resistance
k_o	Value of k for clean pipe or pipe walls
L	Length of pipe
m	Coefficient in Ackers-White Equations (A.4) and (A.8)
N	Coefficient in Equation (12)
n	Coefficient in Ackers-White Equations (A.3) and (A.7)
P	Wetted perimeter of flow
P_o	Wetted perimeter of pipe walls
Q	Volumetric discharge of fluid
Q_s	Volumetric discharge of sediment
R	Hydraulic radius of flow (= A/P)
R_b	Value of R assigned to sediment bed
R_o	Value of R for clear-water flow
R_1	Value of R for sediment depth t_1
R_2	Value of R for sediment depth t_2
R_*	Particle Reynolds number, Equation (54)
R_{*c}	Value of R_* based on composite friction factor λ_c
r	Proportion of pipe length occupied by separated dunes
S_o	Gradient of pipe
s	Specific gravity of sediment particles
t	Thickness of sediment bed (relative to pipe invert)

t_1	Value of t obtained assuming volume of separated dunes distributed uniformly along pipe
t_2	Average value for separated dunes
u_s	Velocity of particles at surface of sediment bed
u_*	Shear velocity, Equation (55)
V	Mean flow velocity
V_L	Limiting flow velocity without deposition
V_o	Value of V for clean pipe
V_s	Self-cleansing velocity
V_t	Value of V at threshold of sediment movement
V_{ts}	Value of V_t for smooth pipe
V_2	Value of V for sediment depth t_2
W_b	Width of sediment bed
W_e	Effective width of sediment bed
W_1	Value of W_b corresponding to sediment depth t_1
W_2	Value of W_b corresponding to sediment depth t_2
w	Fall velocity of sediment
x	Distance along pipe in direction of flow
Y_s	Volume of separated dunes in length L
y	Depth of flow relative to pipe invert
y_a	Active depth of sediment bed
α	Coefficient in Ackers' Equations (17) and (A.12)
α_1	Coefficient
α_2	Coefficient
β	Coefficient in Ackers' Equations (17) and (A.13)
γ	Coefficient in Ackers' Equations (17) and (A.14)
Δ	Root-mean-square variation in bed level
δ	Coefficient in Ackers' Equations (17) and (A.16)
δ_*	Length scale for laminar sub-layer
ε	Coefficient in Ackers' Equations (17) and (A.17)
η	Transport parameter for continuous bed, Equation (50)
η_g	Value of η based on grain shear stress, Equation (52)
θ	Transition coefficient for particle Reynolds number, Equation (74)
λ	Darcy-Weisbach friction factor of flow, Equation (21)
λ_b	Value of λ for total bed shear stress
λ_c	Composite value of λ for pipe and sediment bed
λ_{cd}	Value of λ_c for separated dunes
λ_g	Value of λ for grain shear stress
λ_o	Value of λ for clean pipe
λ_s	Value of λ for effective shear stress
ν	Kinematic viscosity of fluid
ρ	Density of fluid
σ_g	Geometric standard deviation of sediment (= $\sqrt{(d_{84}/d_{16})}$)
τ	Average shear stress exerted by fluid on boundary
τ_b	Total bed shear stress
τ_c	Composite value of τ for pipe and sediment bed
τ_g	Grain shear stress
τ_o	Value of τ for clean pipe or pipe walls
τ_s	Effective shear stress causing sediment transport
τ_t	Shear stress on sediment bed at threshold of movement
Φ	Resistance parameter, Equation (46)
ϕ	Effective angle of friction for sediment
Ω	Transport parameter for limit of deposition, Equation (27)

Contents

Contents continued

1 Introduction

The term "sewer sediment" is used generally to describe the range of settleable solids that can be found deposited in sewerage systems (CIRIA, 1986). The foul water component of sewage contributes mainly organic sludges and low density gross solids, while the storm water component is responsible for most of the higher-density inorganic particles of sand and grit. The majority of deposits in storm water and combined systems are formed by these heavier particles, but in combined sewers they can be covered by a more mobile layer of organic sludge (Crabtree, 1988).

The sediment has two important effects on the performance of sewerage systems. Firstly, deposits can significantly reduce the flow capacity of sewer pipes by decreasing their cross-sectional area and increasing the overall hydraulic resistance. Secondly, pollutants from foul sewage and industrial effluents tend to become attached to the inorganic particles so that the transport of pollutants through a system is linked to the movement of the sediment.

In the UK and many other countries, new sewers and rising mains are normally designed to be "self-cleansing". Minimum gradients and flow velocities are specified which are intended to prevent the build-up of significant amounts of deposition. In many situations it is inevitable that some sediment will deposit during periods of low flow, so it is necessary to ensure that "self-cleansing" conditions occur frequently enough to re-erode the material and prevent it from solidifying. In the case of many existing systems (particularly older combined sewers in city centres), major changes in pipe sizes and gradients cannot be made to reduce amounts of sediment deposition. However, improvements in flow capacity and water quality can be achieved by altering the operation of control structures and overflow weirs, and by installing devices such as storm tanks. In order to design these modifications, it is necessary to be able to simulate the overall performance of the sewer network using a computer model that takes proper account of the effects of sediment movement and deposition.

Therefore, from the research point of view, information on the sediment transporting capacity of pipe flows is required for two different purposes. Firstly, better guidelines are needed for the design of new "self-cleansing" sewers. Existing criteria based on a minimum value of velocity or shear stress do not take account of the pipe size or the amount and type of sediment to be transported. The aim of the new guidelines should be to restrict the amount of sediment deposition to a level at which the hydraulic performance of the sewer system is not significantly reduced. Economic factors also need to be considered, but this is a separate issue from the definition of the limiting hydraulic conditions. The second research objective is to enable the sediment-transporting capacity to be predicted for existing sewers containing significant depths of deposited sediment. The "self-cleansing" condition for new sewers is in fact a special case of this more general requirement.

Most laboratory research on sediment transport in pipes has been carried out with non-cohesive sands and gravels. However, inorganic sediments in combined sewers tend to be partly cohesive due to the effects of biological slimes and grease. The non-cohesive research is nevertheless important and relevant for two reasons. Firstly, the transport of sediment in pipes has been found to be a complex subject, and it is necessary to understand the non-cohesive behaviour before trying to take account of additional effects due to cohesion. Secondly, research described by Alvarez (1990) and Nalluri & Alvarez (1990) indicates that cohesive sediments tend to behave non-cohesively once their threshold of movement is exceeded. The tests were carried out with sands to which synthetic Laponite RD clay was added to produce different degrees of cohesion. The clay significantly increased the shear stress required to move the particles, but once the structure of the deposited bed was disrupted the cohesive effects appeared to be lost.

The present report describes the latest stage of experimental work on non-cohesive sediment transport in pipes carried out by HR Wallingford and funded by the Construction Directorate of the Department of the Environment. Earlier stages have covered:

- Initial literature review (HR Report INT 139)
- Limit of deposition tests in 77mm and 158mm diameter perspex and plastic pipes (HR Report IT 222)
- Limit of deposition tests in 299mm diameter spun concrete pipe (HR Report SR 179)
- Tests with small depths of sediment deposition in 299mm diameter spun concrete pipe (HR Report SR 211)

These studies were mainly concerned with defining the "self-cleansing" conditions appropriate to the design of new sewers. The present work concentrates on the second design problem, that of predicting sediment transport rates and frictional resistance in existing sewers with significant bed deposits. The tests were carried out in a newly-installed 450mm diameter spun concrete pipe. Additional information was also collected on conditions at the limit of deposition for comparison with the earlier work on smaller pipes. Valuable contributions to the results were made by two visiting researchers using the HR test rig: Dr G S Perrusquía of Chalmers University of Technology, Sweden and Mr A Ab Ghani of the University of Newcastle upon Tyne.

2 Previous research

2.1 Self-cleansing conditions

Alternative equations for predicting the limit of sediment deposition in pipes have been reviewed and evaluated in the HR reports listed in Section 1, and only those considered in the present study will now be detailed.

Macke (1982) measured the limit of deposition in smooth pipes with diameters of 192mm, 290mm and 445mm, and used sands with sizes of 0.16mm and 0.37mm. Analysis of the results, together with data from other sources, led to the following equation:

$$Q_s \, \rho g(s-1) \, w^{1.5} = 1.64 \times 10^{-4} \, \tau_c^3 \quad , \text{ for } \tau_c \geq 1.07 \text{ N/m}^2 \qquad (1)$$

where Q_s is the volumetric sediment discharge, s is the specific gravity of the sediment, w is its fall velocity and τ_c is the average shear stress around the pipe; a full list of symbols is given at the start of this report. For comparison purposes in this report, alternative equations will be re-arranged so that the volumetric sediment concentration C_v is a function of the other variables. In this form Macke's equation becomes:

$$C_v = \frac{\lambda_c^3 V_L^5}{30.4\ (s-1) w^{1.5} A} \tag{2}$$

where V_L is the limiting flow velocity without deposition, A is the cross-sectional area of flow and λ_c is the Darcy-Weisbach friction factor for the flow. Both Equations (1) and (2) are dimensional and SI units must be used. The limit of deposition was identified by an instrument which sensed the presence of stationary sediment particles adjacent to the pipe invert.

The results of the previous HR studies with 77mm, 158mm and 299mm diameter pipes were fitted by May (1982, 1989) to a semi-empirical theory of bed load transport; sediment sizes used in the tests were 0.57mm, 0.64mm 0.72mm, 5.8mm and 7.9mm with specific gravities in the range 2.62 to 2.65. The best-fit equation to the data was found to be:

$$C_V = 2.11 \times 10^{-2} (y/D)^{0.36} (D^2/A) (d/R)^{0.6}. \\ [1 - (V_t/V_s)]^4 [\frac{V_s^2}{g(s-1)D}]^{3/2} \tag{3}$$

where d is the sediment size, D the diameter of the pipe, y the depth of flow and R the hydraulic radius. The self-cleansing velocity V_s was defined as the velocity at which all the sediment was observed to be transported by fluid forces. Thus deposition was considered to have occurred if slow-moving separated dunes formed or if particles adjacent to the pipe invert were sliding forwards only as a result of solid-to-solid contacts with faster moving particles above them. The threshold velocity V_t at the start of sediment transport was estimated in the case of smooth pipes from Novak & Nalluri's (1975) equation:

$$V_{ts} = 0.61\ [g(s-1)R]^{½} (d/R)^{0.23} \tag{4}$$

The HR data for the 299mm diameter concrete indicated that the threshold velocity was 1.33 times the smooth-pipe value given by Equation (4).

Ackers (1984) developed a numerical model for sediment transport in pipes using a modified version of the Ackers-White sediment transport equation and the Colebrook-White resistance formula (see Appendix A). The Ackers-White equation was developed from data for rivers and rectangular alluvial channels, and predicts the transport rate per unit width of sediment bed. In order to use it to predict the limit of deposition in pipes, it was necessary to determine values for the effective width of sediment bed that would result in correct rates of transport. Ackers analysed the HR data for the 77mm and 158mm diameter pipes, and found that the effective width at the limit of deposition was equal to approximately 10 times the mean sediment size (ie $W_e = 10\ d_{50}$).

Mayerle, Nalluri & Novak (1991) described the results of experiments to measure the limit of deposition in smooth and rough rectangular channels and in a smooth 152mm diameter pipe. The sediment sizes were varied between 0.50mm and 8.74mm. Two alternative formulae were obtained for the circular pipe. The first did not include the friction factor of the pipe and can be expressed in the form:

$$C_V = 1.73 \times 10^{-3}\ (d/R)^{0.783} \left[\frac{V_s^2}{g(s-1)R}\right]^{2.174} \tag{5}$$

The second formula took account of the increase in friction factor caused by the sediment and can be written as:

$$C_V = 3.63 \times 10^{-7}\ \frac{(d/R)^{0.333}}{\lambda_c}\ D_{gr}^{0.778} \left[\frac{V_s^2}{g(s-1)R}\right]^{2.778} \tag{6}$$

D_{gr} is the dimensionless grain size defined as:

$$D_{gr} = \left(\frac{g(s-1)}{\nu^2}\right)^{1/3} d \tag{7}$$

and the friction factor λ_c is determined from the Colebrook-White formula using a composite roughness k_c given by:

$$\frac{k_c - k_o}{R} = 0.0130\ D_{gr}^{0.24}\ C_v^{0.40} \tag{8}$$

where k_o is the roughness of the pipe without sediment. Overall, the data and equations obtained from these experiments were in reasonable agreement with the corresponding HR results obtained with smooth pipes and also with the 299mm diameter concrete pipe.

Comparison of Equations (2), (3), (5) and (6) illustrates some of the uncertainties that remain about the relative importance of the different parameters. Assuming that each factor is varied separately, the effects of these factors on the sediment concentration can be summarised as follows:

Factor	Relationship to C_V			
	Macke, Eqn (2)	May, Eqn (3)	Mayerle, Eqn (5)	Mayerle, Eqn (6)
V^m	m=5	minimum m=3	m=4.35	m=5.56
D^n	n=-2	maximum n=-2.1	n=-2.96	n=-3.11
d^p	p=-0.75 to -3 (for large to small particles)	variable, small and positive	p=0.783	p=1.11
λ^q	q=3	-	-	q=-1
$\frac{\text{½-full } C_V}{\text{pipe-full } C_V}$	2.0	1.56	1.0	1.0

The behaviour of Equation (3) is more complex because it varies according to the relative magnitude of the ratio V_t/V_s; the values given above are limiting values at high velocities. The equations are in reasonable agreement about the effects of flow velocity and pipe size, but there is conflicting evidence about the influences of sediment size, friction factor and proportional flow depth.

2.2 Transport with deposition

Experimental studies described by Laursen (1956) suggested that the sediment-transporting capacity of a pipe flowing initially part-full will decrease once deposition occurs. If the pipe slope and the water and sediment discharges are kept constant, deposition will continue until the pipe flows full and surcharges. Only when the energy gradient starts to become steeper than the slope of the pipe can the velocity of the flow increase enough to transport the sediment load without further deposition. Laursen and his researchers therefore concentrated on the "ultimate" condition of pipe-full flow, and obtained a graphical relationship between water discharge Q, sediment concentration C_V and depth t of deposit which can be approximated by the equation:

$$C_V = \left[\frac{(1 + t/D)^3}{8 - (1 + t/D)^3}\right]^3 \left[\frac{Q^2}{g(s-1)\,D^5}\right]^{3/2} \qquad (9)$$

The experiments were carried out using 51mm and 152mm diameter smooth pipes. The sediment size was varied between 0.25 mm and 1.6mm and was not found to be a significant factor. The energy gradient i for flows with deposited beds was described by the simple formula:

$$i = b\,\frac{(s-1)}{1.65}\,C_V^{2/3} \qquad (10)$$

where the factor b has a value of b = 1 for duned beds and b = 0.6 for plane beds.

Graf & Acaroglu (1968) analysed data to produce a formula suitable for both alluvial channels and pipes with deposited beds. The equation was expressed in terms of non-dimensional transport and shear parameters but can be written in the more direct form:

$$C_V = 5.32 \times 10^{-2}\, \lambda_c^{2.52}\, (d/R)^{-1.02} \left[\frac{V^2}{g(s-1)\,R}\right]^{2.02} \tag{11}$$

where R is the hydraulic radius of the free-flow area and λ_c is the composite friction factor for the pipe and sediment bed.

Hare (1988) and May et al (1989) described experiments carried out at HR with deposited beds in a 299mm diameter spun concrete pipe. The mean sediment size was 0.72mm and the proportional depth of deposit (averaged along the pipe) was varied up to a maximum of t/D = 0.15. The majority of the tests were carried out with sediment depths below t/D = 0.05 and with separated dunes rather than continuous deposited beds. It was found that the rate of sediment transport with deposition was nearly always higher than that produced by the same flow conditions at the limit of deposition. However, the overall hydraulic resistance increased significantly when the average depth of deposit exceeded about t/D = 0.03. The results suggested that "self-cleansing" sewers might be designed for a sediment depth of t/D = 0.01 without adverse hydraulic effects while allowing somewhat lower minimum velocities and slopes than the strict no-deposit criterion. The sediment transport rate was expressed in the form:

$$C_V = \frac{N}{100}\, (y/d)^{0.36}\, (D^2/A)\, (d/R)^{0.6}\, [1 - (V_t/V)]^4 \cdot \left[\frac{V^2}{g(s-1)\,D}\right]^{3/2} \tag{12}$$

For the limit of deposition case ($V = V_s$), N = 2.11 in accordance with Equation (3). With the criterion relaxed slightly to allow a mean sediment depth of t/D = 0.01, the value of N was found to vary between about N = 14.8 at V = 0.6m/s and N = 4.0 at V = 1.2m/s in the 299mm diameter test pipe. As an interim design method, it was suggested that conservative results for self-cleansing sewers could be obtained using a value of N = 4.0.

Perrusquía (1991, 1992) carried out a systematic experimental investigation of various factors affecting transport in pipes with continuous deposited beds. Factors studied were: the apportionment of the hydraulic resistance between the smooth walls of the pipe and the rougher sediment bed; the development of bed forms and their effect on the flow resistance; and the relationship between the sediment transport rate and other parameters of the flow. The tests were carried out using a 154mm diameter PVC pipe, a 225mm diameter concrete pipe and (at HR Wallingford) a 450mm diameter spun concrete pipe. The overall resistance of a sediment bed can be divided into a grain resistance (due to the sediment size) and a form resistance (due to the occurrence of bed features such as ripples and dunes). Perrusquía found a relationship that can be expressed as:

$$\frac{\tau_b}{\tau_t} = 1.5 + 3.58 \ln (\tau_g/\tau_t) \tag{13}$$

where τ_t is the critical shear stress at the threshold of particle movement, τ_b is the total bed shear stress at a higher stage of sediment transport and τ_g is the component of τ_b due to grain roughness. All three values of shear stress relate to the sediment bed alone so, in Perrusquía's method, the composite resistance of the pipe plus sediment bed should be determined using the Einstein/Vanoni-Brooks separation method. The grain shear stress component is estimated from the rough-turbulent equation:

$$\tau_g = \frac{\rho V^2}{6.24 \ln^2 (12R_b/k_g)} \tag{14}$$

where V is the mean flow velocity, R_b is the portion of the hydraulic radius associated with the sediment bed (found from the above separation method), and the effective grain roughness is given by $k_g = 2.5\ d_{50}$. Perrusquía found that the critical shear stress τ_t for a deposited bed in a pipe could be estimated satisfactorily from the well-established Shields curve. Data from the tests with the 154mm and 225mm diameter pipes were used to establish a sediment transport equation that (in its later 1992 version) can be written in the form:

$$C_v = 15.3 \left(\frac{W_b}{D}\right)\left(\frac{t}{D}\right)^{-0.70}\left(\frac{D^2}{A}\right)\left(\frac{h}{D}\right)^{0.19}\lambda_b^{2.6}\left(\frac{d_{50}}{D}\right)^{-0.63} D_{gr}^{-0.96}\left[\frac{V^2}{g(s-1)D}\right]^{2.1} \tag{15}$$

where W_b is the width of the sediment bed, h is the depth of water above the sediment bed and λ_b is the friction factor for the bed (as determined from the total bed shear stress τ_b). Data obtained with the 450mm diameter pipe did not follow the same trend as the other results and so were not included in the analysis leading to Equation (15).

Kleijwegt (1992) carried out an experimental study similar in scope to that of Perrusquía's described above. The experiments were done using a 302mm diameter uPVC pipe for tests with fixed beds and a 150mm diameter perspex pipe for tests with moveable beds. The latter pipe was equipped with a sediment recirculating-system similar in principle to that used at HR (see Section 3). Extensive statistical analyses of the data were made to determine the validity of various existing formulae for predicting: shear stress at the bed; incipient motion; bed-form type and dimensions; flow resistance; and sediment transport. In the case of sediment transport, the Ackers-White equation gave the best results for continuous deposits with bed forms, while the Engelund-Hansen equation was best for continuous flat beds.

As described in Section 2.1, Ackers (1984) developed the Ackers-White transport equation and the Colebrook-White resistance equation to apply to problems of sediment movement in sewers. The approach is likely to be particularly suitable when there is a significant amount of deposition because the conditions then approach more closely the alluvial-channel case for which the transport equation was originally derived. The composite roughness of a pipe with a deposited bed was calculated from:

$$k_c = \frac{P_o k_o + W_b\, k_b}{P_o + W_b} \tag{16}$$

where P_o is the wetted perimeter of pipe wall, W_b is the width of the sediment bed, and k_o and k_b are the corresponding roughness values in the Colebrook-White equation. The value of k_b for the bed has to be assumed or estimated separately.

Ackers (1991) further developed the method by simplifying the resistance term in the Ackers-White equation and incorporating recent modifications to some of the coefficients (see Appendix A). The resulting transport equation can be expressed (in the standardised form used in this report) as:

$$C_v = J(W_e R/A)^{\alpha}\ (d/R)^{\beta}\ \lambda_c^{\gamma} \left[\frac{V}{\{g(s-1)\ R\}^{1/2}} - K\ \lambda_c^{\delta} (d/R)^{\varepsilon} \right]^m \tag{17}$$

The coefficients J, α, β, γ, K, δ, ε, m depend on the dimensionless grain size D_{gr}, and formulae for their evaluation are given in Appendix A. Values for a representative range of sediment sizes (with s = 2.64) are as follows:

d (mm)	J	α	β	γ	K	δ	ε	m
>2.7	7.84×10^{-3}	1.0	0.287	0	1.91	0	0.400	1.78
0.7	2.02×10^{-2}	0.669	0.0876	0.183	1.42	-0.166	0.433	2.11
0.3	1.51×10^{-2}	0.463	-0.220	0.453	1.23	-0.269	0.454	2.69

Equation (17) has several similarities to the HR Equation (12) including an effective threshold velocity for the start of sediment movement. Ackers (1991) compared Equation (17) with the HR data for the 299mm diameter concrete pipe with small depths of deposition. The agreement was found to be reasonable and within the error bands typical in sediment transport studies. Generally, Equation (17) tended to overestimate the transport rates, but this can be "corrected" by using an effective bed width W_e somewhat less than the actual mean width W_b.

Differences and similarities between the various transport equations for deposited beds can be summarised as follows:

Factor	Relationship to C_v			
	Laursen, Eqn (9)	Graf, Eqn (11)	Perrusquía, Eqn (15)	Ackers, Eqn (17)
V^m	m=3.0	m=4.04	m=4.2	m≈1.8 to 2.7
D^n	n=-1.5	n=-1.0	n=-1.47	n≈-1.2
d^p	-	p=-1.02	p=-1.59	p≈0.29 to -0.22
λ^q	-	q=2.52	q=2.6	q≈0 to 0.45

Perrusquía's Equation (15) shows several similarities to Macke's Equation (2) for the limit of deposition. The coefficients in Ackers' Equation (17) are variable, and the values given above are for high velocities and sediment sizes ≥ 0.3mm. The values of n in the above Table are generally smaller in magnitude than in the corresponding Table in Section 2.1; this suggests that the rate of sediment transport is less sensitive to changes in pipe size when there is a deposited bed than when the flow is at the limit of deposition.

3 Description of experiments

3.1 Test rig

The experiments were carried out with the 450mm diameter concrete pipe installed in a large tilting flume (see Figure 1). The water and sediment discharging from the test pipe were returned to the upstream end by two separate recirculating systems. The sediment was retained within a hopper and pumped as a concentrated slurry back to the inlet of the concrete pipe via a 75mm diameter pipe equipped with an electromagnetic current meter. The remainder of the water flowed from the hopper into a larger outer tank from where two pumps with a total capacity of 220l/s returned it to the upstream end of the flume. This clear-water flow was measured by a British Standard rectangular weir installed upstream of the inlet to the concrete pipe.

The experimental arrangement adopted for the study had the following advantages:

(1) Experiments could be planned and carried out in a systematic way because of the capability for rapid adjustments of the discharge, pipe slope and downstream water level. Thus, for example, it was possible to investigate the effect of flow velocity on the sediment transport rate while keeping other factors such as the water and sediment depths constant.

(2) The sediment recirculating system was much easier to operate than the alternative of using an upstream sediment injector and a downstream collecting tank. The amount of sediment required in the former was much reduced, and this was particularly important when testing a pipe as large as the 450mm one studied here. The recirculating system could be kept running as long as necessary to achieve an equilibrium state within the test pipe. The equilibrium was also reached more quickly because the rates at which sediment entered and left the test pipe were always in balance. The use of a slurry pump did, however, limit the size of sediment that could be recirculated.

An important feature of the test rig was the use of an optical system for measuring the rate of sediment transport. The system was installed near the downstream end of the 75mm diameter recirculating pipe, and consisted of a 1m length of perspex pipe to the outside of which were attached an infra-red light source and detector (see Figure 2). The source and detector were mounted on the vertical centreline of the pipe so that sediment particles travelling along the pipe would interrupt the light beam and vary the output signal from the detector. The signal was passed to a counter which could be set to average the readings over any interval between 1 second and 9999 seconds.

The flow velocity in the recirculating pipe was varied in steps according to the rate of sediment transport, so as to ensure that all the particles moved in suspension or flume traction without any formation of bed deposits. The instrument was calibrated regularly for each sediment size and flow velocity by adding sand at a known rate to the inlet of the recirculating pipe. The calibrations showed a fairly linear relationship between voltage reading and sediment concentration over most of the operating range ; the sensitivity of the instrument was increased if the flow velocity was reduced or the sediment size was increased.

The successful development of the instrument allowed the rate of sediment transport in the test pipe to be measured continuously without affecting the flow or removing sediment from the system. Monitoring the measurements also made it possible to determine when conditions in the test pipe had reached an equilibrium state. More details of the sediment measuring system are given in May et al (1989).

The spun concrete pipe used in the study was manufactured by ROCLA and had a mean internal diameter of 449.5mm. The overall length of the pipe was 21.3m consisting of eight 2.52m sections and a single make-up section at the downstream end. The pipes had spigot-and-socket joints with rubber 'O' ring gaskets, and were assembled with the sockets pointing upstream. A pair of 900mm long x 90mm wide slots was cut in the top of each of the pipes to facilitate the addition of sediment and the measurement of bed and flow features. The slots could be sealed with flush-fitting transparent lids to allow tests with the pipe flowing full and under pressure. Small observation windows were also set into the inverts of the pipes to help identify the start of sediment deposition.

Water levels along the pipe were measured by five electronic digital point gauges set at 2.5m intervals, with each gauge being located about 0.9m downstream of the adjacent pipe socket ; the distance from the pipe inlet to the first gauge was 8.4m. Initially the gauges were mounted over the slots to obtain direct measurements of water levels and avoid the need for pressure tappings, which could become blocked by sediment. However, standing waves produced by the pipe joints and fluctuations in water level due to the passage of dunes made it difficult to determine the slope of the water surface accurately. Pressure tappings were therefore installed at a height of about 0.38D above the invert and connected to stilling wells in which the point gauges were mounted. The tappings worked satisfactorily and helped reduce the fluctuations in water level.

The water level at the downstream end of the pipe was adjusted by means of two side plates which could be moved laterally while allowing sediment to discharge from the pipe into the collecting hopper.

The experiments were carried out using two uniform sands with mean particle sizes of 0.73mm and 0.47mm (Types I and II respectively). The two sizes were first tested separately and then mixed together in the following proportions by weight : equal proportions (Type III), and one part of the 0.73mm sand to two parts of the 0.47mm sand (Type IV). Details of the grading curves are given below; the d_{35} size, for example, is the sieve size through which 35% by weight of a sample is able to pass.

	Type I	Type II	Type III (1:1)	Type IV (1:2)
d_{90} (mm)	0.94	0.76	0.87	0.82
d_{84} (mm)	0.90	0.68	0.79	0.78
d_{65} (mm)	0.80	0.55	0.68	0.66
d_{50} (mm)	0.73	0.47	0.61	0.58
d_{35} (mm)	0.67	0.38	0.54	0.49
d_{16} (mm)	0.58	0.26	0.40	0.33
σ_g (mm)	1.25	1.61	1.41	1.54
s (mm)	2.63	2.64	2.64	2.64

The geometric standard deviation σ_g of the grading curve is defined as $\sigma_g = \sqrt{(d_{84}/d_{16})}$.

3.2 Test procedures

The usual method of carrying out a test was first to set the discharge corresponding to the required velocity and depth of flow in the 450mm diameter pipe. Since the recirculation system for the sediment was operated at a fixed flow rate (appropriate to the likely quantity of sediment transport), changes to the total discharge were made using the clear-water pumps and the rectangular measuring weir. Next, the side plates at the downstream end of the 450mm pipe were adjusted to produce the required water depth at the downstream point gauge. The slope of the pipe was then altered to obtain similar depths and therefore uniform conditions at the other gauge positions. Interaction between the pipe slope and the downstream water level made an iterative procedure necessary, and adjustments were sometimes required during a test because of changes in the flow resistance of the sediment bed. As mentioned in Section 3.1, near-critical flow conditions produced standing waves in the pipe and sometimes made it difficult to obtain equal water depths at the five gauges.

After equilibrium conditions had been reached and measurements made of the water levels and sediment transport rate (using the optical system, see Section 3.1), the flow in the test pipe was stopped suddenly by cutting the pumps and closing the side plates at the downstream end. The water was then allowed to drain slowly away without disturbing the shape of the sediment bed. The bed profile was recorded by measuring either the width or depth of the sediment bed at ten equally-spaced points in each of the eight pipes. The results were used to calculate the mean sediment depth and the root-mean-square variation Δ in bed level ; the mean depth t_1 was defined as the depth that would result if the calculated volume of sediment in the pipe were distributed uniformly along its length. In the case of separated dunes, a second definition of mean depth (t_2) was calculated assuming the sediment to be uniformly distributed along only that portion of the pipe occupied by the dunes.

The head loss gradient i of the flow in the pipe was determined from:

$$i = S_o - \frac{dE}{dx} \tag{18}$$

where S_o is the slope of the pipe and dE/dx is the best-fit gradient of the specific energy relative to the pipe invert. The value of E at each gauge was calculated from:

$$E = y + \frac{Q^2}{2\ g\ (A_t - A_s)^2} \tag{19}$$

where y is the water level relative to the pipe invert, A_t is the total cross-sectional area corresponding to y, and A_s is the cross-sectional area corresponding to the mean sediment depth t_1 described above.

4 Experimental Results

4.1 Clear-water resistance

Tests to determine the hydraulic resistance of the concrete pipe for clear-water flows without any sediment were carried out at the start of the study and during the course of the experiments. The equivalent roughness k of the pipe was calculated from the Colebrook - White equation:

$$\frac{1}{\sqrt{\lambda}} = -2\ \log_{10}\left[\frac{k}{14.8R} + \frac{0.6275\ v}{VR\sqrt{\lambda}}\right] \tag{20}$$

where the Darcy - Weisbach friction factor λ is defined as:

$$\lambda = 8gRi\ /\ V^2 \tag{21}$$

and the energy gradient i is determined from the measurements using equations (18) and (19).

Values of the friction factor λ_o and the roughness k_o for the clean pipe are given in Table 1 for proportional flow depths of y/D = 0.50, 0.75 and 1.0. Analysis of the data gave the following average values and standard deviations:

Prop^n depth y/D	Number of measurements	Average surface roughness k_o (mm)	Standard deviation in k_o (mm)
0.500	40	0.135	0.085
0.748	15	0.162	0.086
1.0	10	0.130	0.168
All data	65	0.141	0.101

The above figures show a reasonably small amount of scatter and no significant variation in effective roughness with the proportional depth of flow. The overall average value of k_o = 0.14mm is used later when determining the composite roughness of the pipe with a deposited sediment bed. This figure agrees well with the value of k_o = 0.15mm recommended in the HR flow tables for spun-concrete pipes in normal condition.

4.2 Limit of deposition

Although additional to the scope of the DOE project, data on the limit of deposition in the 450mm diameter concrete pipe were obtained as a result of separate tests carried out at HR by Mr A Ab Ghani. This information was valuable because it extended the range of the previous HR work on the limit of deposition which was done using 77mm, 158mm and 299mm diameter pipes (see Section 2.1).

Results from the tests with the 450mm pipe and the Type I sand (see Section 3.1) are given in Table 2. The relationship between the mean flow velocity V and the volumetric sediment concentration C_V at the limit of deposition is shown in Figure 3 for a proportional flow depth of y/D = 0.50 and in Figure 4 for a value of y/D = 0.75. The results are analysed and compared with previous data in Section 5.2.

4.3 Transport with separated dunes

In the previous DOE project, tests were carried out in the 299mm diameter concrete pipe to determine the effects of small amounts of sediment deposition. Under these conditions, the sediment did not deposit as a shallow continuous bed but formed a series of larger separated dunes that travelled slowly along the pipe. Although outside the scope of the present DOE study, Mr A Ab Ghani carried out a limited number of tests with separated dunes using the 450mm diameter concrete pipe.

The tests were carried out with the Type I sand, and results are given in Table 3. The variation of the volumetric sediment concentration C_V with the mean flow velocity V and the mean depth of sediment t_1 (averaged along the full pipe length) is illustrated in Figure 5. The tests were carried out with a proportional flow depth of y/D = 0.5, where y was the mean height of the water surface above the invert of the pipe ; the mean depth of water above the sediment bed was $h = y-t_1$. The sediment depth t_2 was the average thickness of the dunes (obtained by averaging their total volume along the length of pipe that they occupied); W_2 was the sediment width corresponding to t_2. Δ was the root-mean-square variation in height of the dunes, neglecting the lengths of clear pipe between them. The data in Table 3 are analysed in Section 5.5.

4.4 Transport with continuous bed

Tests with continuous sediment beds and significant depths of deposition were carried out using four different gradings of sand. As explained in Section 3.1, the sediment types were:

Type I	-	d_{50} = 0.73mm, s = 2.63
Type II	-	d_{50} = 0.47mm, s = 2.64
Type III (1:1 mixture)	-	d_{50} = 0.61mm, s = 2.64
Type IV (1:2 mixture)	-	d_{50} = 0.58mm, s = 2.64

A series of tests was usually carried out with a given amount of sediment added to the recirculating system but with different flow rates and depths of water. This enabled the flow velocity and depth to be varied while keeping an approximately constant mean depth of sediment in the 450mm diameter test pipe. The amount of sediment in the system was then changed and the test procedure repeated. The mixtures were studied in order to determine how their transport rates were related to the corresponding values for the constituent Type I and Type II sands.

It was found in many of the experiments that the flow depth varied significantly along the pipe due to the effects of dunes on the sediment bed and standing waves formed by the spigot-and-socket joints. Although some gauge readings might appear anomalous, there was usually too much variability in the results to justify rejecting the measurements completely. Therefore, in nearly all cases, readings from all five depth gauges were used when calculating the mean water surface slope and flow depth.

The results of the tests with continuous sediment beds are listed in Table 4 (Type I sediment), Table 5 (Type II), Table 6 (Type III) and Table 7 (Type IV). The variation of the volumetric sediment concentration C_v with flow velocity V, mean sediment depth t_1, water level y (above the pipe invert) and sediment type is shown in Figures 6-9. In Tests D.1 to D.9 the proportional depths varied between y/D = 0.356 and 0.671, but in Figure 6 the results are plotted using the symbol for y/D = 0.5. The data in the Tables are analysed in Section 5.4.

5 *Analysis of results*

5.1 Composite resistance

Several alternative methods have in the past been developed for predicting the composite resistance of a channel having two different surface textures. One commonly-used approach involves dividing the flow area between the two roughnesses and assuming each part to have the same mean velocity (eg Horton-Einstein method if using the Manning resistance equation or the Vanoni-Brooks method if using the Darcy-Weisbach equation).

An alternative approach based on shear stress was recommended by Visvalingam (1970) on the basis of systematic experiments with circular pipes having different proportions and types of roughness. The composite shear stress τ_c for the whole pipe was well estimated by the equation:

$$\tau_c = \frac{\tau_1 P_1 + \tau_2 P_2}{P_1 + P_2} \qquad (22)$$

where P_1 is the part of the perimeter occupied by roughness type 1, and τ_1 is the shear stress which would occur if that roughness covered the whole perimeter of the pipe ; subscript 2 refers to the second roughness type. Chow (1959) credits Pavlovskii (1931) with originating this approach. Use of the Darcy-Weisbach resistance Equation (21) gives the following relationship between each component of the shear stress and its corresponding friction factor λ:

$$\tau = \rho \frac{\lambda}{8} V^2 \qquad (23)$$

Substituting in Equation (22) thus gives:

$$\lambda_c = \frac{\lambda_1 P_1 + \lambda_2 P_2}{P_1 + P_2} \qquad (24)$$

The friction factor for each component can be found from the Colebrook-White equation:

$$\frac{1}{\sqrt{\lambda}} = -2 \log_{10} \left[\frac{k}{14.8R} + \frac{0.6275v}{VR\sqrt{\lambda}} \right] \qquad (25)$$

where V and R are respectively the flow velocity and the hydraulic radius for the whole cross-section of the flow, k is the equivalent sand roughness, and v is the kinematic viscosity of the fluid.

Visvalingam's method avoids the problem of having to divide the flow area somewhat arbitrarily between the two roughness types and also has the advantage of being simple to apply. The method has therefore been used throughout the analysis described in later sections of this chapter. In the case of a pipe with a deposited sediment bed, Equation (24) can be written:

$$\lambda_c = \frac{P_o \lambda_o + W_b \lambda_b}{P_o + W_b} \qquad (26)$$

where the subscript o refers to the pipe wall and the subscript b to the sediment bed.

Some uncertainty exists about the value of k_g to be used in the Colebrook-White Equation (25) when determining the grain resistance of a sediment bed with a particle size d. Examples include:

van Rijn (1982)	:	$k_g = 3\ d_{90}$
Henderson (1984)	:	$k_g = 1.5$ to $3\ d_{65}$
Perrusquía (1991)	:	$k_g = 2.5\ d_{50}$

Perrusquía (1991) : $k_g = 2.5\ d_{50}$

Some of these values may apply to flat beds at the threshold of movement rather than to beds with well-developed sediment transport. Evidence from the present tests suggested that the effective values of k_g for flat beds were somewhat lower than those given above. It was therefore assumed in the following analysis that $k_g = 1.23\ d_{50}$ which is equivalent to the value used by Ackers (1991) for single-size sediments (see Appendix A). In practice, differences between alternative assumptions tend to be absorbed into the values of other empirically-derived constants. The effect of any resulting errors should not be large provided an equation is applied using the same assumptions as were made when analysing the original data.

5.2 Limit of deposition

The experimental results obtained with the 450mm diameter concrete pipe are compared in Figures 3 and 4 with the predictions of some existing formulae for the limit of deposition. May I is the previous HR Equation (3) for smooth pipes, with the threshold velocity given by Equation (4); this method gives very similar results to Macke's Equation (2). May II is the corresponding curve for rough pipes using Equation (3) but with the threshold velocity equal to 4/3 times the value for smooth pipes given by Equation (4); this method was derived from the results of earlier HR tests with a 299mm diameter concrete pipe. Mayerle I is Equation (5), and Mayerle II is Equation (6) which takes account of the friction factor λ_c of the water/sediment flow. Experimental values of λ_c were used when determining the curves for Macke and Mayerle II in Figures 3 and 4.

The new data for the limit of deposition in the 450mm diameter pipe do not tie in with any of the existing formulae particularly well, but overall they are closest to the curves for smooth pipes given by Macke and May I. The transport rates appear to be somewhat higher than would have been expected from the earlier HR tests with the 299mm diameter concrete pipe.

As explained in Appendix B, a new theoretical model of bed-load transport in pipes was developed in order to assist the analysis of the experimental data. The model was based on a simplified description of the physical processes involved, and was designed to apply both to conditions at the limit of deposition and to transport with a deposited bed. It was therefore decided to analyse the new data for the limit of deposition in the 450mm diameter concrete pipe together with all the previous HR results for smooth and rough pipes. The earlier results for the 77mm and 158mm diameter smooth pipes and the 299mm diameter concrete pipe are summarised in Tables 8 and 9 but more details are contained in HR Reports IT 222 and SR 221.

The theoretical model described in Appendix B suggests that the volumetric sediment concentration C_v at the limit of deposition can be combined into a transport parameter:

$$\Omega = C_v\ (A/D^2) \left[\frac{\lambda_s V^2}{8gf\ (s-1)\ D}\right]^{-3/2} \tag{27}$$

which should depend on the mobility of the sediment particles as represented by the parameter:

$$G_s = \left[\frac{\lambda_s V^2}{8gf\ (s-1)\ d_{50}}\right]^{1/2} \qquad (28)$$

The factor f is linked to the effective coefficient of friction between the particles and the pipe invert, and for smooth pipes is defined as having a value of f=1.

The friction factor λ_s is the value corresponding to the shear stress exerted on the sediment particles by the flow ; note that this is not equal to the shear stress τ_o acting on the pipe walls (see Appendix B). The value of λ_s is closely linked to the grain resistance λ_g of the particles as determined from the Colebrook-White equation:

$$\frac{1}{\sqrt{\lambda_g}} = -2 \log_{10}\left[\frac{d_{50}}{12R} + \frac{0.6275v}{VR\sqrt{\lambda_g}}\right] \qquad (29)$$

As explained in Section 5.1, R is the hydraulic radius corresponding to the whole cross-sectional area of the flow and the effective sand roughness is described by the relation $k_g = 1.23\ d_{50}$. The value of λ_g applies for circular pipes flowing full, but under part-full conditions the shear stress acting at the pipe invert is modified by the effect of secondary currents and the air-water interface. Analysis of the HR data indicated that the following empirical correction to λ_g was necessary:

$$\lambda_s = \lambda_g\ (y/D)^{2/5} \qquad (30)$$

The transport and mobility parameters used in the analysis of the data were therefore:

$$\Omega = C_v\ (A/D^2)\ (y/D)^{-3/5}\left[\frac{\lambda_g V^2}{8gf\ (s-1)\ D}\right]^{-3/2} \qquad (31)$$

$$G_s = (y/D)^{1/5}\left[\frac{\lambda_g V^2}{8gf\ (s-1)\ d_{50}}\right]^{1/2} \qquad (32)$$

with λ_g being determined from Equation (29).

Values of the parameters Ω and G_s for the earlier HR tests with the 77mm and 158mm diameter smooth pipes are listed in Table 8 and plotted in Figure 10 ; by definition, the friction coefficient f was assumed to have a value of f=1. The data cover quite a wide range of conditions (V=0.43m/s to 1.21m/s ; y/D=0.38 to 1.0 ; and d_{50}=0.57mm to 7.9mm) and show the expected type of parabolic curve (see Appendix B). The following equations for predicting the value of Ω at the limit of deposition were fitted to the data and are plotted in Figure 10:

$\Omega = 0$; $G_s \leq 0.15$ (33)

$\Omega = 8.25\ G_s - 1.24$; $0.15 < G_s \leq 0.55$ (34)

$\Omega = 1.78\ G_s + 2.32$; $0.55 < G_s \leq 0.9$ (35)

Equation (35) can probably be extrapolated somewhat beyond the experimental limit of $G_s = 0.9$, but at high values of particle mobility the sediment will begin to be transported in suspension, causing Ω to increase considerably. The values of limiting sediment concentration predicted by Equations (33) to (35) are listed in Table 8 and compared with the measured values in Figure 11. It can be seen that the agreement is generally satisfactory over the full range of conditions studied. The accuracy of the predictions was evaluated in terms of the variance in the quantity log $(\hat{C}_V/C_V)$ where $\hat{C}_V$ is the predicted concentration and C_V is the corresponding measured concentration for each test ; this method takes equal account of overestimates and underestimates. Omitting two outlying points from the analysis (y/D = 0.384 and 0.395 from Test Series H in Table 8), it was found that the ratio $\hat{C}_V/C_V$ had an average value of 1.00 and standard deviations of +0.29 and -0.24.

Analysis of the data for the 299mm and 450mm diameter concrete pipes indicated that the limiting concentrations were lower than would occur in smooth pipes of similar size. This is believed to be due to a higher coefficient of friction between the particles and the rougher surface texture of the concrete pipes. It was found that a value of the friction coefficient f=1.2 enabled the data to be described by the same Equations (33) to (35) that apply to smooth pipes (with f=1). Values of the parameters Ω and G_s for the tests with the concrete pipes (calculated with f=1.2) are listed in Table 9 and plotted in Figure 12. It can be seen that there is considerably more scatter than occurred with the data for the smooth pipes. This is thought to be due to the difficulty of obtaining uniform flow conditions in the concrete pipes where the spigot-and-socket joints set up strong standing waves ; these increased the degree of turbulence and caused the mean velocity and depth to vary with distance along the pipe. Some groups of data in Figure 12 plot above or below the mean line but no consistent pattern is apparent when the results for all four pipe sizes (smooth and rough) are viewed together. Overall, the data for the concrete pipes show a similar pattern to those for the smooth pipes. The values of limiting sediment concentration predicted by Equations (33) to (35) are listed in Table 9 and plotted in Figure 13. The scatter is substantial in proportionate terms for concentrations below about 5ppm, but in absolute terms the differences and values are small in comparison with those normally occurring in sewers. The accuracy of the predictions was calculated using the method described above for the smooth pipes. For all 75 tests with concrete pipes, the ratio $\hat{C}_V/C_V$ was found to have an average value of 0.97 with standard deviations of +0.73 and -0.46. For the 59 tests with measured concentrations of 5ppm or more, the average value was 1.00 with standard deviations of +0.53 and -0.35.

Analysis of the resistance data in Table 2 shows that the effect of the sediment on the overall roughness of the 450mm diameter concrete pipe was minimal for conditions at the limit of deposition. The average values of equivalent sand roughness in the Colebrook-White equation were k_c=0.12mm for y/D=0.50 and k_c=0.11mm for y/D=0.75. By comparison, the overall average for a larger number of tests under clear-water conditions was found to be k_o=0.14mm (see Section 4.1) ; taking account of the standard deviations, the differences between these roughness estimates are not significant. Therefore, the depth/discharge relationship for the limit of deposition in a rough pipe (eg concrete) can be satisfactorily determined using the clear-water roughness value of the pipe. In the case of smooth pipes, the earlier HR tests with 77mm and 158mm diameter pipes indicated that the friction factor λ_c at the limit of deposition was typically about 5% higher than the corresponding clear-water value λ_o ; the percentage change is likely to be less for larger pipes because the sediment covers a proportionally smaller amount of the pipe perimeter.

The results obtained in this Section for predicting flow conditions at the limit of deposition are summarised in Section 7.1.

5.3 Resistance of sediment bed

In order to be able to predict sediment transport rates in a pipe with a deposited bed, it is first necessary to estimate the hydraulic resistance of the bed since this influences the relationship between discharge, flow velocity and water depth.

Many previous studies of alluvial channels have demonstrated the benefit of separating the total bed resistance into two components : a grain resistance due to the size and shape of the sediment particles ; and a variable form resistance due to the development of ripples and/or dunes. Above the threshold of movement, the form resistance initially increases to a maximum which is related to the size and steepness of the dunes. At higher stages of sediment transport, the bed becomes flatter and the total resistance tends towards the value corresponding to the grain roughness. The form resistance is also affected by the Froude number of the flow because local changes in the level of the bed produce local changes in water depth and velocity.

This description suggests that the relationship between the total shear stress τ_b acting on the sediment bed and the component τ_g due to the grain roughness depends on the rate of sediment transport and the Froude number:

$$F_r = \sqrt{\frac{BV^2}{gA}} \qquad (36)$$

where B is the surface width of the flow and A is the net cross-sectional area. As explained in Appendix B, the rate of sediment transport depends in turn on the mobility of the particles, which can be described by the Shields parameter:

$$F_g^2 = \frac{\tau_g}{\rho g(s-1)d_{50}} \qquad (37)$$

The parameter is expressed in terms of the grain shear stress τ_g since this is the component chiefly responsible for bed-load movement. The functional relationship between total shear stress and grain shear stress can therefore be written:

$$\frac{\tau_b}{\tau_g} = \text{fn}\ (F_g,\ F_r) \tag{38}$$

In most studies of alluvial channels, it is difficult to vary F_g without also changing F_r, and the dependence on the Froude number is therefore sometimes neglected. However, in the present case, tests under pipe-full conditions (ie F_r=0) enabled the relationship between τ_b/τ_g and F_g to be investigated directly. To simplify the analysis it was assumed that the effects of F_g and F_r could be separated so that:

$$\tau_b - \tau_g = \text{fn}_1\ (F_g)\ \text{fn}_2\ (F_r) \tag{39}$$

It is convenient to express the values of shear stress τ_b and τ_g in terms of the corresponding friction factors λ_b and λ_g using Equation (23). Equation (37) can thus be written as:

$$F_g = \left[\frac{\lambda_g V^2}{8g(s-1)d_{50}}\right]^{½} \tag{40}$$

while the corresponding parameter for the total bed resistance is defined as:

$$F_b = \left[\frac{\lambda_b V^2}{8g(s-1)d_{50}}\right]^{½} \tag{41}$$

Equation (39) can then be expressed in the alternative form:

$$F_b - F_g = \text{fn}_3\ (F_g)\ \text{fn}_4\ (F_r) \tag{42}$$

The values of the composite friction factor λ_c for the pipe as a whole (given in Tables 4 to 7) were calculated using Equation (21) and the best-fit gradient of the energy line (see Section 3.2). The total friction factor λ_b for the sediment bed was then found using the composite roughness method described in Section 5.1. The relative proportions of pipe wall and sediment bed were determined using the mean flow depth y and the mean sediment depth t_1 (averaged along the pipe to give the same volume of deposit) ; the concrete pipe was assumed to have a constant roughness of k_o=0.14mm. Table 10 gives for each test the calculated values of λ_o (for the pipe wall), λ_b (for the total bed resistance) and λ_g (for the grain resistance) ; the last was found directly from the Colebrook-White Equation (29) using the known velocity and cross-sectional geometry of the flow. By definition, the friction factor λ_f associated with the form resistance of the bed is given by $\lambda_f=\lambda_b-\lambda_g$. Table 10 also gives the value of the equivalent sand roughness k_b (in the Colebrook-White equation) corresponding to the total friction factor λ_b for the bed.

Perhaps surprisingly, there is not a very good correlation between k_b and the root-mean-square variation Δ in the level of the sediment bed (see Tables 4 to 7). At lower flow velocities $k_b \approx 2\Delta$ very approximately, but at higher velocities k_b decreases much more rapidly than Δ. Viewed overall, the calculated values of λ_b and k_b show a fairly large amount of scatter. As mentioned in

Section 5.2, the formation of standing waves in the pipe sometimes made it difficult to establish or measure uniform flow conditions precisely. Whatever method is used to calculate the composite roughness, any errors in estimating λ_c, or the flow depth and velocity, or the effective roughness k_o of the pipe wall tend to become concentrated in the values of λ_b and k_b assigned to the sediment bed. The scatter is therefore magnified with the result that some tests gave values of λ_b and k_b that were less than those for a clean pipe ; these values are almost certainly incorrect. It is therefore necessary to view the resistance data as a whole when looking for patterns in the results.

Following the method of analysis described above, Figure 14 shows the results for the pipe-full tests in terms of the parameters $F_{b,o}$ (for the total bed resistance with F_r=0) and F_g (for the corresponding grain resistance). The following equations were fitted to the data:

$$F_{b,o} - F_g = 0 \text{ ; for } F_g \leq 0.22 \tag{43}$$

$$F_{b,o} - F_g = 1.63\,(F_g - 0.22)^{0.44} - (F_g - 0.22) \text{ ; for } 0.22 < F_g \leq 0.5 \tag{44}$$

$$F_{b,o} - F_g = 1.15 - F_g \text{ ; for } 0.5 < F_g \leq 1.0 \tag{45}$$

The present experiments did not cover grain mobility values exceeding F_g=0.5 under pipe-full conditions, so Equation (45) is based on typical results found in previous studies of alluvial channels (see, for example, White et al (1987)). The lower limit of F_g=0.22 corresponds to the threshold of movement, and agrees quite satisfactorily with accepted values of the Shields parameter (eg F_g^2=0.040 to 0.056).

The second stage in the analysis involved using the data for part-full flow to investigate the effect of the Froude number on the form resistance, as expressed by the quantity:

$$\Phi = \frac{F_b - F_g}{F_{b,o} - F_g} \tag{46}$$

F_b is the value obtained from Equation (41) for a test with part-full flow (F_r > 0), and $F_{b,o}$ is the value predicted by Equations (43) to (45) for the same grain mobility F_g but a zero Froude number. The values of the quantity Φ in Equation (46) are plotted against F_r in Figure 15. The data show a fair degree of scatter but this is to be expected because any errors in the experimental measurements and calculation procedures are concentrated into this final plot ; negative values of Φ are plotted along the horizontal axis because the total bed resistance ought under no conditions to be less than the grain resistance. The relationship shown by Figure 15 between Φ and the Froude number was described by the following equations:

$$\Phi = 1.0 \text{ ; for } F_r \leq 0.125 \tag{47}$$

$$\Phi = \frac{8}{7}\,(1 - F_r) \text{ ; for } 0.125 < F_r \leq 1.0 \tag{48}$$

$$\Phi = 0.0 \text{ ; for } 1.0 < F_r \leq 1.25 \tag{49}$$

The value of F_r=1.25 represents the upper limit of the present experimental data, but Equation (49) can probably be extended to somewhat higher values of Froude number.

The results obtained by using Equations (43) to (49) to predict the friction factors $\hat{\lambda}_b$ for the total bed resistance and $\hat{\lambda}_c$ for the composite pipe resistance are listed for each test in Table 10. Figure 16 compares the predicted and measured values of λ_c. The points are not distributed equally about the 45° line because several of the tests wtih the Type I sediment gave zero or negative values of the factor Φ (see Figure 15). These values were not used when determining Equations (47) to (49) so the friction factors predicted for these tests are higher than those calculated directly from the experimental data. The results for the three other sediment types are more consistent, and reflect the improved method of measuring water levels adopted during the course of the testing (see Section 3.1).

The results obtained in this Section for predicting the flow resistance of continuous deposited beds are summarised in Section 7.2.

5.4 Transport with continuous bed

The values of sediment concentration measured with continuous deposited beds in the 450mm diameter concrete pipe are plotted versus flow velocity in Figures 6 to 9. Also shown are lines corresponding to the formulae developed by Laursen (Equation (9)) and Graf & Acaroglu (Equation (11)).

Laursen's equation applies only for pipe-full conditions and is therefore not shown in Figures 8 and 9 because sediment Types III and IV were tested only with the pipe flowing part-full. The equation predicts that the rate of sediment transport should not vary with the particle size. Figures 6 and 7 show that Equation (9) does not explain the experimental results satisfactorily.

The lines drawn for Graf & Acaroglu's equation were calculated assuming a typical composite friction factor of λ_c=0.040. The equation does not fit the results consistently, and this conclusion was confirmed by more detailed study of the data.

The formulae developed by Ackers (see Equation (17) and Appendix A) are of particular interest because they have already been used in several sewer flow models (eg MOSQITO) and provide a unifying link with the much larger body of research on sediment transport in alluvial channels. Equation (17) requires values of the composite friction factor λ_c of the pipe, and in order to make comparisons with the present tests it was decided to use the predicted values of $\hat{\lambda}_c$ in Table 10 rather than the directly-calculated values in Tables 4 to 7. As described in Section 5.3, the predictions were obtained from Equations (43) to (49), which in turn were derived from the experimental measurements. The predicted values, therefore, provide a smoothed version of the resistance data and make it easier to assess the performance of the Ackers method. Also, in design situations, the composite roughness of the pipe must be estimated in any case, and it is therefore necessary to consider a sediment-transport formula in combination with a selected resistance formula.

The values of sediment concentration predicted by Equation (17) for each test are listed in Table 11 and compared with the measured values in Figure 17.

Overall the agreement is quite reasonable, particularly when one considers that Equation (17) was adapted directly from the Ackers-White equation for alluvial channels, with changes being limited to those associated with the pipe geometry. The accuracy of the predictions was assessed in terms of the variance in the quantity log ($\hat{C}_v/C_v$) where $\hat{C}_v$ and C_v are the predicted and measured concentrations for a test. Omitting results for two doubtful Tests D.7 and D.10, the average value of the ratio $\hat{C}_v/C_v$ was 1.16 with standard deviations of +1.53 and -0.66. Some of the variance was probably due to intrinsic errors in the experimental data while some was the result of more systematic differences. It can be seen from Figure 17 that, for the coarsest particle size (Type I, d_{50}=0.73mm), Equation (17) tends to underestimate the concentrations at lower transport rates but gives good results at the higher rates (eg 500ppm to 1000ppm). For the finest particle size (Type II, d_{50}=0.47mm), the concentrations are consistently overestimated by a factor of 2 or more.

A possible explanation of this behaviour is as follows. In the Ackers method, the mode of sediment transport is assumed to vary between 100% bed-load and 100% suspended-load according to the size of the particles (see Equations (A.2) and (A.6) for the transition coefficient n in Appendix A). Therefore, the 0.47mm sand used in the tests would be expected to move more in the form of suspended load than the coarser 0.73mm sand. Since transport in suspension is more efficient than movement as bed-load, relatively higher concentrations are predicted for the finer material. In practice, however, the mode of transport varies with the flow velocity as well as the particle size. In the present experiments, the velocities were not high enough to transport any of the sands in suspension so the relative mobilities of the finer materials may have been overestimated by Equation (17). It is not possible to suggest specific modifications to the Ackers method without much more data analysis because all the coefficients detailed in Appendix A are inter-related and cannot be varied in isolation. However, according to the above explanation, it could be worthwhile investigating a change in the formula for the transition coefficient n so that all sediment sizes are assumed to move as bed-load (ie with n=0) until the particle mobility exceeds a certain limit.

A similar type of comparison was made between the experimental data and the sediment transport formula developed by Perrusquía (Equation (15)). This formula requires values of the friction factor λ_b corresponding to the total bed resistance. In order to reduce the adverse effect caused by scatter in the experimental data, it was decided to use the smoothed values of $\hat{\lambda}_b$ (given by Equations (43) to (49)) rather than those calculated directly from the measurements. The basis of the comparison was therefore the same as described above for the Ackers method. The sediment transport rates predicted by Equation (15) were found to be very significantly higher than the measured values for concentrations below about C_v=500ppm. The reason appears to be that Equation (15) is very sensitive to variations in the bed friction factor λ_b. The present tests showed that the highest values of λ_b tended to occur at low flow velocities and Froude numbers when the size of the bed forms was not significantly reduced by interactions with the free surface. At higher velocities, the friction factor reduced towards the values corresponding to the grain roughness (see Section 5.3). As a result, Equation (15) tends to predict fairly constant sediment concentrations over quite a wide range of flow velocities. Better results may perhaps be obtained using Perrusquía's own method of predicting the total bed resistance (see

Equation (13)). However, in design situations, Equation (15) will remain very sensitive to any errors in estimating the bed roughness.

As mentioned previously, a theoretical model of bed-load transport in pipes was developed in order to assist the analysis of the experimental results from this study. In the case of deposited beds, the model described in Appendix B suggests that the transport parameter:

$$\eta = C_v \, (D/W_b) \, (A/D^2) \left[\frac{\lambda_s V^2}{8g(s-1)\,D}\right]^{-1} \tag{50}$$

should depend on the mobility parameter:

$$F_s = \left[\frac{\lambda_s V^2}{8g(s-1)\,d_{50}}\right]^{½} \tag{51}$$

The value of the parameter η is zero if F_s is less than the value corresponding to the threshold of movement. Above this value, η increases with increasing F_s but the curve is expected to flatten off as the efficiency of the bed-load transport process tends towards an asymptotic value. At higher values of F_s, η will start to increase again when the sediment begins to be transported in suspension.

The friction factor λ_s in Equations (50) and (51) relates to the sediment bed and should correspond to the part of the fluid shear stress that is effective in producing sediment transport. Previous research on alluvial channels suggests that the grain shear stress is mainly responsible for bed-load transport and that the component associated with the form resistance only becomes effective when the sediment begins to move in suspension. For this reason the experimental data for the 450mm diameter concrete pipe were first correlated using the parameters:

$$\eta_g = C_v \, (D/W_b) \, (A/D^2) \left[\frac{\lambda_g V^2}{8g(s-1)\,D}\right]^{-1} \tag{52}$$

$$F_g = \left[\frac{\lambda_g V^2}{8g(s-1)\,d_{50}}\right]^{½} \tag{53}$$

The friction factor λ_g corresponds to the grain resistance, and was determined using Equation (29) and Visvalingam's method for composite roughness (see Section 5.1). The data are plotted in Figure 18 in terms of η_g and F_g. It can be seen that the points for each of the four sediment sizes are correlated quite well and that the individual curves have the expected parabolic shape. However, it is also clear that the data sets are distinct and that in the experiments the coarser particles (eg Type I) were transported more easily than the finer ones (eg Type II). Unlike the results for the limit of deposition (see Section 5.2), the proportional depth of flow in the pipe does not affect the correlation significantly. This may be because the deposited bed gave rise to a more rectangular cross-section with a shear-stress distribution that varied less with changes in flow depth.

Figure 18 shows that it is necessary to take further account of sediment size in order to bring all the data towards a single curve. The question that then arises is what linear dimension of the problem should the sediment size be compared to? One possibility is the width W_b of the deposited bed, but there is no obvious reason why the ratio d/W_b should affect the mobility of the sediment (unless the size of the particles is such that the bed width is made up by only a few particles). Other possibilities for the linear dimension are the flow depth h and the hydraulic radius R. The ratio d/h is unlikely to be significant unless the particles are large enough to produce individual interactions with the free surface. The ratio d/R is important in determining the flow resistance of the sediment bed but this factor is already taken into account in the calculation of the friction factor λ_g. A fourth alternative is the thickness δ_* of the laminar sub-layer, and this is more promising because research on boundary layer problems has established the importance of the ratio d/δ_* in determining the transition between smooth-turbulent and rough-turbulent flow. If a particle is submerged within the laminar sub-layer, it is likely to experience lower forces than a particle which is large enough to project into the turbulent wall region. [The Colebrook-White Equation (29) does not take full account of this factor because it was developed for commercial pipes which have a much more gradual transition between smooth-turbulent and rough-turbulent flow than do mobile sediment beds].

The size of the sediment and the thickness of the laminar sub-layer are usually compared in terms of the particle Reynolds number:

$$R_* = \frac{u_* d_{50}}{\nu} \tag{54}$$

where ν is the kinematic viscosity of the liquid and u_* is the shear velocity defined, in terms of the shear stress τ at the bed, as:

$$u_* = \sqrt{\frac{\tau}{\rho}} \tag{55}$$

Referring back to the original correlation parameters η and F_s in Equations (50) and (51), it seems likely that the value of the effective friction factor λ_s initially increases as the sediment particle becomes larger in relation to the thickness of the laminar sub-layer. However, beyond a certain point, the particle is no longer shielded, and λ_s becomes constant and equal to λ_g, the value of grain resistance for fully-rough turbulent flow. A function that can be expected to approximate this type of behaviour is the hyperbolic tangent function:

$$\tanh(x) = \frac{e^{2x} - 1}{e^{2x} + 1} \tag{56}$$

The formula for λ_s that best correlated the data was found to be:

$$\lambda_s = \lambda_g \tanh\left(\frac{R_{*c}}{25}\right) \qquad (57)$$

where λ_g is the value of the friction factor given by Equation (29). Using Equations (23) and (55) to substitute for u_*, the definition of the particle Reynolds number can be expressed as:

$$R_{*c} = \sqrt{\frac{\lambda_c}{8}}\left(\frac{Vd_{50}}{\nu}\right) \qquad (58)$$

where λ_c is the friction factor corresponding to the composite roughness of the pipe. Alternatives to the use of λ_c and the value of the constant in Equation (57) were tested but were less satisfactory. According to Equation (57), the value of λ_s becomes effectively equal to λ_g when $R_{*c} > 50$ approximately.

The transport and mobility parameters used finally to correlate the experimental data were therefore:

$$\eta = C_v\ (D/W_b)\ (A/D^2)\left[\frac{\lambda_g V^2 \tanh(R_{*c}/25)}{8g(s-1)\ D}\right]^{-1} \qquad (59)$$

$$F_s = \left[\frac{\lambda_g V^2 \tanh(R_{*c}/25)}{8g(s-1)\ d_{50}}\right]^{1/2} \qquad (60)$$

Values of the parameters for the tests with the 450mm diameter concrete pipe are listed in Table 11 and are plotted in Figure 19. There is still a fair degree of scatter but it is considered that some of this is present in the basic experimental data (see Figures 6 to 9) and will remain whatever method of analysis is tried. It should also be remembered that Figure 19 is plotted in natural co-ordinates (as opposed to log co-ordinates) and contains values of C_v varying between 3.5ppm and 1290ppm.

The pattern of the data in Figure 19 was described by the following four equations, each covering a different range of the mobility parameter:

$$\eta = 0\ ;\ \text{for } F_s \leq 0.1 \qquad (61)$$

$$\eta = 1.6\ (F_s - 0.1)\ ;\ \text{for } 0.1 < F_s \leq 0.225 \qquad (62)$$

$$\eta = 0.2 + 2.13\ (F_s - 0.225)^{0.6}\ ;\ \text{for } 0.225 < F_s \leq 0.40 \qquad (63)$$

$$\eta = 0.95\ ;\ \text{for } 0.40 < F_s \leq 0.65 \qquad (64)$$

The upper limit of $F_s = 0.65$ corresponds approximately to the maximum value of particle mobility studied in the present experiments. The particles will begin to be transported in suspension at some higher stage of mobility, causing η to increase beyond the value of 0.95.

The sediment concentrations predicted by Equations (61) to (64) are listed in Table 11 and compared with the measured values in Figure 20. It can be seen that the previous systematic differences between the four sediment sizes are generally resolved and that the agreement is best for concentrations exceeding about 300ppm. The accuracy of the method was evaluated as before in terms of the variance in the quantity log $(\hat{C}_V/C_V)$ and omitting results for Tests D.7 and D.10. The average value of the ratio $\hat{C}_V/C_V$ was 1.00 with standard deviations of +0.76 and -0.43. Some of the variance is believed to be due to intrinsic errors in the experimental data.

The results obtained in this Section and in Section 5.3 for predicting flow conditions in a pipe with a continuous sediment bed are summarised in Section 7.2.

5.5 Transport with separated dunes

This mode of transport is the most complex type of bed-load movement because separated dunes bring an additional degree of freedom to the problem: for a given amount of deposited sediment in a pipe, there is potentially an infinite number of combinations of average dune size and spacing. It is therefore interesting to establish whether the results obtained in Sections 5.3 and 5.4 can be applied to the case of separated dunes.

In the previous HR study with the 299mm diameter concrete pipe (HR Report SR 221), it was suggested that sediment transport equations for continuous beds might be applicable if the total volume of the separated dunes were assumed to be distributed as a uniform continuous deposit along the pipe. Sediment transport rates could then be calculated using the mean width and blockage area of the equivalent bed. This approach has the advantage that it would be simple to implement in numerical models of sewers such as MOSQITO which calculate changes in the volume of deposited material during a sequence of storm events. On this basis, it would not be necessary to consider whether the material was in the form of a continuous bed or in separated dunes.

The experimental data in Table 3 for the 450mm diameter concrete pipe were therefore analysed using the values of t_1, W_1 etc for the equivalent continuous bed having the same total volume as the separated dunes (Method A). The first stage involved calculating the flow resistance of the bed and the composite resistance of the pipe predicted by the method developed in Section 5.3 (Equations (43) to (49)). The predicted values of $\hat{\lambda}_c$ are listed in Table 12, and it can be seen that the effect of the sediment on the resistance was significantly over-estimated. In the second stage, the rates of sediment transport were predicted using these estimates of $\hat{\lambda}_c$ together with the transport equations developed in Section 5.4 (Equations (59) to (64)). The predicted concentrations $\hat{C}_V$ are listed in Table 12, and it can be seen that they were typically about 3 times the measured values. If the measured values of the composite friction factor λ_c had been used instead of those estimated from Section 5.3, the predicted concentrations would have been reduced by only about 10%. These results suggest that separated dunes cannot be considered as hydraulically equivalent to a continuous uniform bed having the same volume of deposited material.

An alternative approach is to base the calculations on the average dimensions of the dunes (t_2, W_2 in Table 3), as obtained by dividing their total volume by the sum of their lengths ; this approach is denoted as Method B in Table 12. The composite resistance of the pipe $\hat{\lambda}_{cd}$ and the sediment concentration $\hat{C}_{vd}$ were first calculated from the equations in Sections 5.3 and 5.4 as though the "average" dune were part of a continuous bed having the same thickness and width ; the concentrations were determined from the predicted values of $\hat{\lambda}_{cd}$. If the separated dunes occupied a certain proportion r of the total pipe length, the overall values of the composite roughness and the sediment concentration were determined from the following equations:

$$\hat{\lambda}_c = (1-r)\hat{\lambda}_o + r\,\hat{\lambda}_{cd} \tag{65}$$

$$\hat{C}_v = r\,\hat{C}_{cd} \tag{66}$$

where $\hat{\lambda}_o$ was the calculated friction factor for the clean pipe. The predicted values of $\hat{\lambda}_c$ and $\hat{C}_v$ obtained with Method B are listed in Table 12. It can be seen that the agreement with the measured values is encouragingly good and clearly superior to that achieved using Method A. Although the equivalent continuous bed in Method A has the same volume as the separated dunes, the surface area of the bed is significantly higher. This is believed to be the reason why Method A overestimates the resistance and the sediment transport rate.

These results suggest that transport and resistance equations for continuous sediment beds can also apply to separated dunes provided correct account is taken of the size of the dunes and the distance of clear pipe between them. A relationship between the relative size and spacing of the separated dunes has not been established from the present limited number of tests, but this will be necessary if it is required to predict flow conditions for this mode of transport. Based on findings from alluvial channel research, it might be expected that the size and spacing of the dunes will evolve towards the most "efficient" solution. Thus, for a given discharge and hydraulic gradient, this solution would correspond to the maximum rate of sediment transport. Alternatively, for a given discharge and sediment load, the optimum solution would correspond to the minimum hydraulic gradient. This suggested "regime" condition could be investigated numerically using the resistance and transport equations developed in Sections 5.3 and 5.4.

6 Conclusions

1 The average clear-water roughness of the 450mm diameter spun concrete pipe used in the experiments was k_o = 0.14mm in the Colebrook-White equation. This value is in line with previously published data for this type of pipe.

2 A new theoretical model of bed-load transport in pipes provides a unified description of sediment movement at the limit of deposition and with continuous deposited beds. The model identified non-dimensional transport and mobility parameters which were found to be relevant to the analysis of the experimental results.

3 The flow velocities occurring in the experiments (0.4m/s to 1.3m/s) were not sufficient to transport the sands (d_{50} = 0.47mm to 0.73mm, s = 2.6) in suspension. In many sewers, therefore, bed-load movement is likely to be the predominant mode of transport for medium sands and coarser particles of similar density. The sands used in the tests were non-cohesive.

4 A new equation for the sediment concentration at the limit of deposition was obtained by analysing HR data for smooth pipes (D = 77mm and 158mm) and concrete pipes (D = 299mm and 450mm). The equation indicates that the transport capacity in a rough pipe is less than for equivalent conditions in a smooth pipe because of the higher coefficient of dynamic friction between the particles and the pipe invert. The results were consistent with the friction coefficient being 20% higher in the rough pipes than in the smooth ones.

5 The test with continuous deposited beds showed that the form resistance of the sediment surface varied with both the particle mobility and the Froude number of the flow.

6 The sediment transport equations due to Ackers (1991) were found to be in reasonable agreement with the transport rates measured in the tests with continuous beds. The predicted values were best for the coarsest sand size (d_{50} = 0.73mm) but overestimated the measured concentrations for the finest size (d_{50} = 0.47mm) by a factor of about two. More accurate and consistent results were obtained from a new transport equation based on the theoretical model of bed-load movement mentioned above.

7 The tests with continuous beds were carried out using four different sizes of sand : Types III and IV were obtained by mixing Type I (d_{50} = 0.73mm) and Type II (d_{50} = 0.47mm) in different proportions. The transport rates measured with the mixtures were intermediate between the corresponding values for the original Type I and Type II sands. The results for all four sediments were correlated satisfactorily by the d_{50} size of the grading.

8 The flow resistance and sediment transport rate for separated dunes can be described by the same equations as apply to continuous deposited beds. Good agreement was obtained when the average dimensions and spacing of the dunes were taken into account. An alternative approach based on an equivalent continuous bed having the same volume as the separated dunes over-estimated the effect of the sediment significantly.

9 A full summary of the new results for the limit of deposition and for transport with continuous beds and separated dunes is provided in Chapter 7.

7 Summary of results

7.1 Limit of deposition

It is assumed that the depth and velocity of flow in a pipe are known and that it is required to find the limiting value of sediment concentration above which deposition will occur. Symbols are defined at the beginning of the report, and out-of-sequence equation numbers indicate their use earlier in the text.

First find the friction factor λ_o for the equivalent clear-water flow using the known roughness k_o of the pipe material and the Colebrook-White equation:

$$\frac{1}{\sqrt{\lambda_o}} = -2\log_{10}\left[\frac{k_o}{14.8R} + \frac{0.6275v}{VR\sqrt{\lambda_o}}\right] \qquad (20)$$

If the pipe is smooth (eg plastic or perspex), the value of the friction factor at the limit of deposition can be assumed (typically) to be $\lambda_c = 1.05\ \lambda_o$. If the pipe is rough (eg concrete), the effect of the sediment is negligible and it can be assumed that $\lambda_c = \lambda_o$. The hydraulic gradient required to produce the specified flow in the pipe is:

$$i = \frac{\lambda_c V^2}{8gR} \qquad (21)$$

In order to take account of the fluid forces acting on the sediment, calculate the friction factor λ_g corresponding to the grain resistance from:

$$\frac{1}{\sqrt{\lambda_g}} = -2\log_{10}\left[\frac{d_{50}}{12R} + \frac{0.6275\ v}{VR\sqrt{\lambda_g}}\right] \qquad (29)$$

Calculate the particle mobility from:

$$G_s = (y/D)^{1/5}\left[\frac{\lambda_g V^2}{8gf(s-1)d_{50}}\right]^{1/2} \qquad (32)$$

If the pipe is smooth, the friction coefficient for particle-to-pipe contact has a value of f = 1 ; if the pipe is rough (eg concrete), f = 1.2.

Determine the value of the transport parameter Ω from whichever of the following equations applies:

(i) $G_s \leq 0.15 : \ \Omega = 0$ (33)

(ii) $0.15 < G_s \leq 0.55 : \ \Omega = 8.25\ G_s - 1.24$ (34)

(iii) $0.55 < G_s \leq 0.9 : \ \Omega = 1.78\ G_s + 2.32$ (35)

The upper value of $G_s = 0.9$ corresponds to the limit of the present tests. The maximum volumetric sediment concentration possible without causing deposition can finally be found from:

$$C_v = \Omega(A/D^2)^{-1}(y/D)^{3/5}\left[\frac{\lambda_g V^2}{8gf(s-1)D}\right]^{3/2} \tag{31}$$

If the design problem is specified differently (eg given C_v, find limiting V), an iterative procedure is necessary.

7.2 Transport with continuous bed

It is assumed that there is a continuous sediment bed in the pipe with a certain mean depth (calculated by averaging the volume of deposited material uniformly along the pipe). The depth and velocity of flow are known, and it is required to find the hydraulic gradient and the rate of sediment transport.

The first step in the procedure is to determine the composite roughness of the pipe. Calculate the friction factor λ_o for the pipe walls using Equation (20) in Section 7.1 ; the hydraulic radius R should correspond to the total free flow area above the sediment bed. Similarly, determine the friction factor λ_g for the grain resistance from Equation (29) in Section 7.1. The form resistance of the bed depends partly on the grain mobility of the sediment particles defined as:

$$F_g = \left[\frac{\lambda_g V^2}{8g(s-1)d_{50}}\right]^{1/2} \tag{40}$$

A second factor is the Froude number of the flow given by:

$$F_r = \left(\frac{BV^2}{gA}\right)^{1/2} \tag{36}$$

The mobility parameter F_b for the total bed resistance (grain + form resistance) varies with F_g and F_r according to the following equations:

(i) $F_g \leq 0.22$; all F_r : $F_b = F_g$ (67)

(ii) $0.22 < F_g \leq 0.5$; $F_r \leq 0.125$: $F_b = 0.22 + 1.63\ (F_g - 0.22)^{0.44}$ (68)

(iii) $0.22 < F_g \leq 0.5$; $0.125 < F_r \leq 1.0$:

$$F_b = F_g + \frac{8}{7}(1 - F_r)\left[1.63(F_g - 0.22)^{0.44} - (F_g - 0.22)\right] \tag{69}$$

(iv) $0.22 < F_g \leq 0.5$; $1.0 < F_r \leq 1.25$: $F_b = F_g$ (70)

(v) $0.5 < F_g \leq 1.0$; $F_r \leq 0.125$: $F_b = 1.15$ (71)

(vi) $0.5 < F_g \leq 1.0$; $0.125 < F_r \leq 1.0$: $F_b = F_g + \frac{8}{7}(1-F_r)(1.15-F_g)$ (72)

(vii) $0.5 < F_g \leq 1.0$; $1.0 < F_r \leq 1.25$: $F_b = F_g$ (73)

The upper values of $F_g = 1.0$ and $F_r = 1.25$ correspond approximately to the limits of the present experiments. Having determined F_b from the appropriate equation, the friction factor for the total bed resistance is found from:

$$\lambda_b = \frac{8g(s-1)F_b^2 d_{50}}{V^2} \tag{41}$$

The composite friction factor for the pipe is given by:

$$\lambda_c = \frac{P_o\lambda_o + W_b\lambda_b}{P_o + W_b} \tag{26}$$

where the lengths of wetted perimeter corresponding to the pipe wall (P_o) and the sediment bed (W_b) are known from the cross-sectional geometry. The hydraulic gradient required to produce the specified flow is given by Equation (21) in Section 7.1.

These values of the friction factor, together with the other specified properties of the flow, enable the sediment transport rate in the pipe to be predicted using any of the design equations so far developed. One possibility which gave reasonable results in the present study is the Ackers (1991) method (see Equation (17) and Appendix A). Alternatively, the transport rate can be estimated using the following HR method developed in Section 5.4.

First calculate the particle Reynolds number given by:

$$R_{*c} = \sqrt{\frac{\lambda_c}{8}}\left(\frac{Vd_{50}}{\nu}\right) \tag{58}$$

and then the related transition factor:

$$\theta = \frac{\exp(R_{*c} / 12.5) - 1}{\exp(R_{*c} / 12.5) + 1} \tag{74}$$

The effective mobility of the sediment particles is defined by the parameter:

$$F_s = \left[\frac{\theta\lambda_g V^2}{8g(s-1)d_{50}}\right]^{1/2} \tag{75}$$

The value of F_s is related to the transport parameter η by the following equations:

(i) $F_s \leq 0.1 : \eta = 0$ (61)

(ii) $0.1 < F_s \leq 0.225 : \eta = 1.6 (F_s - 0.1)$ (62)

(iii) $0.225 < F_s \leq 0.40 : \eta = 0.2 + 2.13 (F_s - 0.225)^{0.6}$ (63)

(iv) $0.40 < F_s \leq 0.65 : \eta = 0.95$ (64)

The upper value of $F_s = 0.65$ corresponds approximately to the limit of the present tests. Having determined the value of η from the appropriate equation, the volumetric sediment concentration is finally calculated from:

$$C_v = \eta \left(\frac{W_b}{D} \right) \left(\frac{A}{D^2} \right)^{-1} \left[\frac{\theta \lambda_g V^2}{8g(s-1)D} \right] \tag{76}$$

If the design problem is specified differently (eg given C_v and discharge, find flow depth), an iterative procedure is necessary.

7.3 Transport with separated dunes

It is assumed that the pipe contains separated dunes, and that the average dimensions and spacing of the dunes are known. Given the flow depth and water discharge, it is required to find the hydraulic gradient and the rate of sediment transport.

Separate calculations are carried out for the flow over a dune and for the flow in the section of clear pipe between adjacent dunes. If Y_s is the volume of the dunes in a length L of pipe and r is the proportion of the length L occupied by dunes, calculate the average cross-sectional area of a dune as:

$$A_s = \frac{Y_s}{r\,L} \tag{77}$$

From the known diameter of the pipe, find the average thickness t_2 and bed width W_2 corresponding to A_s. It is assumed that the depth of water above the pipe invert is uniform along the length L.

For the flow over a dune, calculate the cross-sectional area of the flow and hence the hydraulic radius R_2 and the corresponding local velocity V_2. The composite friction factor λ_{cd} for the dune and the pipe walls is then determined assuming the dune to be part of a continuous sediment bed of thickness t_2. The calculations are carried out using the procedure described in the first part of Section 7.2 up to Equation (26). Having found λ_{cd}, the corresponding sediment concentration C_{vd} for the flow over the dune can be estimated using the equations in the second part of Section 7.2.

For the flow in the section of clear pipe between the dunes, the hydraulic radius R_o and the flow velocity V_o are found from the known discharge and water level. The friction factor λ_o for the clear-water flow is determined from Equation (20) in Section 7.1.

In the final step, the overall values of hydraulic gradient and sediment concentration are calculated from the equations:

$$i = (1-r)\,\frac{\lambda_o V_o^2}{8gR_o} + r\,\frac{\lambda_{cd} V_2^2}{8gR_2} \qquad (78)$$

$$C_v = r\,C_{vd} \qquad (79)$$

8 Recommendations for further study

1 The flow resistance of continuous deposited beds under pipe-full conditions (zero Froude number) should be investigated for higher values of particle mobility.

2 Data from other studies should be analysed according to the new theoretical model of bed-load movement in order to confirm or improve the correlations between the transport and mobility parameters.

3 Experimental data on suspended-load transport in pipes are required to help identify or develop a suitable model for predicting the movement of silts, fine sands and low-density particles.

4 Experimental data on separated dunes should be analysed to determine whether the size and spacing of the dunes correspond to optimised solutions of the resistance and transport equations (ie maximum sediment concentration and/or minimum hydraulic gradient).

9 Acknowledgements

The experimental programme was co-ordinated by Mrs P M Brown and Ms M Escarameia and the measurements were made by Mr L J Eldred, Mr S Mambretti, Mr R Payne and Mr I R Willoughby. Important contributions to the HR test programme were made by Dr G S Perrusquía from the Department of Hydraulics, Chalmers University of Technology, Gõteborg and by Mr A Ab Ghani from the Department of Civil Engineering, University of Newcastle upon Tyne.

10 References

ACKERS P. (1984). Sediment transport in sewers and the design implications. Intern. Conf. on Planning, Construction, Maintenance and Operation of Sewerage Systems, BHRA/WRc, Reading, England, September, pp215-230.

ACKERS P. (1991). Sediment aspects of drainage and outfall design. Proc Intern. Symp. on Environmental Hydraulics, Hong Kong, December, pp19-29. (Eds. J.H.W. Lee & Y.K. Cheung, A.A. Balkema, Rotterdam).

ALVAREZ E.M. (1990). The influence of cohesion on sediment movement in channels of circular cross-section. PhD Thesis, University of Newcastle upon Tyne.

CHOW V.T. (1959). Open-channel hydraulics. McGraw-Hill Kogakusha, Tokyo.

CIRIA (1986). Sediment movement in combined sewerage and storm-water drainage systems. Research Project 366, Phase 1 - Project report.

CRABTREE R.W. (1988). A classification of combined sewer sediment types and characteristics. Water Research Centre, Report No ER324E.

GRAF W.H. & ACAROGLU E.R. (1968). Sediment transport in conveyance systems : Part 1. Bull. Intern. Assoc. Sci. Hydr., XIII année, No 2, June, pp20-39.

HARE G.R. (1988). Sediment movement in sewers : interim report. HR Wallingford, Report SR 179.

HENDERSON R.J. (1984). A guide to hydraulic roughness in sewers. Water Research Centre, External Report No 131E.

HR WALLINGFORD (1990). Sediment transport : the Ackers and White theory revised. HR Wallingford, Report SR 237.

KLEIJWEGT R.A. (1992). On sediment transport in circular sewers with non-cohesive deposits. PhD thesis, Technical University of Delft.

LAURSEN E.M. (1956). The hydraulics of a storm-drain system for sediment-transporting flow. Bull. No 5, Iowa Highway Research Board.

MACKE E. (1982). About sedimentation at low concentrations in partly filled pipes. Mitteilungen, Leichtweiss - Institut für Wasserbau der Technischen Universität Braunschweig, Heft 76/1982, pp1-151, (in German).

MAY R.W.P. (1975). Deposition of grit in pipes : literature survey. HR Wallingford, Report INT 139.

MAY R.W.P. (1982). Sediment transport in sewers. HR Wallingford, Report IT 222.

MAY R.W.P., BROWN P.M., HARE G.R. & JONES K.D. Self-cleansing conditions for sewers carrying sediment. HR Wallingford, Report SR 221.

MAYERLE R., NALLURI C. & NOVAK P. (1991). Sediment transport in rigid bed conveyance. Jnl. Hydraulic Research, Vol 29, No 4, pp475-495.

NALLURI C. & ALVAREZ E.M. (1992). The influence of cohesion on sediment behaviour. Water Sci. Tech., Vol 25, No 8, pp151-164.

NOVAK P. & NALLURI C. (1975). Sediment transport in smooth fixed bed channels. Jnl. Hydr. Div., Amer. Soc. Civ. Engrs., Vol 101, HY9, September, pp1139-1154.

PAVLOVSKII N.N. (1931). On a design formula for uniform movement in channels with non-homogeneous walls. Trans. All-Union Scientific Research Institute of Hydraulic Engineering, Leningrad, Vol 3, pp157-164.

PERRUSQUÍA G.S. (1991). Bedload transport in storm sewers : Stream traction in pipe channels. PhD thesis, Dept. Hydraulics, Chalmers University of Technology, Göteborg, Report Series A:22.

PERRUSQUÍA G.S. (1992). Sediment transport in pipe channels. Dept. Hydraulics, Chalmers University of Technology, Göteborg, Report Series B:55.

RIJN L. C. van (1982). Equivalent roughness of alluvial bed. Jnl. Hydr. Div., Amer. Soc. Civ. Engrs., Vol 108, HY10, October, pp1215-1218.

VISVALINGAM M. (1970). Flow through partly lined conduits. PhD thesis, Imperial College of Science and Technology, London.

WHITE W.R., BETTESS R. & WANG SHIQIANG (1987). Frictional characteristics of alluvial streams in the lower and upper regimes. Proc. Instn. Civ. Engrs., Part 2, Vol 83, December, pp685-700.

Tables

Table 1 Clear-water roughness of 450mm diameter concrete pipe

Test No	y/D	V (m/s)	F_r	T (°C)	λ_o	k_o (mm)
A.1	0.503	0.492	0.37	15.0	0.0242	0.881*
A.2	0.504	0.780	0.59	16.2	0.0212	0.523*
A.3	0.504	1.177	0.89	13.4	0.0178	0.226
A.4	0.499	1.181	0.90	14.7	0.0175	0.211
A.5	0.511	1.067	0.80	16.4	0.0191	0.338
A.6	0.499	0.703	0.53	11.0	0.0181	0.192
A.10	0.502	0.496	0.38	14.0	0.0174	0.101
A.11	0.505	0.694	0.52	16.0	0.0159	0.062
A.12	0.500	0.908	0.69	14.0	0.0178	0.210
A.13	0.503	1.080	0.82	13.0	0.0147	0.041
A.14	0.500	0.486	0.37	15.0	0.0188	0.218
A.15	0.502	0.887	0.67	13.5	0.0174	0.178
A.16	0.504	1.091	0.82	13.5	0.0159	0.103
A.17	0.500	0.408	0.31	15.5	0.0181	0.124
A.18	0.499	0.597	0.45	15.5	0.0179	0.178
A.19	0.499	0.801	0.61	13.5	0.0176	0.182
A.20	0.496	1.012	0.77	13.0	0.0165	0.127
A.21	0.501	0.395	0.30	16.0	0.0195	0.249
A.22	0.502	0.397	0.30	16.5	0.0204	0.344
A.23	0.502	0.524	0.40	15.5	0.0177	0.140
A.24	0.498	0.606	0.46	15.5	0.0160	0.048
A.25	0.499	0.609	0.46	15.5	0.0159	0.047
A.26	0.503	0.781	0.59	15.5	0.0166	0.114
A.27	0.496	0.996	0.76	16.0	0.0161	0.109
A.30	0.498	0.609	0.46	15.5	0.0161	0.054
A.31	0.501	0.791	0.60	15.5	0.0169	0.134
A.32	0.499	0.975	0.74	16.0	0.0173	0.179
A.33	0.499	0.510	0.39	16.0	0.0159	0.021
A.34	0.498	0.708	0.54	16.0	0.0163	0.088
A.35	0.498	0.808	0.61	16.0	0.0160	0.081
A.36	0.493	0.914	0.70	15.5	0.0169	0.144

Table 1 Continued

Test No	y/D	V (m/s)	F_r	T (°C)	λ_o	k_o (mm)
A.37	0.500	0.987	0.75	15.5	0.0173	0.182
A.38	0.509	1.075	0.81	16.5	0.0152	0.071
A.39	0.497	0.707	0.54	16.5	0.0167	0.112
A.40	0.500	0.505	0.38	16.0	0.0165	0.055
A.41	0.498	0.602	0.46	15.5	0.0168	0.097
A.42	0.501	1.194	0.91	14.0	0.0192	0.341
A.43	0.497	0.755	0.58	14.0	0.0159	0.066
A.44	0.495	0.860	0.66	14.0	0.0154	0.053
A.45	0.500	0.552	0.42	13.5	0.0165	0.055
A.46	0.497	0.654	0.50	13.0	0.0168	0.101
A.47	0.500	0.841	0.64	13.5	0.0151	0.037
A.50	0.754	0.670	0.37	14.0	0.0178	0.237
A.51	0.750	0.514	0.29	14.0	0.0191	0.333
A.52	0.749	0.812	0.45	14.0	0.0181	0.285
A.53	0.751	0.602	0.33	13.5	0.0164	0.108
A.54	0.750	0.407	0.23	13.5	0.0161	0.016
A.55	0.739	1.017	0.57	14.0	0.0170	0.212
A.60	0.747	0.502	0.28	15.5	0.0169	0.123
A.61	0.750	0.700	0.39	15.5	0.0173	0.205
A.62	0.751	0.798	0.44	14.5	0.0168	0.173
A.63	0.747	0.904	0.51	14.5	0.0168	0.188
A.64	0.750	0.600	0.33	14.0	0.0166	0.123
A.65	0.748	0.754	0.42	14.0	0.0152	0.057
A.66	0.747	0.662	0.36	14.0	0.0161	0.101
A.67	0.745	0.856	0.48	15.0	0.0153	0.085
A.68	0.747	0.709	0.39	15.0	0.0170	0.180

Table 1 Continued

Test No	y/D	V (m/s)	F_r	T (°C)	λ_o	k_o (mm)
A.70	1.0	0.424	-	13.8	0.0193	0.230
A.71	1.0	0.424	-	13.9	0.0182	0.133
A.72	1.0	0.437	-	14.3	0.0183	0.155
A.73	1.0	0.431	-	14.5	0.0179	0.118
A.74	1.0	0.426	-	14.2	0.0199	0.296
A.75	1.0	0.426	-	13.6	0.0194	0.245
A.76	1.0	0.460	-	12.0	0.0204	0.349
A.77	1.0	0.467	-	12.1	0.0127	-0.156
A.78	1.0	0.454	-	12.3	0.0171	0.057
A.79	1.0	0.453	-	12.5	0.0135	-0.132

* 2 No extreme values omitted when calculating averages
Tests A.10 to A.79 were carried out by Mr A Ab Ghani

Table 2 Data for limit of deposition

Test No	y/D	R (m)	V (m/s)	F_r	λ_c	k_c (mm)	C_v (ppm)
B.1	0.497	0.112	0.609	0.46	0.0160	0.050	4.9
B.2	0.503	0.113	0.786	0.59	0.0168	0.131	12.9
B.3	0.496	0.112	0.983	0.75	0.0182	0.247	22.1
B.4	0.500	0.112	0.510	0.39	0.0161	0.031	3.6
B.5	0.497	0.112	0.709	0.54	0.0171	0.138	7.1
B.6	0.498	0.112	0.808	0.62	0.0161	0.088	7.8
B.7	0.495	0.112	0.912	0.70	0.0169	0.151	11.4
B.8	0.500	0.112	0.986	0.75	0.0180	0.232	18.3
B.9	0.509	0.114	1.069	0.80	0.0156	0.089	20.5
B.10	0.498	0.112	0.705	0.54	0.0174	0.157	4.7
B.11	0.500	0.112	0.504	0.38	0.0176	0.128	1.6
B.12	0.497	0.112	0.600	0.46	0.0175	0.144	5.3
B.13	0.494	0.112	1.216	0.93	0.0181	0.249	37.7
B.14	0.497	0.112	0.754	0.57	0.0163	0.091	12.8
B.15	0.500	0.112	0.853	0.65	0.0159	0.081	18.8
B.16	0.499	0.112	0.553	0.42	0.0165	0.060	3.3
B.17	0.495	0.112	0.652	0.49	0.0169	0.106	5.1
B.18	0.499	0.112	0.843	0.64	0.0153	0.045	13.9
B.20	0.747	0.135	0.502	0.28	0.0174	0.166	2.3
B.21	0.749	0.136	0.701	0.39	0.0163	0.126	7.4
B.22	0.750	0.136	0.790	0.44	0.0177	0.250	11.5
B.23	0.747	0.136	0.904	0.51	0.0142	0.027	17.9
B.24	0.750	0.136	0.600	0.33	0.0147	0.002	3.6
B.25	0.749	0.136	0.753	0.42	0.0155	0.079	7.2
B.26	0.746	0.135	0.662	0.37	0.0162	0.107	5.0
B.27	0.744	0.135	0.857	0.48	0.0160	0.127	14.0
B.28	0.745	0.135	0.706	0.40	0.0165	0.143	6.8

Tests carried out by Mr A Ab Ghani

Table 3 Data for separated dunes

Test No	y/D	t_1/D t_2/D (%)	Prop of dunes (%)	R_1 R_2 (m)	W_1 W_2 (m)	V_1 V_2 (m/s)	F_{r1} F_{r2}	λ_c	k_c (mm)	Δ (mm)	C_v (ppm)
C.1	0.498	0.278 1.51	7.6	0.1121 0.1116	0.0474 0.1097	0.653 0.657	0.498 0.502	0.0181	0.187	8.2	4.6
C.2	0.501	0.422 1.50	14.8	0.1124 0.1120	0.0584 0.1092	0.741 0.745	0.563 0.567	0.0176	0.170	7.7	13.2
C.3	0.501	0.767 1.78	28.2	0.1123 0.1119	0.0785 0.1188	0.843 0.848	0.641 0.646	0.0183	0.241	8.8	34.8
C.4	0.496	0.422 1.53	14.7	0.1117 0.1113	0.0584 0.1104	0.607 0.610	0.464 0.468	0.0210	0.455	8.5	6.3
C.5	0.501	0.644 1.54	27.3	0.1124 0.1120	0.0720 0.1108	0.708 0.711	0.538 0.542	0.0203	0.401	8.7	15.4
C.6	0.500	0.933 1.90	34.3	0.1121 0.1116	0.0865 0.1228	0.502 0.505	0.382 0.385	0.0197	0.292	10.5	3.6

Table 4 Data for transport with continuous bed (Type I sand)

Test No	y/D	t_1/D	R (m)	W (m)	V (m/s)	F_r	λ_c	k_c (mm)	Δ (mm)	C_v (ppm)
D.1	0.356	0.162	0.0636	0.332	0.486	0.55	0.0211	0.182	7.4*	276
D.2	0.467	0.194	0.0823	0.355	0.516	0.49	0.0242	0.605	12.6*	133
D.3	0.621	0.167	0.1115	0.335	0.454	0.33	0.0424	6.04	-	38
D.4	0.447	0.178	0.0812	0.344	0.494	0.47	0.0522	7.69	13.1*	217
D.5	0.501	0.178	0.0916	0.344	0.520	0.45	0.0531	8.03	19.7*	171
D.6	0.671	0.195	0.1132	0.356	0.531	0.36	0.0630	17.0	28.6*	75
D.7	0.472	0.174	0.0870	0.340	0.375	0.34	0.1456	62.9	33.1*	281
D.8	0.565	0.191	0.0995	0.354	0.509	0.41	0.0904	31.9	34.1*	104
D.9	0.440	0.185	0.0784	0.349	0.555	0.54	0.0799	19.7	37.7*	303
D.10 **	0.493	0.209	0.0844	0.366	0.780	0.719	0.0225	0.487	20.9	(1100)
D.11	0.456	0.211	0.0764	0.367	0.792	0.787	0.0246	0.648	17.9	1044
D.12	0.507	0.223	0.0844	0.374	0.606	0.556	0.0412	4.21	11.6	351
D.13	0.529	0.241	0.0849	0.385	0.519	0.471	0.0625	12.5	15.3	55.2
D.14	0.507	0.210	0.0870	0.366	0.881	0.792	0.0152	0.016	17.5	941
D.15	0.510	0.215	0.0863	0.370	0.973	0.879	0.0076	-0.122	18.3	923
D.16	0.481	0.202	0.0833	0.361	1.317	1.229	0.0037	-0.134	17.2	1280
D.17	0.524	0.209	0.0903	0.365	1.013	0.884	0.0172	0.128	11.4	947
D.18	0.511	0.228	0.0842	0.377	0.556	0.512	0.0438	5.00	15.3	270
D.19	0.518	0.227	0.0858	0.376	0.666	0.603	0.0451	5.55	15.9	512
D.20	0.507	0.220	0.0851	0.372	0.825	0.753	0.0345	2.50	13.8	800
D.30	0.505	0.260	0.0764	0.394	0.512	0.502	0.0338	2.04	10.2	49.3
D.31	0.509	0.228	0.0840	0.377	0.536	0.493	0.0510	7.51	18.6	440
D.32	0.512	0.225	0.0849	0.375	0.802	0.732	0.0189	0.195	15.8	788
D.33	0.504	0.198	0.0886	0.358	0.588	0.523	0.0299	1.60	20.3	114
D.34	0.519	0.176	0.0951	0.343	0.607	0.512	0.0443	5.86	26.0	252
D.35	0.511	0.184	0.0924	0.349	0.793	0.684	0.0228	0.582	21.7	413
D.36	0.513	0.171	0.0948	0.339	0.968	0.820	0.0131	-0.035	20.2	823

Table 4 Continued

Test No	y/D	t_f/D	R (m)	W (m)	V (m/s)	F_r	λ_c	k_c (mm)	Δ (mm)	C_v (ppm)
D.40	0.486	0.128	0.0972	0.300	0.950	0.800	0.0222	0.550	18.0	780
D.41	0.505	0.138	0.0990	0.310	0.801	0.662	0.0284	1.49	14.1	205
D.42	0.504	0.144	0.0979	0.315	0.605	0.504	0.0631	14.8	9.6	212
D.43	0.500	0.150	0.0963	0.321	1.200	1.012	-	-	16.1	1290
D.44	0.543	0.200	0.0951	0.360	0.954	0.797	0.0420	5.06	7.8	783
D.45	0.505	0.204	0.0876	0.362	0.702	0.629	0.0395	3.88	7.4	507
D.50	1.0	0.288	0.0922	0.407	0.736	-	0.0089	-0.144	37.6	76.5
D.51	1.0	0.244	0.0965	0.386	0.659	-	0.0672	16.8	45.9	322
D.52	1.0	0.244	0.0965	0.386	0.759	-	0.0573	11.6	47.5	297
D.53	1.0	0.270	0.0940	0.399	0.907	-	0.0449	6.0	51.8	378
D.54	1.0	0.224	0.0983	0.375	0.939	-	0.0851	28.1	57.6	606

* values of Δ are average dune heights (crest to trough)

** values derived from only three water level gauges

Tests D.1 to D.9 carried out by Dr G S Perrusquía

Tests D.10 to D.20 carried out by Mr A Ab Ghani

Table 5 Data for transport with continuous bed (Type II sand)

Test No	y/D	t_1/D	R (m)	W (m)	V (m/s)	F_r	λ_c	k_c (mm)	Δ (mm)	C_v (ppm)
E.1	0.499	0.215	0.0843	0.369	0.525	0.484	0.0561	9.56	14.4	19.2
E.2	0.502	0.211	0.0857	0.367	0.616	0.561	0.0521	8.10	14.1	103
E.3	0.509	0.198	0.0896	0.358	0.675	0.595	0.0507	7.90	16.1	211
E.4	0.515	0.202	0.0899	0.361	0.764	0.670	0.0410	4.43	8.6	355
E.5	0.511	0.208	0.0879	0.365	0.889	0.793	0.0301	1.65	12.8	554
E.6	0.504	0.200	0.0883	0.359	0.985	0.878	0.0252	0.855	10.8	638
E.7	0.503	0.193	0.0893	0.355	1.069	0.946	0.0187	0.222	14.1	798
E.8	0.501	0.180	0.0913	0.346	1.137	0.992	0.0191	0.261	14.4	798
E.10	1.0	0.217	0.0989	0.371	0.511	-	0.0460	6.74	40.3	11.5
E.11	1.0	0.224	0.0983	0.375	0.618	-	0.0560	11.2	26.6	42.2
E.12	1.0	0.218	0.0989	0.371	0.715	-	0.0534	9.99	45.9	113

Table 6 Data for transport with continuous bed (Type III sand)

Test No	y/D	t_1/D	R (m)	W (m)	V (m/s)	F_r	λ_c	k_c (mm)	Δ (mm)	C_v (ppm)
F.1	0.513	0.219	0.0864	0.372	0.636	0.574	0.0544	9.11	21.1	378
F.2	0.503	0.214	0.0854	0.369	0.542	0.494	0.0535	8.62	17.3	203
F.3	0.506	0.218	0.0851	0.371	0.440	0.401	0.0648	13.6	16.5	148
F.4	0.506	0.214	0.0858	0.369	0.724	0.657	0.0466	6.06	15.7	438
F.5	0.502	0.202	0.0875	0.361	0.778	0.698	0.0489	7.03	9.1	561
F.6	0.503	0.197	0.0886	0.357	0.972	0.865	0.0366	3.14	14.3	649
F.10	0.498	0.219	0.0835	0.372	0.659	0.611	0.0385	3.41	21.1	283
F.11	0.501	0.202	0.0873	0.361	0.778	0.700	0.0473	6.43	9.1	424
F.12	0.513	0.205	0.0889	0.363	0.754	0.668	0.0467	6.30	9.7	463
F.13	0.500	0.215	0.0846	0.369	0.716	0.657	0.0429	4.75	14.7	311
F.20	0.756	0.218	0.1169	0.371	0.398	0.246	0.0437	6.90	21.5	3.5
F.21	0.756	0.227	0.1157	0.377	0.591	0.368	0.0629	17.3	33.3	136
F.22	0.757	0.220	0.1168	0.372	0.475	0.294	0.0475	8.69	23.0	28.9
F.30	0.775	0.227	0.1167	0.377	0.571	0.345	0.0665	19.8	33.3	96.1

Table 7 Data for transport with continuous bed (Type IV sand)

Test No	y/D	t_f/D	R (m)	W (m)	V (m/s)	F_r	λ_c	k_c (mm)	Δ (mm)	C_v (ppm)
G.1	0.509	0.189	0.0911	0.352	0.591	0.515	0.0627	13.5	17.6	454
G.2	0.499	0.210	0.0853	0.366	0.506	0.462	0.0364	2.89	16.9	51.8
G.3	0.498	0.197	0.0877	0.358	0.709	0.636	0.0490	7.09	13.7	425
G.4	0.510	0.202	0.0889	0.361	0.779	0.690	0.0461	6.10	13.4	425

Table 8 Derived data for limit of deposition: smooth pipes

Test Conditions

H : D = 158mm, d_{50} = 0.64mm, s = 2.65
I : D = 158mm, d_{50} = 5.8mm, s = 2.65
J : D = 158mm, d_{50} = 7.9mm, s = 2.65
K : D = 76.7mm, d_{50} = 0.57mm, s = 2.65

Test Series	y/D	V (m/s)	Measured C_v (ppm)	G_s	Ω	Predicted $\hat{C}_v$ (ppm)
H	1.0	0.429	4.7	0.2669	0.755	6.0
	1.0	0.451	5.7	0.2803	0.791	7.7
	1.0	0.481	7.8	0.2985	0.896	10.6
	1.0	0.506	10.0	0.3137	0.990	13.6
	1.0	0.565	16.8	0.3495	1.202	23.0
	1.0	0.598	32.1	0.3695	1.944	29.9
	1.0	0.625	36.6	0.3859	1.945	36.6
	1.0	0.658	38.3	0.4060	1.749	46.2
	1.0	0.695	47.1	0.4284	1.830	59.0
	1.0	0.785	77.2	0.4830	2.093	101
	1.0	0.892	177	0.5480	3.287	177
	1.0	0.997	250	0.6117	3.338	255
	1.0	1.090	352	0.6681	3.607	342
	1.0	1.198	353	0.7336	2.732	468
H	0.738	0.509	12.9	0.2888	1.295	11.4
	0.752	0.598	28.8	0.3394	1.817	24.7
	0.743	0.706	39.4	0.3987	1.513	53.4
	0.742	0.809	77.1	0.4560	1.977	98.3
	0.777	0.869	113	0.4933	2.399	133

Table 8 Continued

Test Series	y/D	V (m/s)	Measured C_v (ppm)	G_s	Ω	Predicted $\hat{C}_v$ (ppm)
H	0.500	0.513	11.2	0.2767	0.807	14.5
	0.500	0.569	35.0	0.3063	1.860	24.2
	0.501	0.609	44.2	0.3275	1.926	33.5
	0.501	0.629	53.7	0.3382	2.127	39.1
	0.504	0.656	75.8	0.3526	2.667	47.4
H	0.384	0.484	53.9	0.2552	3.505	13.3
	0.395	0.558	75.4	0.2940	3.330	26.8
	0.373	0.705	86.9	0.3683	1.807	86.5
	0.374	0.803	130	0.4188	1.846	156
	0.370	0.916	148	0.4765	1.406	283
	0.372	1.011	397	0.5256	2.831	434
	0.383	1.069	507	0.5567	3.164	531
I	1.0	0.777	144	0.2355	1.235	82.0
	1.0	0.888	207	0.2691	1.190	170
	1.0	0.997	478	0.3020	1.943	308
	1.0	1.082	687	0.3277	2.185	460
	1.0	1.186	918	0.3592	2.218	713
J	1.0	0.777	132	0.2169	0.911	80.0
	1.0	0.888	214	0.2479	0.990	174
	1.0	0.997	413	0.2783	1.350	323
	1.0	1.082	522	0.3020	1.335	489
	1.0	1.186	612	0.3310	1.189	767

Table 8 Continued

Test Series	y/D	V (m/s)	Measured C_v (ppm)	G_s	Ω	Predicted $\hat{C}_v$ (ppm)
K	1.0	0.484	58.5	0.3515	1.651	58.8
	1.0	0.599	170	0.4331	2.566	155
	1.0	0.695	346	0.5011	3.371	297
	1.0	0.803	509	0.5776	3.238	526
	1.0	0.901	740	0.6470	3.349	767
	1.0	1.013	1150	0.7264	3.679	1130
	1.0	1.096	1430	0.7851	3.622	1470
	1.0	1.211	2110	0.8666	3.975	2050

Table 9 Derived data for limit of deposition: concrete pipes

Test Conditions

L : D = 299mm, d_{50} = 0.72mm, s = 2.62
B : D = 450mm, d_{50} = 0.73mm, s = 2.63 (See also Table 2)

Test Series	y/D	V (m/s)	Measured C_v (ppm)	G_s	Ω	Predicted $\hat{C}_v$ (ppm)
L	1.0	0.893	29.9	0.4412	2.310	31.1
	1.0	1.006	45.5	0.4964	2.470	52.6
	1.0	0.800	14.5	0.3957	1.554	18.9
	1.0	0.698	7.6	0.3459	1.213	10.1
	1.0	0.500	0.67	0.2491	0.288	1.9
	1.0	0.603	4.1	0.2994	1.007	5.0
	1.0	1.196	69.7	0.5893	2.265	104
	1.0	1.099	55.3	0.5419	2.308	77.4
	1.0	0.549	2.1	0.2730	0.695	3.1
	1.0	1.386	98.7	0.6820	2.065	169
L	0.734	1.016	42.5	0.4594	2.293	47.3
	0.75	0.805	8.3	0.3662	0.899	16.4
	0.73	1.129	41.6	0.5095	1.632	75.5
	0.75	0.502	0.31	0.2300	0.136	1.5
	0.75	1.107	66.1	0.5019	2.795	68.6
	0.74	0.809	20.7	0.3672	2.202	16.8
	0.75	0.603	1.5	0.2754	0.396	4.0
L	0.511	0.972	70.1	0.4187	3.260	47.6
	0.504	0.896	22.2	0.3857	1.297	33.2
	0.490	1.021	32.7	0.4375	1.262	61.4
	0.499	0.702	6.7	0.3027	0.797	10.6
	0.494	0.812	27.5	0.3492	2.114	21.3

Table 9 Continued

Test Series	y/D	V (m/s)	Measured C_v (ppm)	G_s	Ω	Predicted $\hat{C}_v$ (ppm)
L (cont'd)	0.513	0.870	30.5	0.3754	1.976	28.7
	0.498	1.08	51.5	0.4753	1.585	87.1
	0.502	1.191	55.7	0.5111	1.394	119
	0.519	1.237	136	0.5323	3.123	137
	0.49	0.714	9.6	0.3073	1.068	11.6
	0.49	0.822	20.8	0.3531	1.526	22.8
	0.52	0.864	29.4	0.3734	1.972	27.4
	0.51	0.983	24.1	0.4233	1.081	50.2
	0.51	1.066	35.2	0.4587	1.241	72.2
	0.52	1.119	87.5	0.4824	2.721	88.1
	0.50	1.290	221	0.5529	4.335	168
	0.52	0.948	35.4	0.4093	1.802	42.0
	0.53	1.035	47.2	0.4474	1.885	61.4
	0.50	1.386	230	0.5937	3.656	212
	0.50	1.498	251	0.6414	3.161	275
	0.50	1.191	110	0.5108	2.739	119
	0.50	1.294	175	0.5547	3.397	170
	0.50	0.599	4.4	0.2590	0.848	4.6
	0.50	0.499	1.0	0.2164	0.328	1.7
	0.50	1.497	280	0.6409	3.531	274
	0.50	0.495	4.5	0.2147	1.509	1.6
L	0.38	0.801	19.5	0.3357	1.195	25.0
	0.38	1.100	98.0	0.4594	2.342	107
	0.37	0.598	8.0	0.2509	1.129	5.9
	0.38	0.597	2.5	0.2512	0.361	5.7
	0.38	1.396	443	0.5819	5.208	285

Table 9 Continued

Test Series	y/D	V (m/s)	Measured C_v (ppm)	G_s	Ω	Predicted $\hat{C}_v$ (ppm)
B	0.497	0.609	4.9	0.2467	1.943	2.0
	0.503	0.786	12.9	0.3177	2.432	7.3
	0.496	0.983	22.1	0.3957	2.118	21.1
	0.500	0.510	3.6	0.2138	2.423	0.8
	0.497	0.709	7.1	0.2866	1.796	4.4
	0.498	0.808	7.8	0.3261	1.342	8.4
	0.495	0.912	11.4	0.3672	1.375	14.8
	0.500	0.986	18.3	0.3974	1.751	21.3
	0.509	1.069	20.5	0.4313	1.568	30.3
	0.498	0.705	4.7	0.2851	1.211	4.3
	0.500	0.504	1.6	0.2049	1.115	0.6
	0.497	0.600	5.3	0.2431	2.195	1.8
	0.494	1.216	37.7	0.4885	1.913	55.0
	0.497	0.754	12.8	0.3045	2.700	6.0
	0.500	0.853	18.8	0.3442	2.766	10.9
	0.499	0.553	3.3	0.2245	1.746	1.2
	0.495	0.652	5.1	0.2637	1.647	2.9
	0.499	0.843	13.9	0.3401	2.113	10.3
B	0.747	0.502	2.3	0.2158	2.200	0.6
	0.749	0.701	7.4	0.3000	2.644	3.5
	0.750	0.790	11.5	0.3376	2.885	6.2
	0.747	0.904	17.9	0.3854	3.005	11.5
	0.750	0.600	3.6	0.2573	2.039	1.6
	0.749	0.753	7.2	0.3219	2.081	4.9
	0.746	0.662	5.0	0.2834	2.111	2.6
	0.744	0.857	14.0	0.3654	2.749	9.0
	0.745	0.706	6.8	0.3018	2.372	3.6

Table 10 Derived data for resistance with continuous bed

Test No	Derived friction coefficients				Predicted friction coefficients	
	λ_o	λ_g	λ_b	k_b (mm)	$\hat{\lambda}_b$	$\hat{\lambda}_c$
D.1	0.0204	0.0286	0.0215	0.21	0.0862	0.0613
D.2	0.0191	0.0266	0.0281	1.13	0.0910	0.0602
D.3	0.0182	0.0246	0.0741	23.9	0.0753	0.0429
D.4	0.0193	0.0267	0.0777	19.2	0.0912	0.0598
D.5	0.0187	0.0258	0.0848	25.9	0.0941	0.0580
D.6	0.0178	0.0243	0.1204	60.6	0.1024	0.0551
D.7	0.0197	0.0265	0.2542	131	0.0265	0.0234
D.8	0.0183	0.0252	0.1634	85.9	0.0952	0.0565
D.9	0.0192	0.0269	0.1237	43.8	0.0870	0.0585
D.10	0.0182	0.0261	0.0257	0.86	0.0560	0.0398
D.11	0.0186	0.0268	0.0285	1.15	0.0487	0.0369
D.12	0.0187	0.0263	0.0574	10.2	0.0832	0.0561
D.13	0.0190	0.0263	0.0932	28.9	0.0932	0.0625
D.14	0.0179	0.0258	0.0131	-0.05	0.0452	0.0333
D.15	0.0177	0.0258	-0.0002	-ve	0.0357	0.0279
D.16	0.0175	0.0259	-0.0066	-ve	0.0259	0.0223
D.17	0.0175	0.0254	0.0170	0.11	0.0346	0.0269
D.18	0.0189	0.0263	0.0611	11.7	0.0897	0.0602
D.19	0.0184	0.0261	0.0647	13.6	0.0746	0.0509
D.20	0.0181	0.0260	0.0466	6.02	0.0508	0.0370
D.30	0.0195	0.0272	0.0421	4.02	0.0910	0.0647
D.31	0.0190	0.0264	0.0736	17.7	0.0917	0.0616
D.32	0.0181	0.0260	0.0195	0.23	0.0538	0.0388
D.33	0.0185	0.0259	0.0393	3.86	0.0873	0.0563
D.34	0.0182	0.0254	0.0699	18.0	0.0875	0.0533
D.35	0.0178	0.0254	0.0274	1.21	0.0589	0.0393
D.36	0.0174	0.0251	0.0089	-0.11	0.0403	0.0289

Table 10 Continued

Test No	Derived friction coefficients				Predicted friction coefficients	
	λ_o	λ_g	λ_b	k_b (mm)	$\hat{\lambda}_b$	$\hat{\lambda}_c$
D.40	0.0173	0.0250	0.0280	1.42	0.0422	0.0286
D.41	0.0175	0.0249	0.0412	4.99	0.0606	0.0372
D.42	0.0181	0.0252	0.1145	48.2	0.0818	0.0508
D.43	0.0170	0.0249	-	-	0.0249	0.0208
D.44	0.0174	0.0251	0.0644	15.0	0.0427	0.0306
D.45	0.0182	0.0259	0.0565	10.2	0.0695	0.0467
D.50	0.0179	0.0255	-0.0112	-ve	0.1859	0.0701
D.51	0.0180	0.0252	0.1880	100	0.1909	0.0680
D.52	0.0177	0.0251	0.1546	76.4	0.1815	0.0651
D.53	0.0175	0.0252	0.1081	41.9	0.1631	0.0615
D.54	0.0173	0.0249	0.2604	152	0.1577	0.0565
E.1	0.0190	0.0239	0.0833	23.1	0.0867	0.0580
E.2	0.0186	0.0236	0.0776	20.3	0.0720	0.0489
E.3	0.0182	0.0232	0.0778	21.3	0.0645	0.0434
E.4	0.0180	0.0231	0.0601	12.1	0.0526	0.0369
E.5	0.0178	0.0231	0.0399	4.03	0.0366	0.0283
E.6	0.0176	0.0230	0.0313	1.88	0.0291	0.0240
E.7	0.0175	0.0229	0.0197	0.29	0.0251	0.0216
E.8	0.0173	0.0227	0.0207	0.38	0.0230	0.0203
E.10	0.0184	0.0229	0.1188	51.8	0.1740	0.0612
E.11	0.0180	0.0228	0.1543	77.6	0.1671	0.0596
E.12	0.0177	0.0226	0.1473	72.8	0.1538	0.0552

Table 10 Continued

Test No	Derived friction coefficients				Predicted friction coefficients	
	λ_o	λ_g	λ_b	k_b (mm)	$\hat{\lambda}_b$	$\hat{\lambda}_c$
F.1	0.0185	0.0250	0.0814	22.5	0.0755	0.0510
F.2	0.0189	0.0252	0.0795	21.2	0.0894	0.0592
F.3	0.0194	0.0254	0.0984	32.0	0.0894	0.0596
F.4	0.0183	0.0249	0.0680	15.3	0.0613	0.0428
F.5	0.0181	0.0247	0.0736	18.5	0.0546	0.0383
F.6	0.0176	0.0245	0.0523	8.50	0.0337	0.0264
F.10	0.0186	0.0252	0.0528	8.16	0.0700	0.0485
F.11	0.0181	0.0247	0.0706	16.9	0.0543	0.0382
F.12	0.0180	0.0246	0.0700	16.9	0.0586	0.0404
F.13	0.0183	0.0250	0.0610	11.8	0.0618	0.0433
F.20	0.0183	0.0235	0.0788	28.6	0.0235	0.0205
F.21	0.0175	0.0231	0.1234	64.6	0.1031	0.0542
F.22	0.0179	0.0233	0.0882	35.7	0.1023	0.0535
F.30	0.0175	0.0231	0.1343	74.7	0.1065	0.0548
G.1	0.0184	0.0244	0.1017	36.5	0.0834	0.0530
G.2	0.0190	0.0250	0.0495	7.07	0.0927	0.0609
G.3	0.0182	0.0245	0.0741	18.8	0.0631	0.0430
G.4	0.0180	0.0243	0.0692	16.5	0.0542	0.0379

Table 11 Derived data for transport with continuous bed

Test No	F_s	η	Measured C_v (ppm)	Predicted $\hat{C}_v$ (ppm)	
				Ackers	HR
D.1	0.237	0.689	276	122	140
D.2	0.246	0.433	133	115	126
D.3	0.191	0.368	38	16.0	15.0
D.4	0.233	0.788	217	88.0	87.4
D.5	0.243	0.695	171	94.1	96.3
D.6	0.241	0.454	75	67.9	62.5
D.7	0.135	3.416	281	-ve	4.6
D.8	0.233	0.528	104	68.8	62.5
D.9	0.270	0.769	303	182	209
D.10	0.385	1.499	(1100)	601	667
D.11	0.395	1.154	1044	727	846
D.12	0.295	0.801	351	248	277
D.13	0.248	0.179	55.2	119	130
D.14	0.435	1.053	941	832	849
D.15	0.481	0.834	923	1110	1050
D.16	0.671	0.568	1280	2820	2140
D.17	0.499	0.856	947	1160	1050
D.18	0.268	0.740	270	171	191
D.19	0.326	0.978	512	351	386
D.20	0.408	0.971	800	716	783

Table 11 Continued

Test No	F_s	η	Measured C_v (ppm)	Predicted $\hat{C}_v$ (ppm)	
				Ackers	HR
D.30	0.248	0.132	49.3	138	157
D.31	0.258	1.300	440	144	161
D.32	0.396	1.008	788	660	733
D.33	0.283	0.315	114	194	212
D.34	0.289	0.776	252	188	198
D.35	0.387	0.667	413	533	566
D.36	0.473	0.951	823	907	822
D.40	0.461	1.082	780	847	685
D.41	0.386	0.408	205	453	458
D.42	0.286	0.745	212	164	170
D.43	0.590	1.020	1290	1550	1200
D.44	0.468	0.892	783	905	834
D.45	0.343	0.929	507	398	432
D.50	0.371	0.226	76.5	367	295
D.51	0.325	1.389	322	210	170
D.52	0.380	0.938	297	359	284
D.53	0.462	0.755	378	697	476
D.54	0.475	1.300	606	678	443

Table 11 Continued

Test No	F_s	η	Measured C_v (ppm)	Predicted $\hat{C}_v$ (ppm)	
				Ackers	HR
E.1	0.256	0.091	19.2	187	98.1
E.2	0.307	0.350	103	338	199
E.3	0.338	0.647	211	426	253
E.4	0.387	0.831	355	631	391
E.5	0.453	0.908	554	996	580
E.6	0.504	0.855	638	1304	709
E.7	0.551	0.922	798	1604	822
E.8	0.589	0.851	798	1834	891
E.10	0.245	0.147	11.5	91.1	31.6
E.11	0.313	0.322	42.2	222	91.2
E.12	0.374	0.618	113	377	161
F.1	0.316	0.941	378	327	283
F.2	0.264	0.714	203	172	143
F.3	0.202	0.885	148	48.6	27.3
F.4	0.363	0.824	438	511	451
F.5	0.390	0.952	561	616	544
F.6	0.490	0.718	649	1130	859

Table 11 Continued

Test No	F_s	η	Measured C_v (ppm)	Predicted $\hat{C}_v$ (ppm)	
				Ackers	HR
F.10	0.329	0.612	283	392	346
F.11	0.390	0.717	424	617	546
F.12	0.377	0.862	463	546	477
F.13	0.359	0.581	311	505	448
F.20	0.136	0.087	3.5	0.09	2.3
F.21	0.279	0.771	136	139	100
F.22	0.210	0.297	28.9	38.7	17.1
F.30	0.267	0.614	96.1	115	81.1
G.1	0.289	1.611	454	224	172
G.2	0.244	0.226	51.8	129	91.1
G.3	0.355	0.925	425	467	380
G.4	0.392	0.773	425	619	510

Table 12 Derived data for transport with separated dunes

Test No	Measured		Predicted - Method A		Predicted - Method B	
	λ_c	C_v (ppm)	$\hat{\lambda}_c$	$\hat{C}_v$ (ppm)	$\hat{\lambda}_c$	$\hat{C}_v$ (ppm)
C.1	0.0181	4.6	0.0218	18.1	0.0181	3.8
C.2	0.0176	13.2	0.0217	40.3	0.0183	12.5
C.3	0.0183	34.8	0.0216	92.7	0.0189	42.5
C.4	0.0210	6.3	00235	15.2	0.0191	5.2
C.5	0.0203	15.4	0.0233	42.2	0.0197	19.5
C.6	0.0197	3.6	0.0268	5.1	0.0222	2.8

Method A - calculated using equivalent continuous bed

Method B - calculated using average dune thickness and proportion of clear pipe

Figures

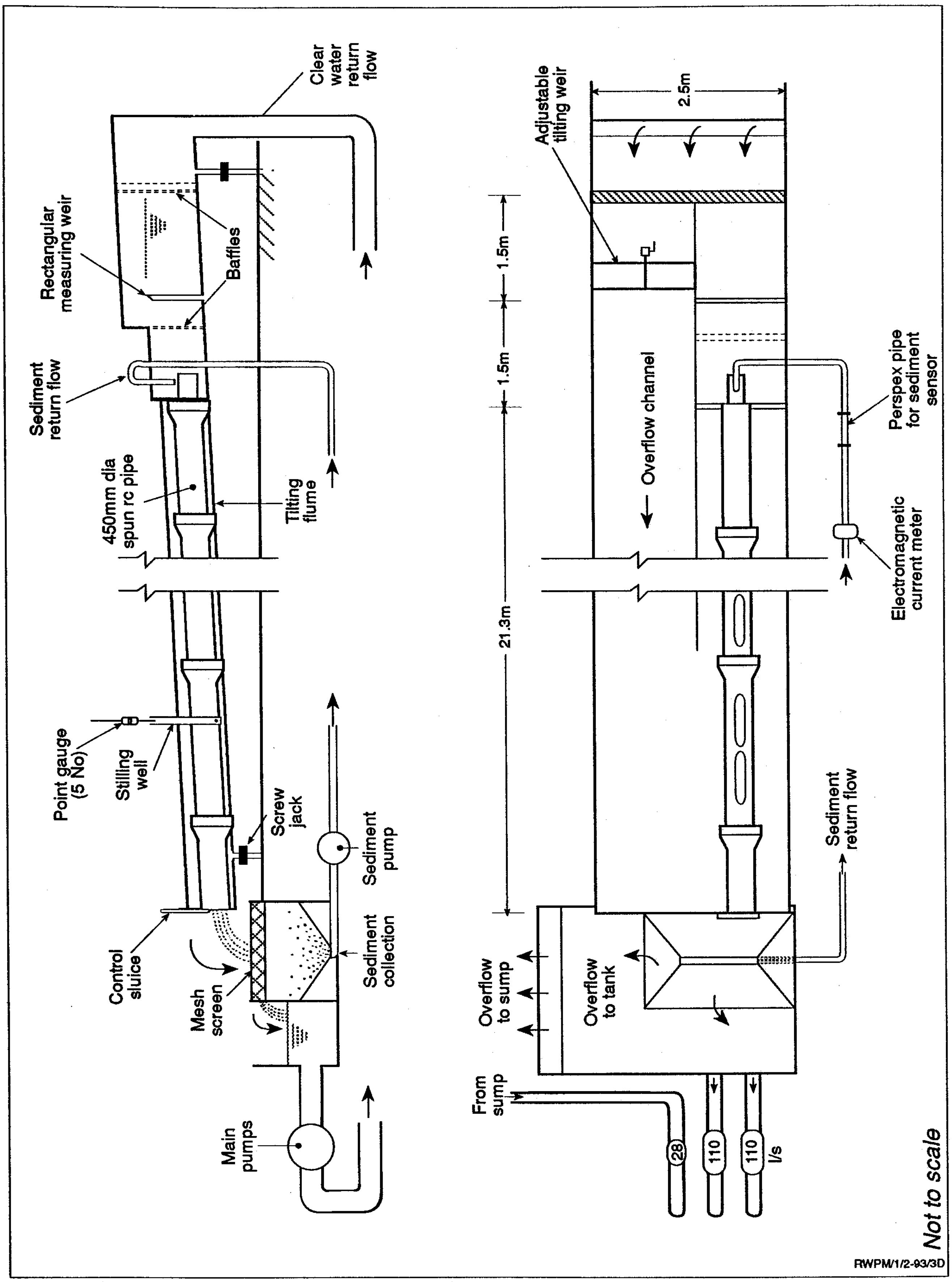

Figure 1 Layout of test rig

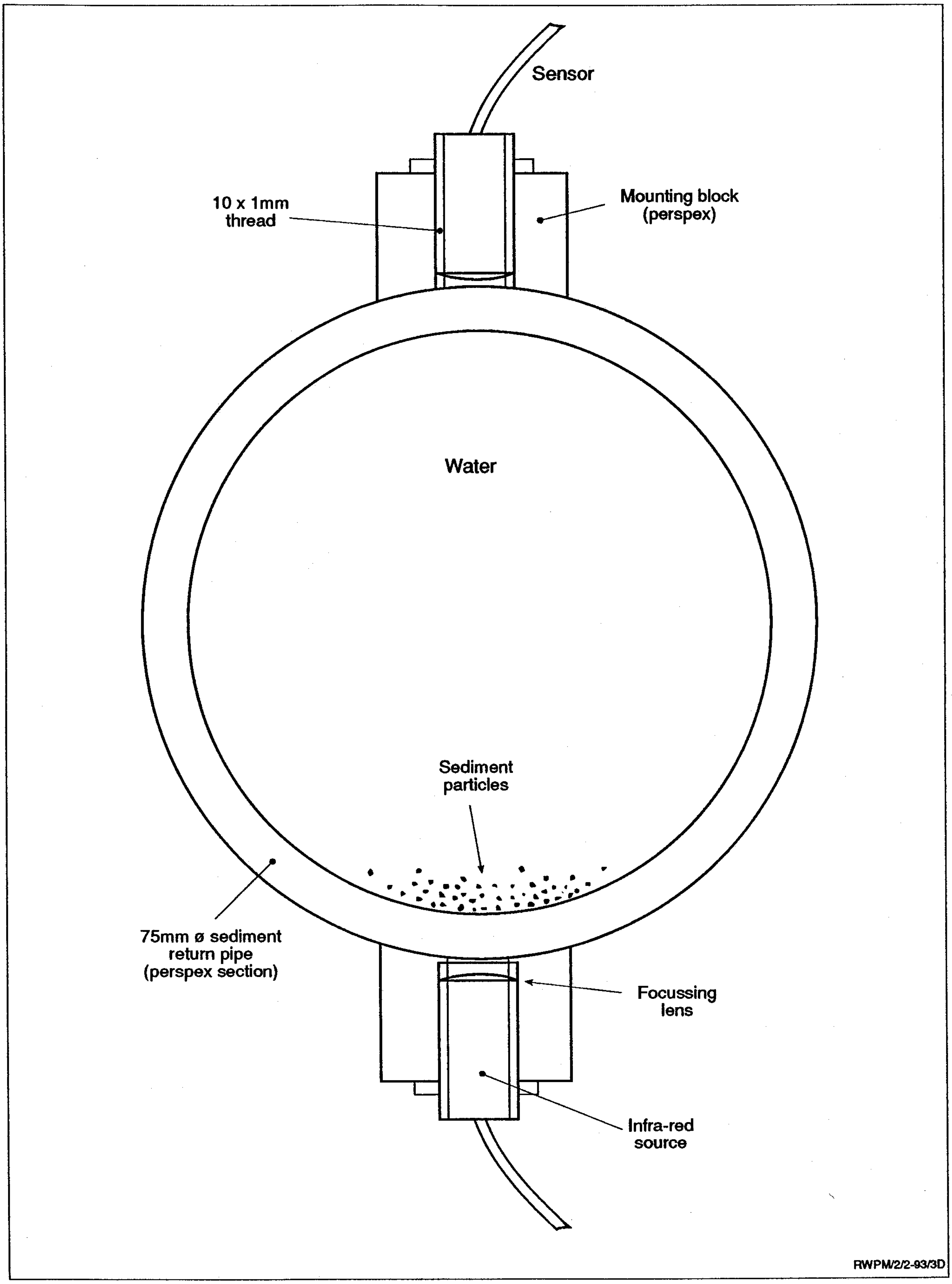

Figure 2 Cross-section through sediment sensor

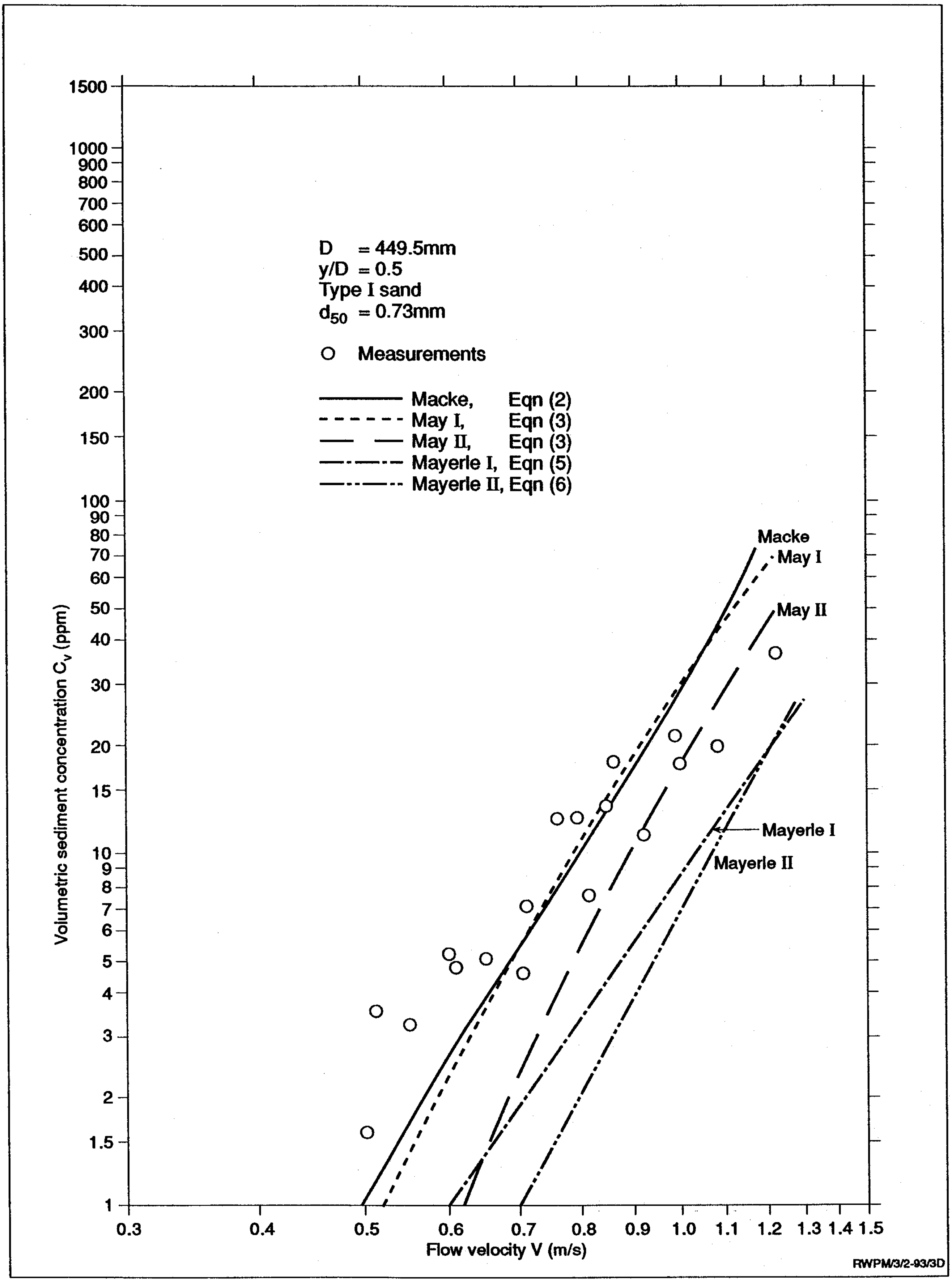

Figure 3 Data for limit of deposition (y/d = 0.5)

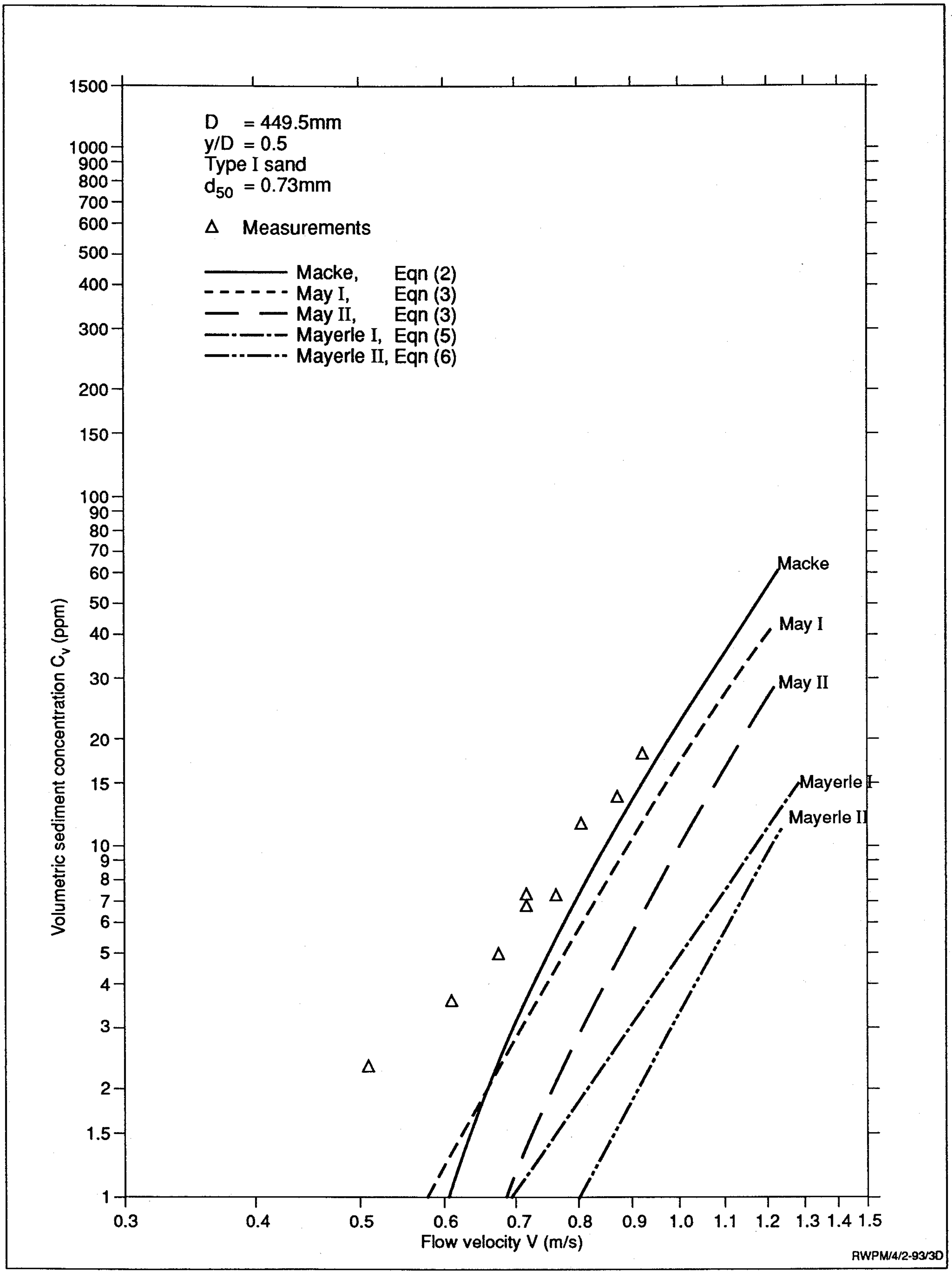

Figure 4 Data for limit of deposition (y/d = 0.75)

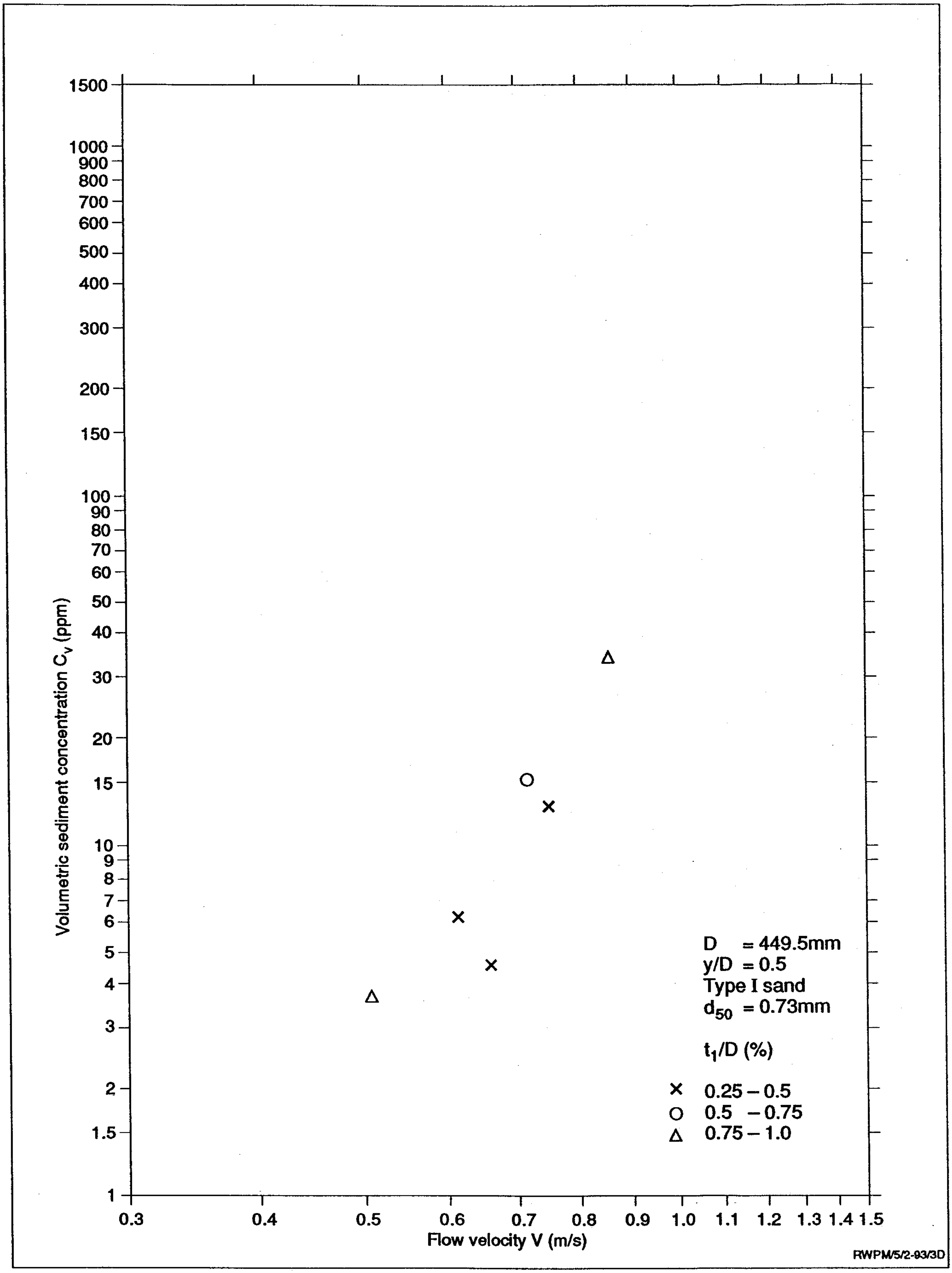

Figure 5 Data for separated dunes (y/d = 0.5)

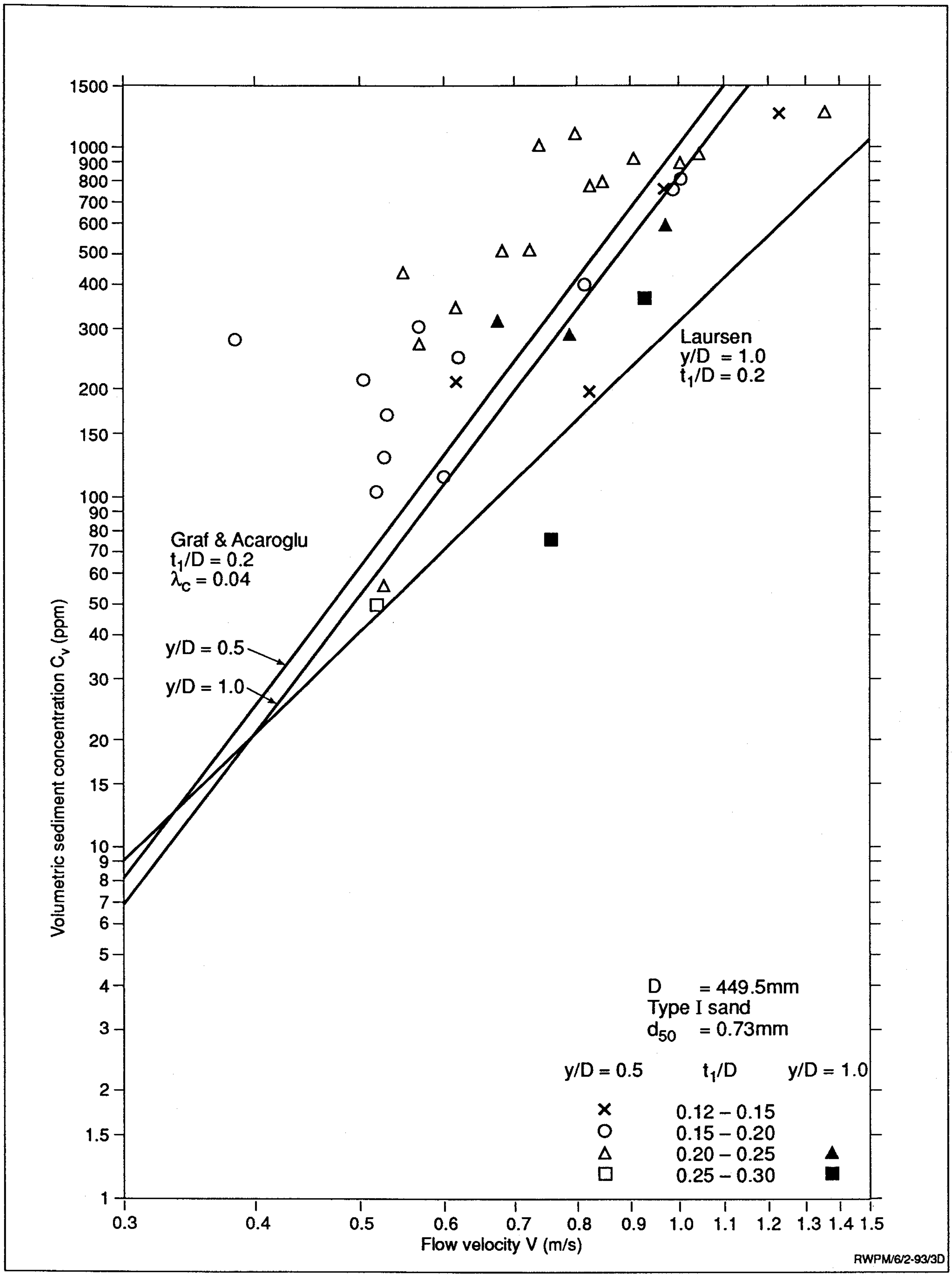

Figure 6 Data for transport with continuous bed (Type I sand)

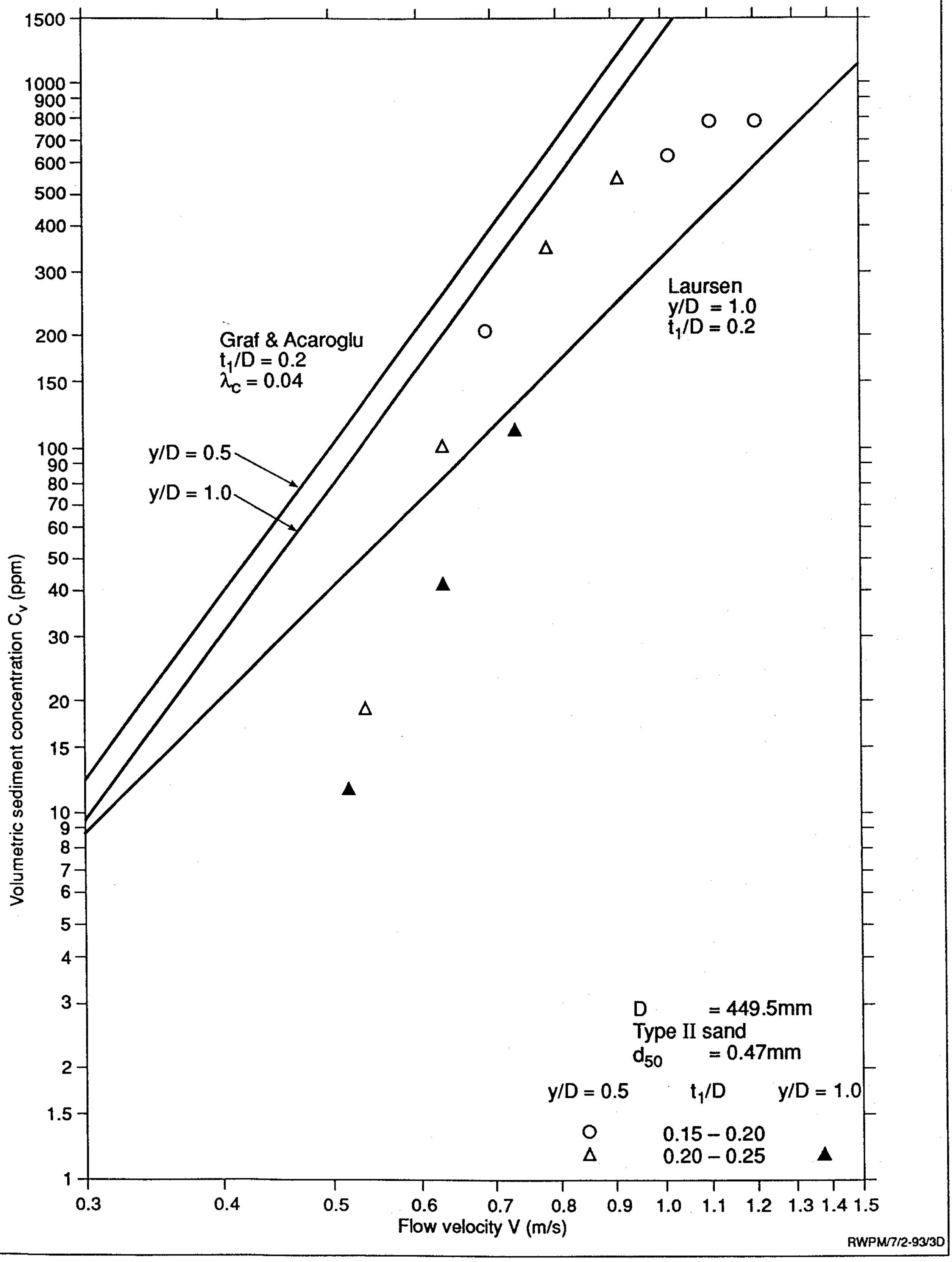

Figure 7 Data for transport with continuous bed (Type II sand)

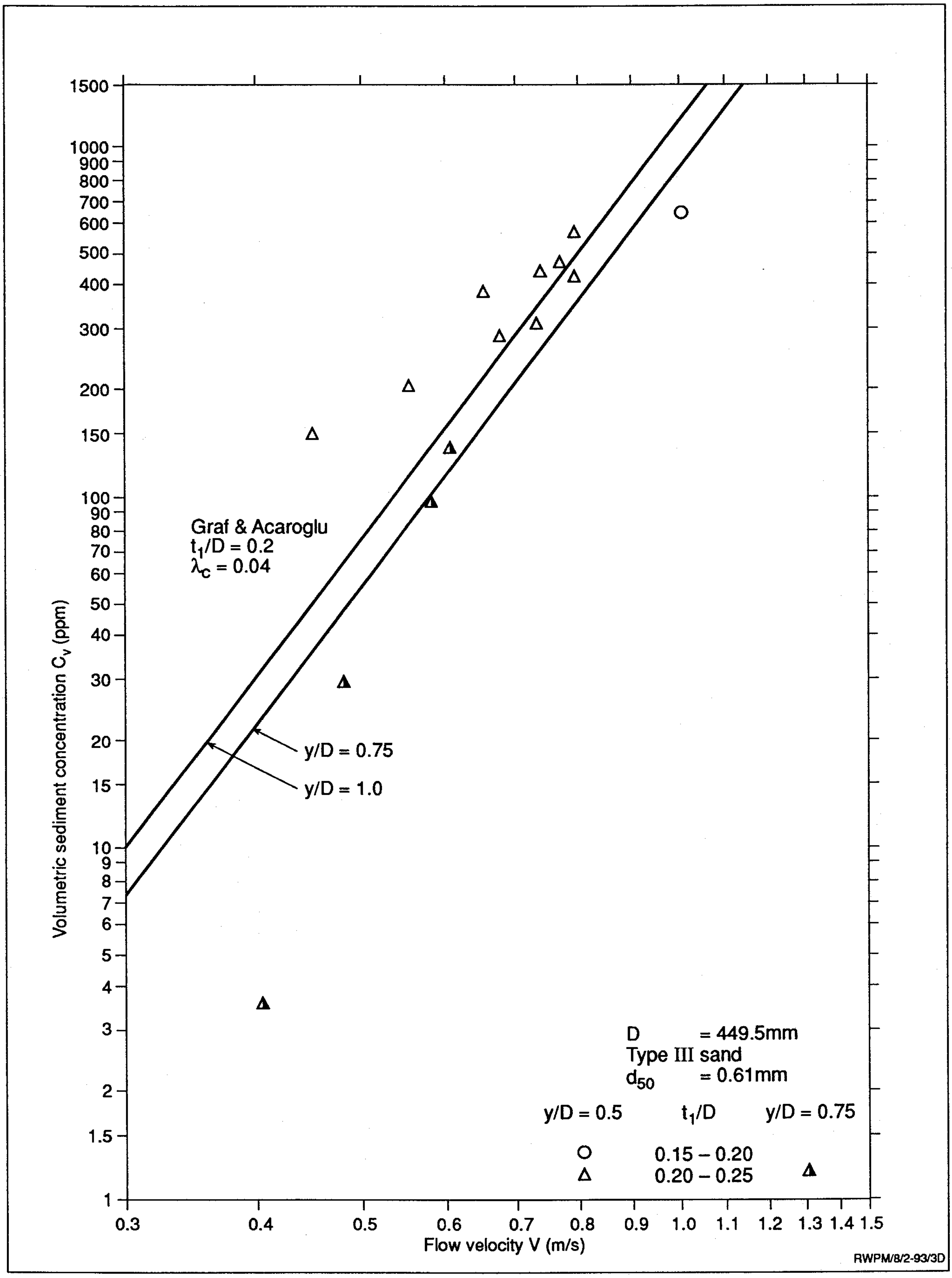

Figure 8 Data for transport with continuous bed (Type III sand)

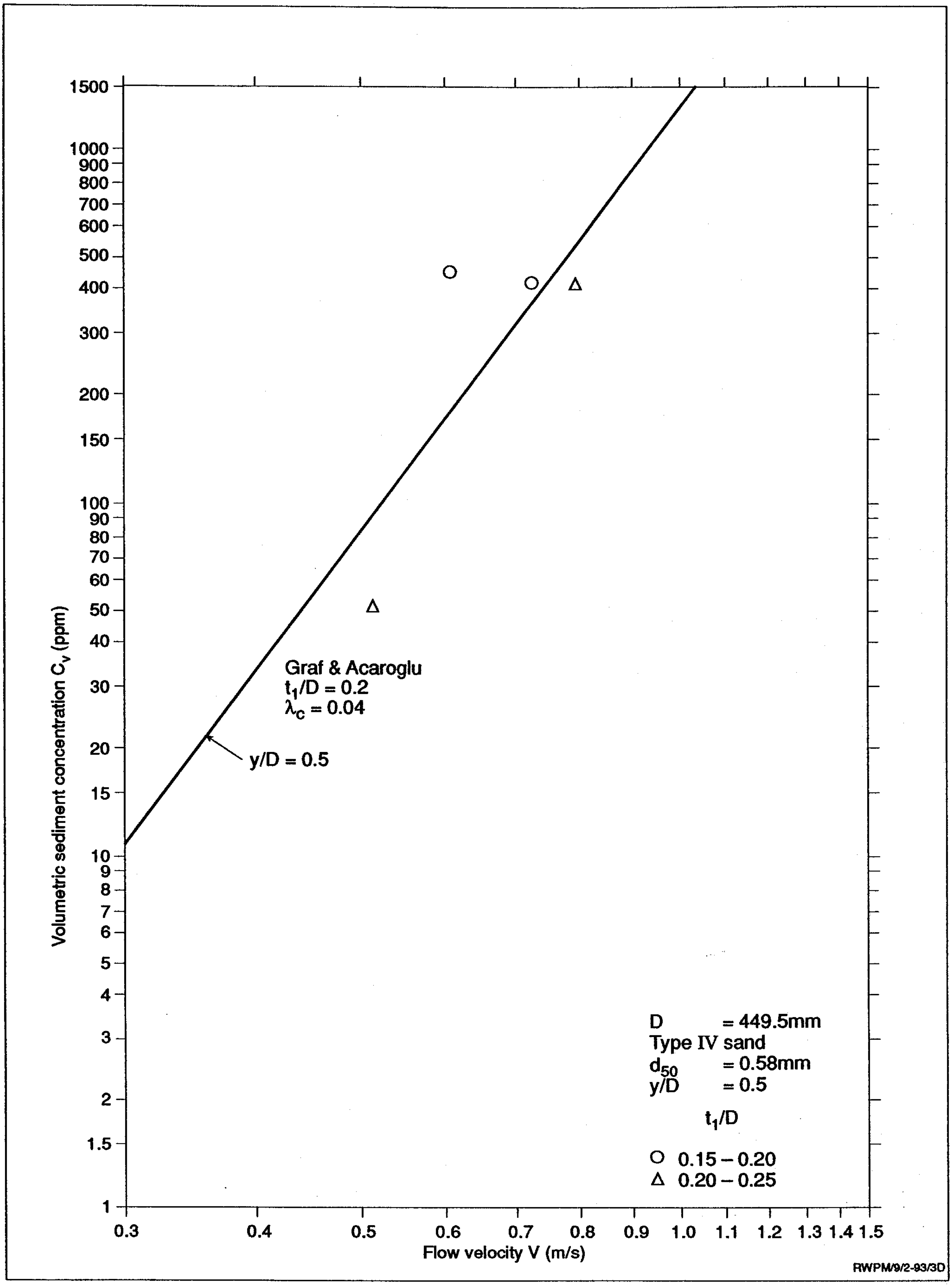

Figure 9 Data for transport with continuous bed (Type IV sand)

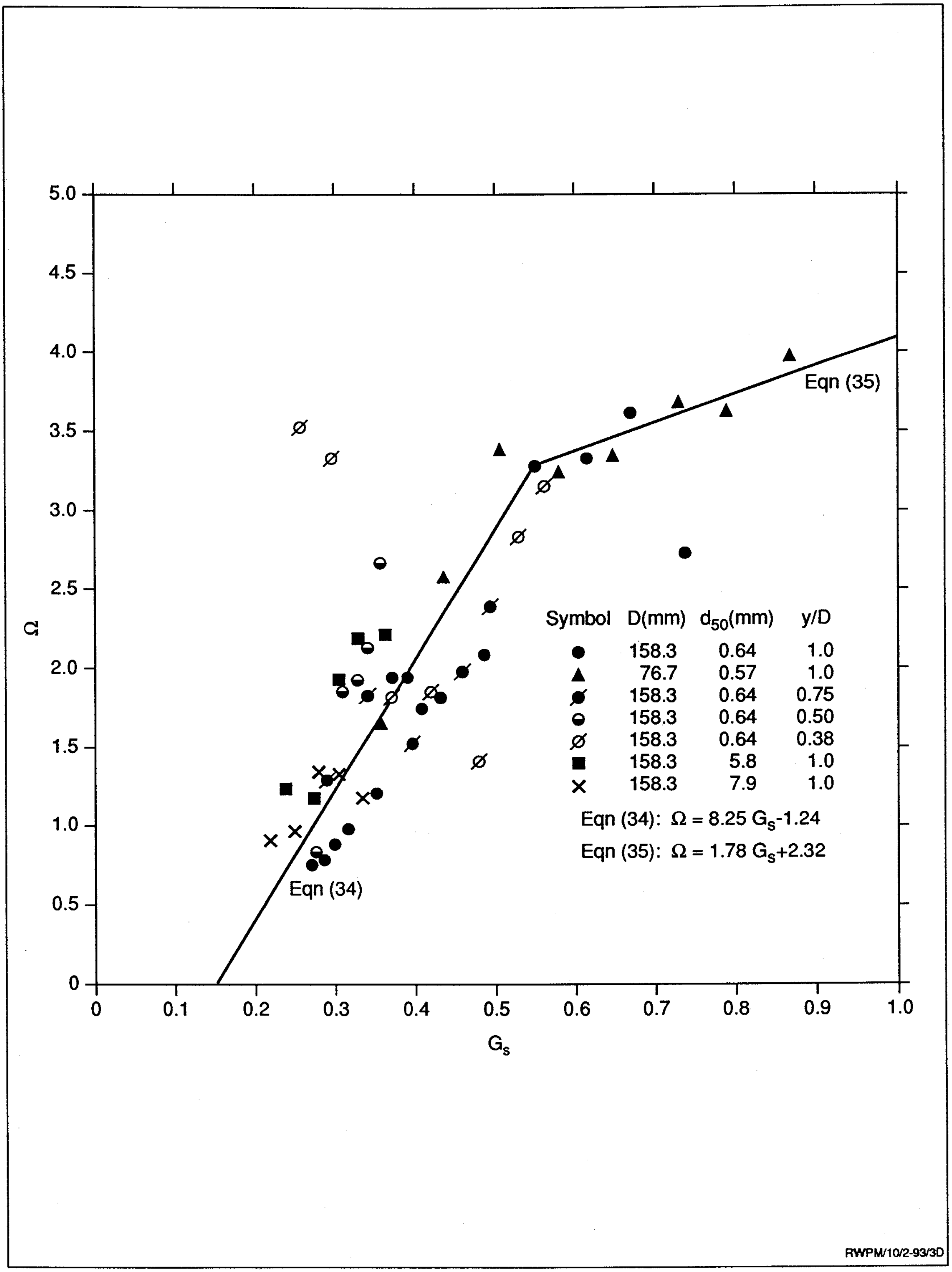

Figure 10 Ω versus G_s for limit of deposition: smooth pipes

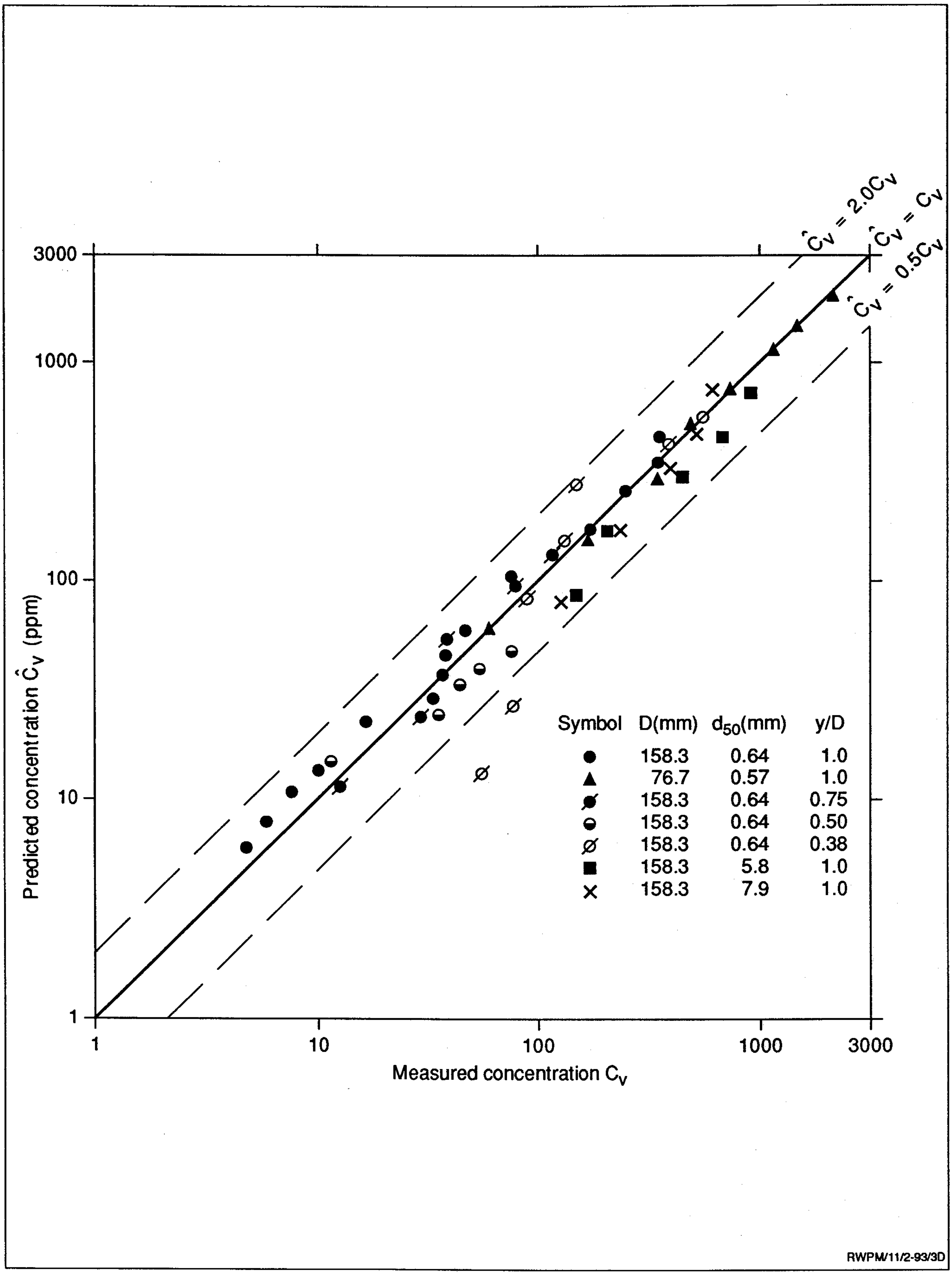

Figure 11 Predicted and measured sediment concentrations for limit of deposition: smooth pipes

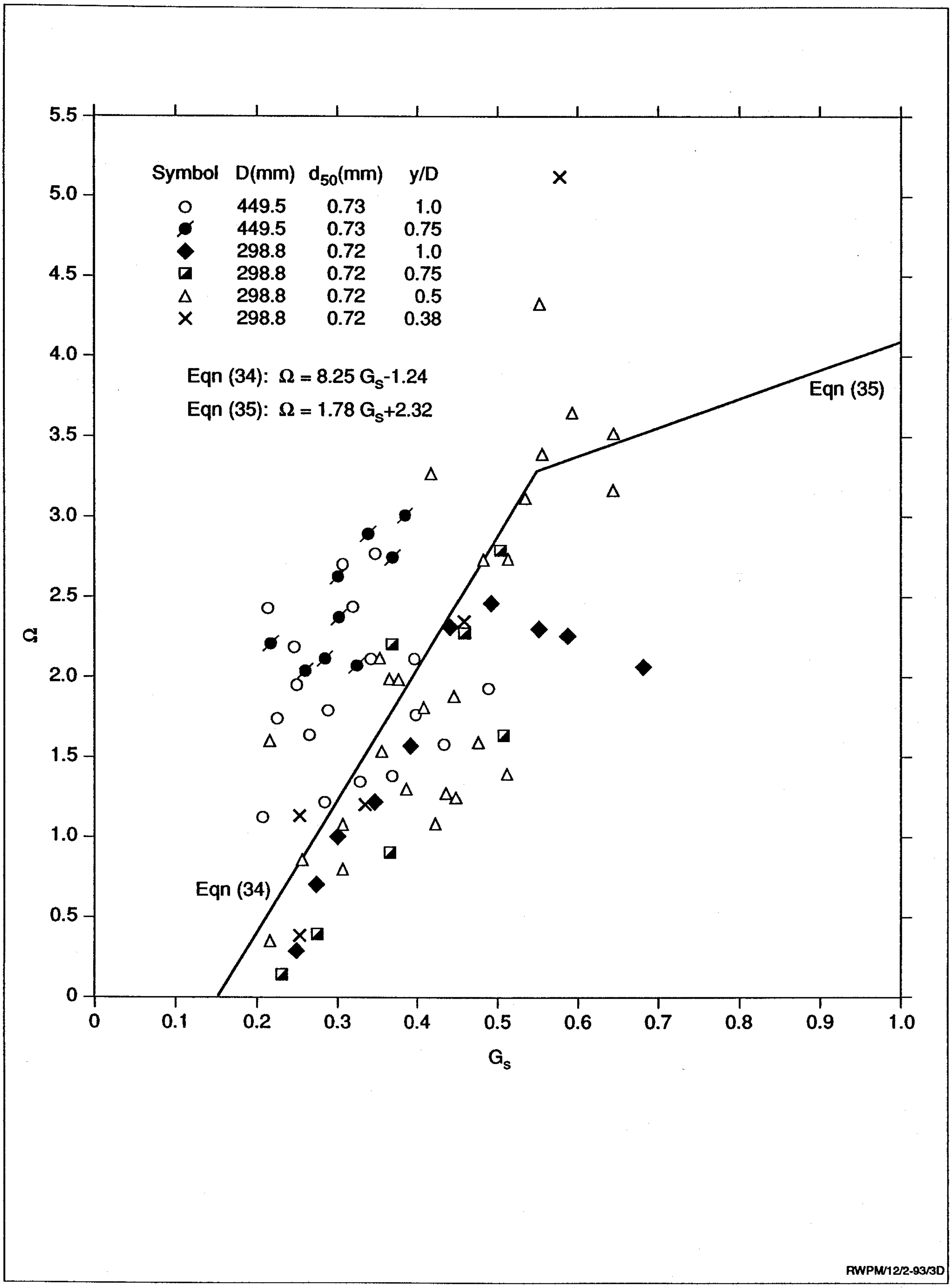

Figure 12 Ω versus G_s for limit of deposition: concrete pipes

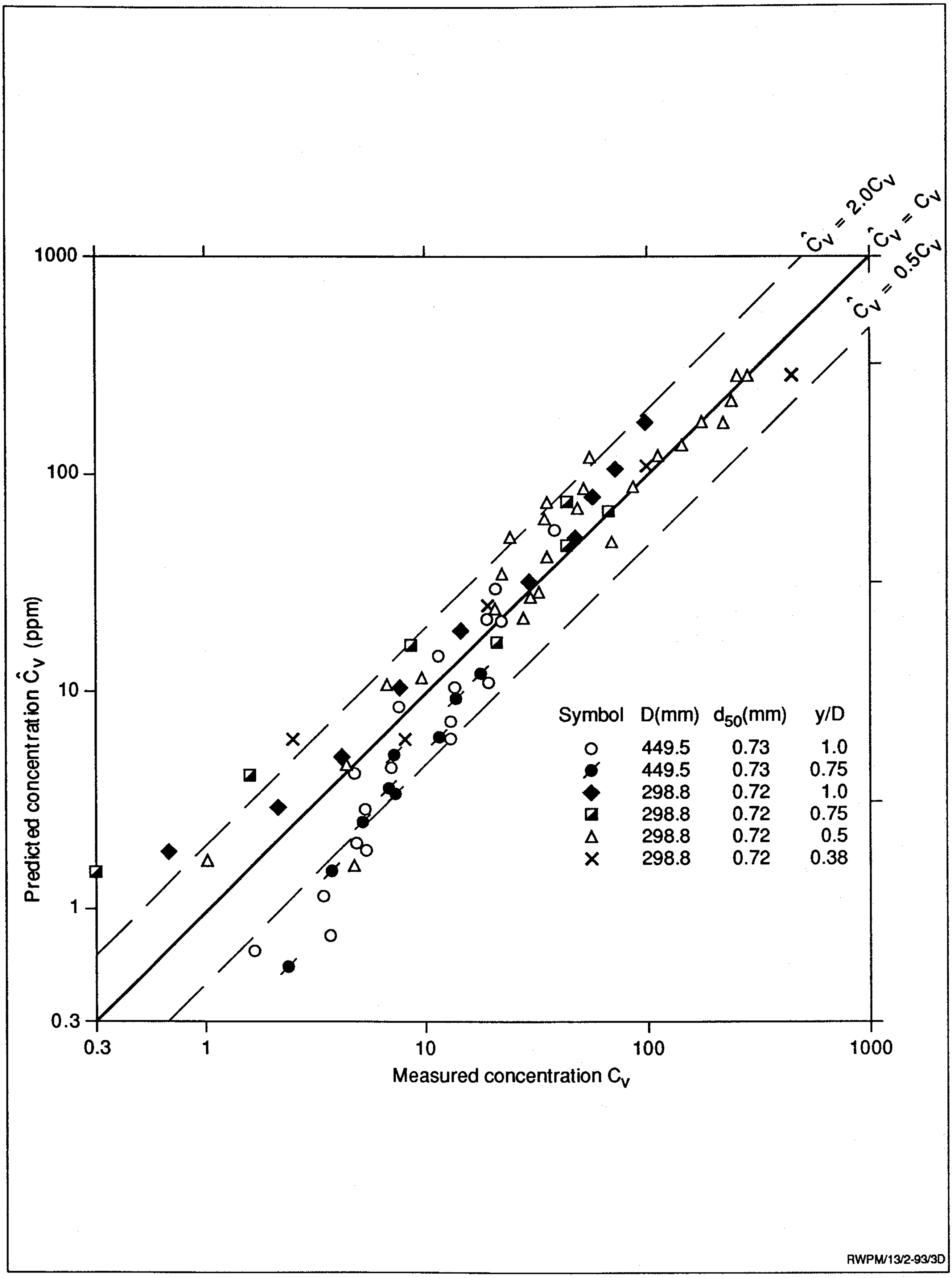

Figure 13 Predicted and measured sediment concentrations for limit of deposition: concrete pipes

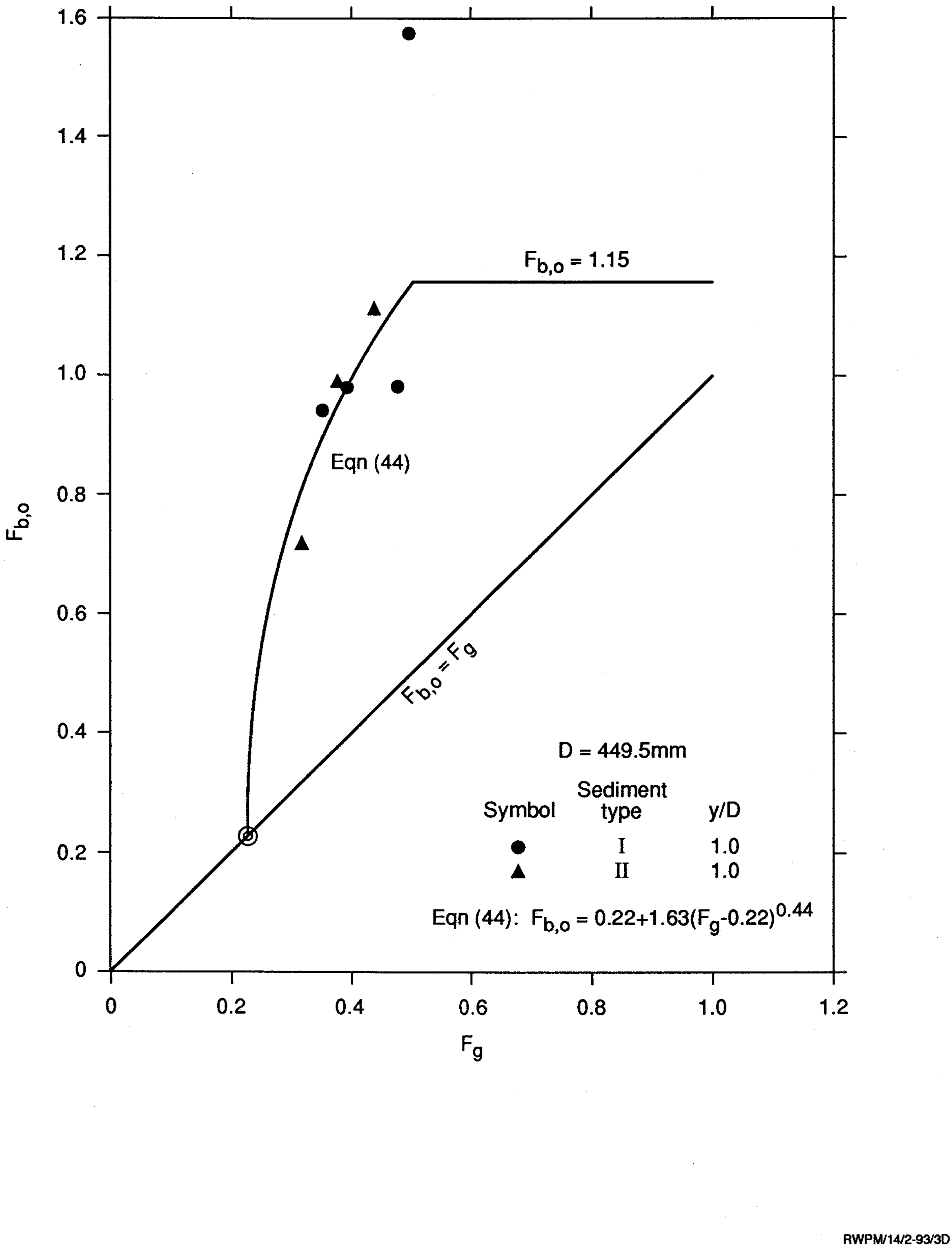

Figure 14 Resistance of sediment bed for pipe-full flow

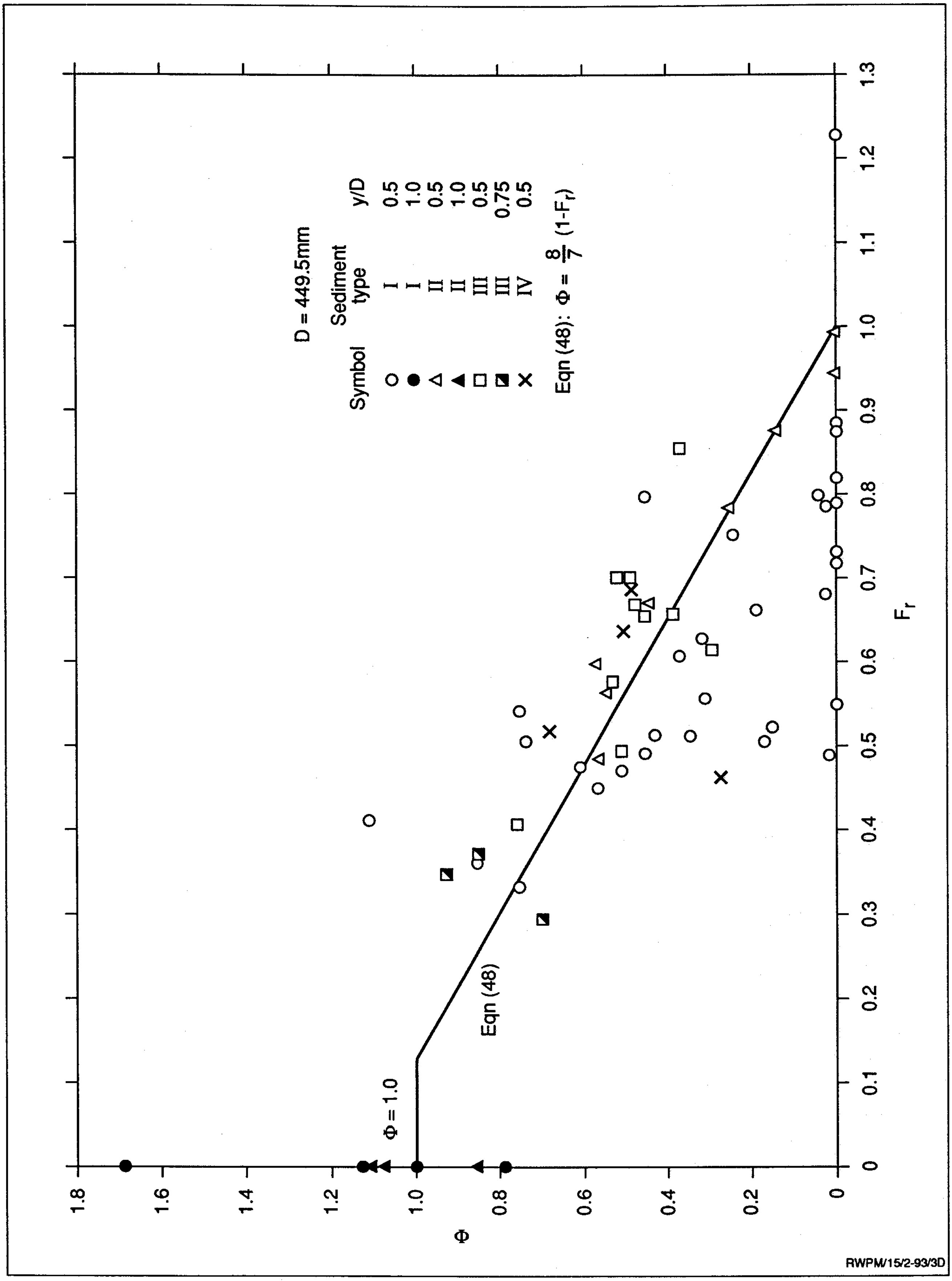

Figure 15 Effect of Froude number on resistance of sediment bed

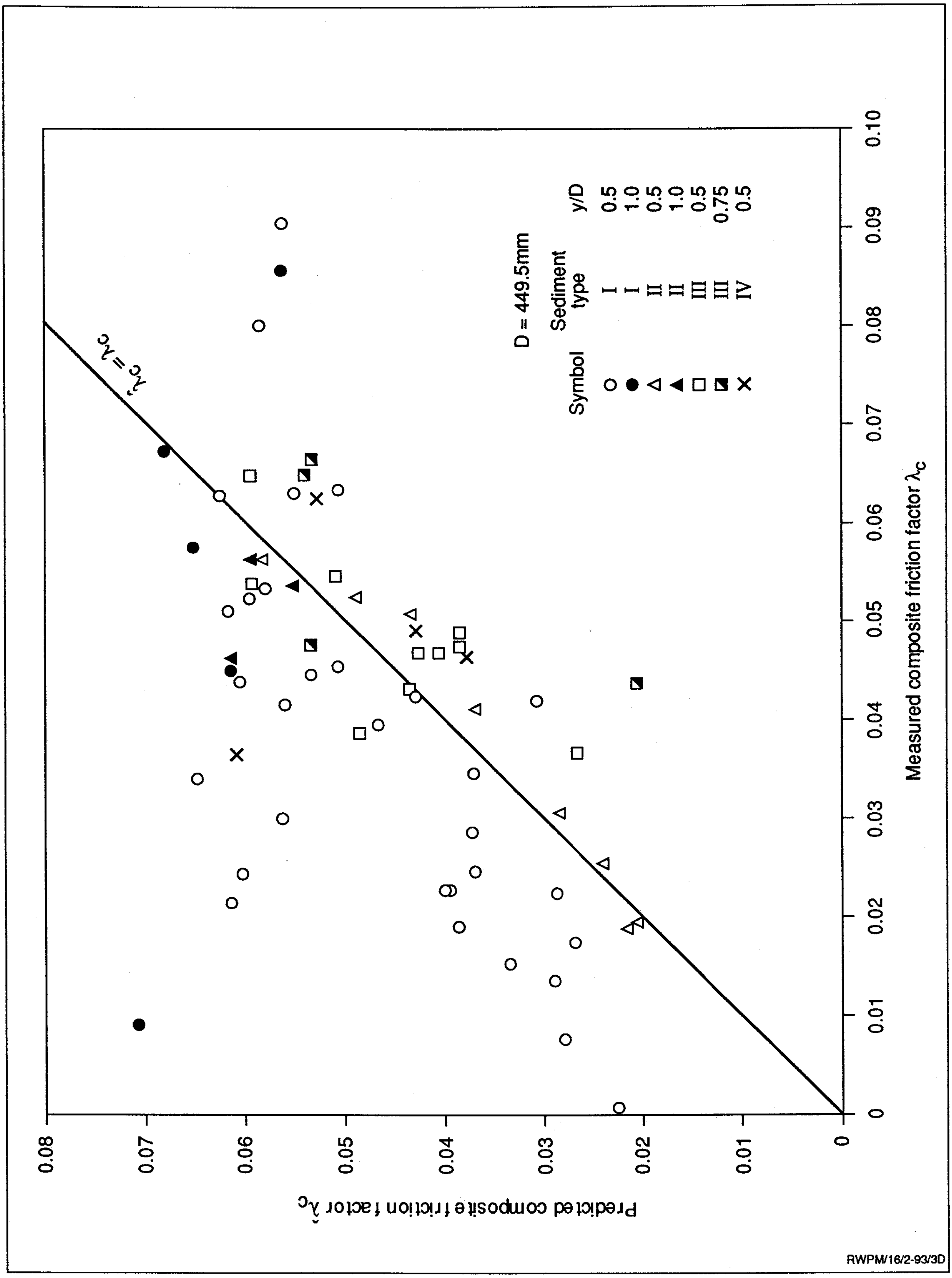

Figure 16 **Predicted and measured composite roughness with continuous bed**

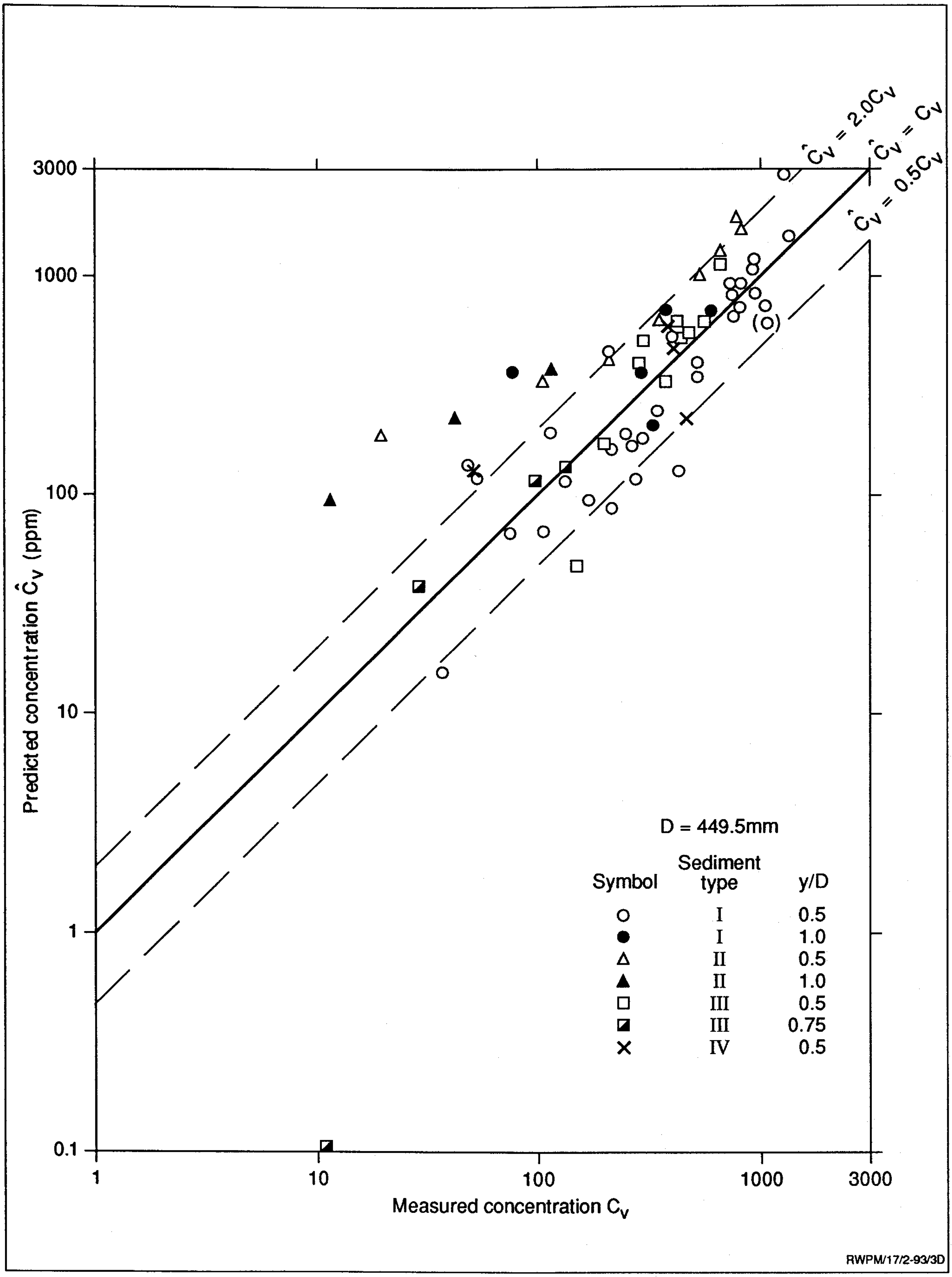

Figure 17 Predicted and measured sediment concentrations for transport with continuous bed: Ackers method

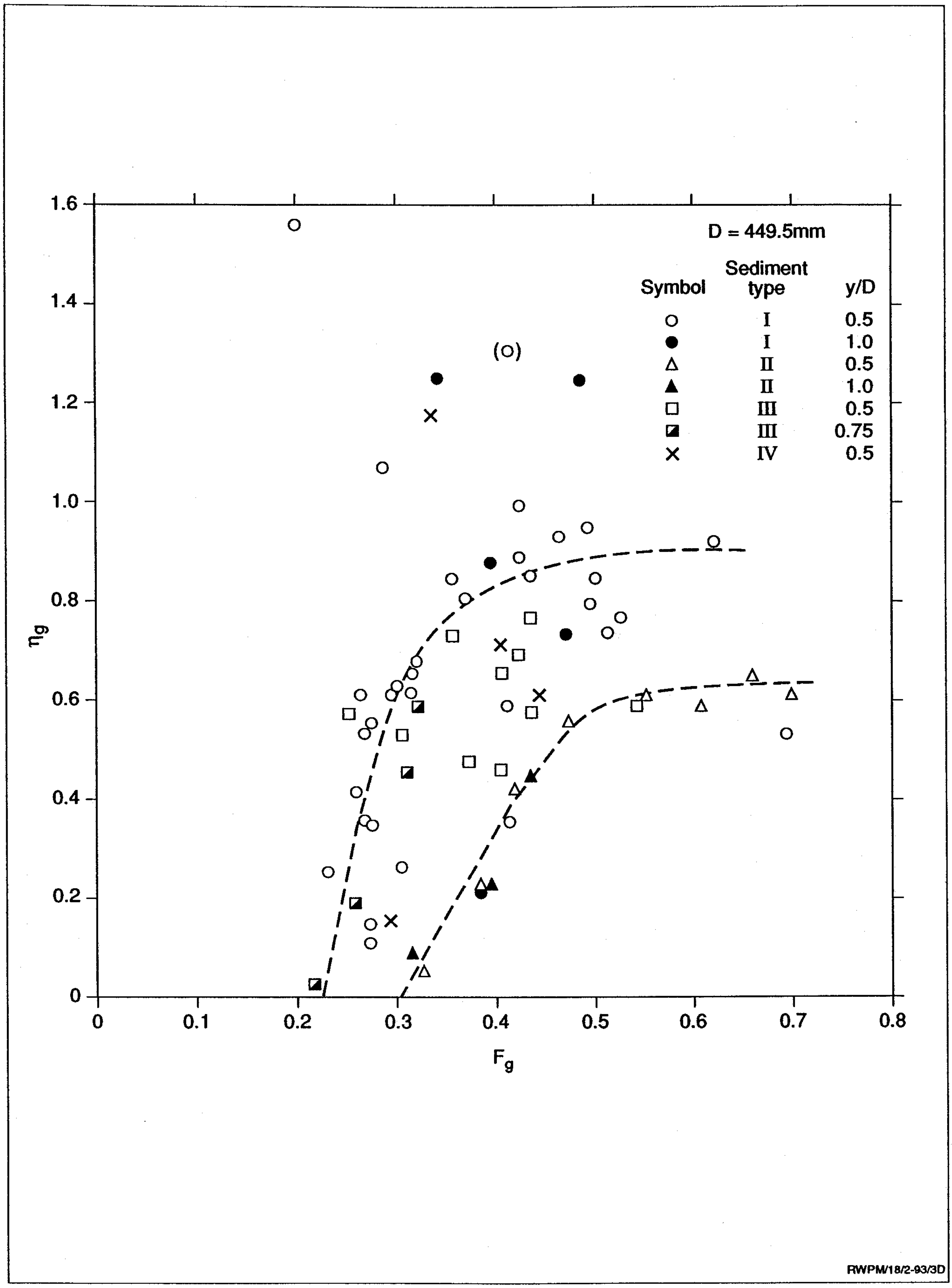

Figure 18 η_g versus F_g for transport with continuous bed

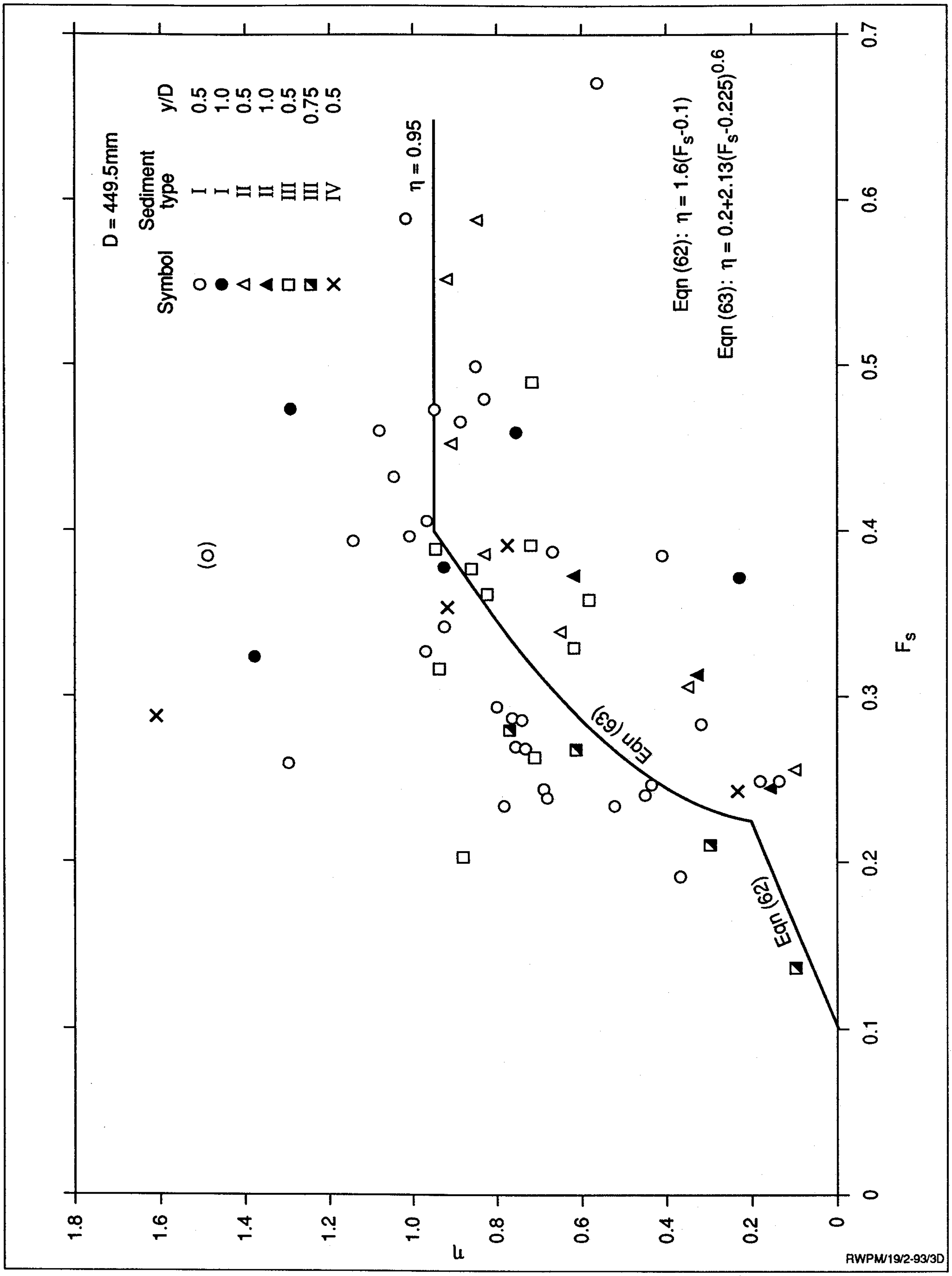

Figure 19 η versus F_s for transport with continuous bed

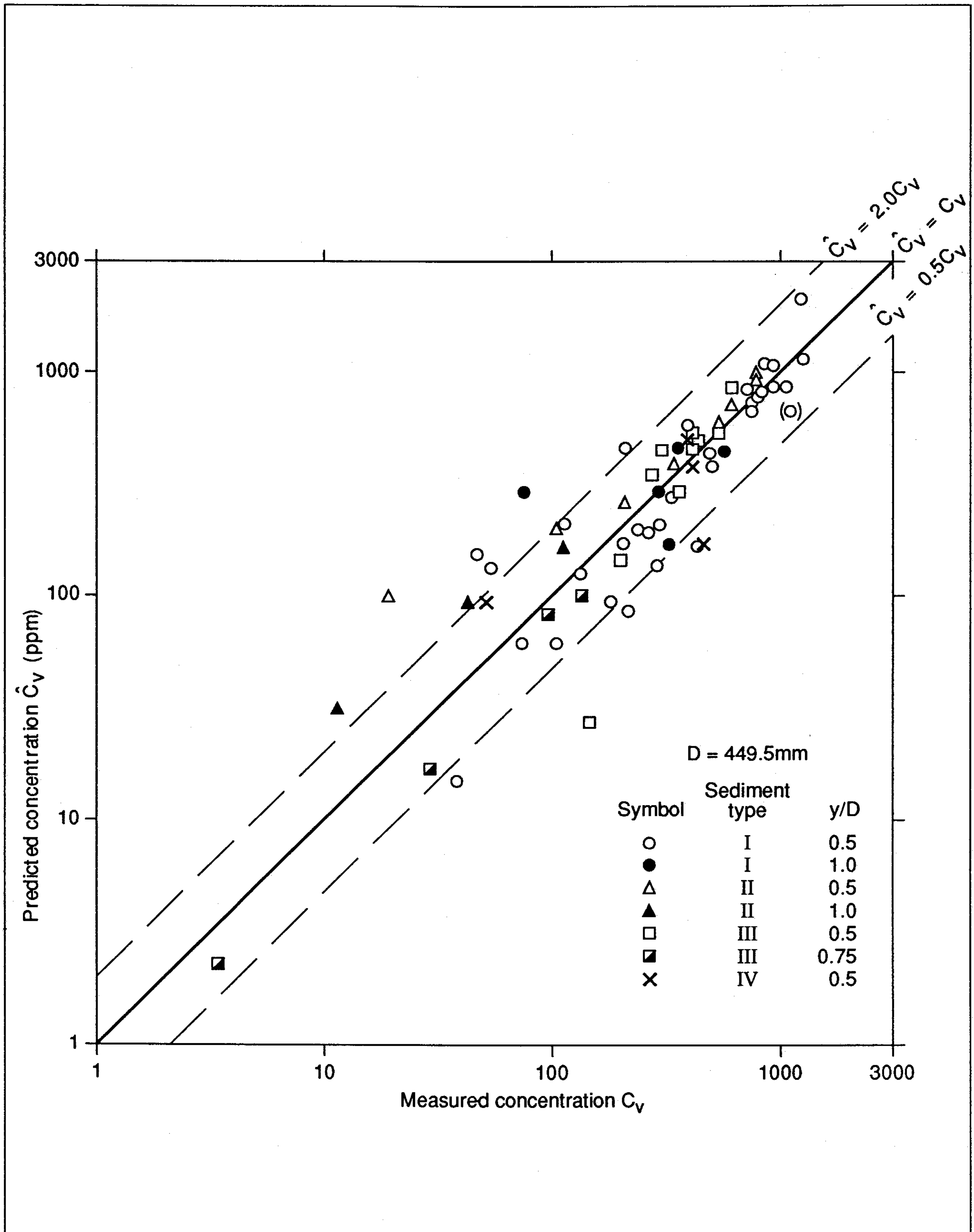

Figure 20 Predicted and measured sediment concentrations for transport with continuous bed: HR method

Appendices

Appendix A

Ackers equations for sediment transport in pipes

Appendix A Ackers equations for sediment transport in pipes

This method is based on the general theory developed by Ackers & White (1973) for sediment transport in alluvial channels, but with appropriate modifications to allow for the geometry of circular pipes. In the latest version, Ackers (1991) incorporated the results of a recent HR review of the Ackers-White equation (see HR Report SR 237) which recommended the use of slightly modified coefficients. The method was also simplified through replacement of a logarithmic term describing the grain resistance by an equivalent power-law term. The resulting transport equation presented by Ackers expresses the flow velocity as a function of the sediment concentration, but for the present report the equation has been transposed to express concentration as a function of velocity:

$$C_v = J\,(W_e R/A)^{\alpha}\,(d/R)^{\beta}\lambda_c^{\gamma}\left[\frac{V}{\{g(s-1)R\}^{1/2}} - K\lambda_c^{\delta}\,(d/R)^{\varepsilon}\right]^m \qquad (A.1)$$

The coefficients J, α, β, γ, K, δ, ε and m all depend on the dimensionless grain size:

$$D_{gr} = \left[\frac{g(s-1)}{v}\right]^{1/3} d \qquad (A.2)$$

Other quantities are defined in the list of Symbols at the beginning of this report. The coefficients in Equation (A.1) are related to four parameters in the Ackers-White equation:

$$n = 1.00 - 0.56 \log_{10} D_{gr} \qquad (A.3)$$

$$m = 1.67 + 6.83/D_{gr} \qquad (A.4)$$

$$A_{gr} = 0.14 + 0.23 / \sqrt{D_{gr}} \qquad (A.5)$$

$$\log_{10} H = - 3.46 + 2.79 \log_{10} D_{gr} - 0.98 (\log_{10} D_{gr})^2 \qquad (A.6)$$

For coarse sediments with $D_{gr} > 60$:

$$n = 0 \qquad (A.7)$$

$$m = 1.78 \qquad (A.8)$$

$$A_{gr} = 0.17 \qquad (A.9)$$

$$H = 0.025 \qquad (A.10)$$

The other coefficients are given by the following formulae:

$$J = \frac{8^{n(1-m)/2}\, H}{11.3^{m(1-n)}\, A_{gr}^{m}} \qquad \text{(A.11)}$$

$$\alpha = 1 - n \qquad \text{(A.12)}$$

$$\beta = (10-4m-mn)/10 \qquad \text{(A.13)}$$

$$\gamma = n(m-1)/2 \qquad \text{(A.14)}$$

$$K = 11.3^{(1-n)}\, g^{n/2}\, A_{gr} \qquad \text{(A.15)}$$

$$\delta = -\, n/2 \qquad \text{(A.16)}$$

$$\varepsilon = (4+n)/10 \qquad \text{(A.17)}$$

Appendix B

Theoretical model for bed-load transport in pipes

Appendix B Theoretical model for bed-load transport in pipes

Flow velocities in gravity pipes and sewers can be sufficient to carry low-density solids, silts and fine sands in suspension, but coarser sands and gravels will normally only be transported as bed load. In all the tests so far carried out at HR to investigate the limit of deposition and transport with deposited beds, the sands and gravels were observed to move as bed load.

Although dimensional analysis can be useful when processing data from sediment transport experiments, uncertainties still remain about the most appropriate ways of grouping the various quantities into non-dimensional variables. The following analysis is therefore carried out to describe the main features of bed-load transport in pipes and help identify the relationships between the principal quantities. The description of the physical processes is necessarily very much simplified, but the analysis is intended to apply both to conditions at the limit of deposition and to transport with a deposited bed since the governing factors are essentially the same.

It is assumed that bed-load transport occurs in a pipe of diameter D which may be flowing either full or part-full. The mean thickness of the sediment bed is t and the level of the water surface above the pipe invert is y ; the depth of flow above the bed is therefore (y-t). The cross-sectional area of the flow is A and the wetted perimeter is P (equal to the length of wetted pipe wall P_o plus the width of the sediment bed W_b) ; the mean velocity of the flow is V. The sediment particles transported by the flow have a specific gravity s and a mean size d (assumed equivalent to the d_{50} size of the grading curve).

The particles in the surface layer of the sediment bed are transported by fluctuating lift and drag forces exerted on them by the fluid. However, only the components of these forces averaged over time and space will be considered in the analysis. The lift forces can therefore be neglected because the overall mean value acting on a sediment bed is zero (assuming no general curvature of the flow or the bed). The mean drag force exerted on a particle depends on its size, its drag coefficient and the local flow velocity in its vicinity. Averaging the individual drag forces acting on particles occupying unit surface area of the bed gives a mean shear stress τ_s which the flow can be considered as exerting on the sediment bed. The shear stress and the mean flow velocity are linked by the Darcy-Weisbach resistance equation, which can be written in the form:

$$\tau_s = \rho \frac{\lambda_s}{8} V^2 \qquad \text{(B.1)}$$

The friction factor λ_s therefore implicitly contains information about the particle size, the drag coefficient and the velocity profile near the bed.

It is important to note that the drag force acting on an isolated particle in a pipe is not directly related to the shear stress τ_o and friction factor λ_o for the pipe as a whole. These values are dependent on the surface texture of the walls and are usually much smaller than the values τ_s and λ_s that apply to the sediment. Design criteria or transport formulae based on pipe shear stress τ_o can therefore be misleading if the sediment moves as bed-load.

When a sediment particle begins to move, its speed u_s adjusts until the mean drag force exerted by the flow balances the mean frictional resistance exerted on it by the other particles or by the invert of the pipe. The effective shear stress acting on the surface layer is therefore given by:

$$\tau_s = \rho \frac{\lambda_s}{8} (V - u_s)^2 \tag{B.2}$$

The magnitude of the shear stress also determines the thickness y_a of the active layer within which the sediment transport occurs (either due to fluid forces or to particle-particle contacts). If ϕ is the effective angle of friction acting on the underside of the active layer and e is the voids ratio of the layer (volume of voids/volume of particles), then the time-averaged balance between the shear force and the frictional resistance gives:

$$y_a = \frac{(1+e)\ \tau_s}{\rho g(s-1)\ \tan\phi} \tag{B.3}$$

At low stages of sediment transport, it can be shown that y_a may often be less than d, ie the depth of the active layer is less than one grain thickness. This in fact implies that only a proportion of the particles in the surface layer is in motion at any one time ; the drag force acting on one of these exposed particles is higher than the average and sufficient to exceed the frictional resistance exerted by the bed. However, a description based on changes in the proportion of surface particles in motion or one based on changes in the effective thickness of the active layer give similar types of result, and the active layer concept is preferred as it also applies to higher stages of sediment transport.

The above analysis demonstrates the linkage between three important aspects of the problem : the velocity of the particles ; the shear stress exerted on them by the flow ; and the thickness of the active layer in which the sediment transport occurs. The mean velocity of the particles in the active layer will be related in some way to the velocity u_s of the particles at the surface. The volumetric rate of sediment transport Q_s can therefore be expressed as:

$$Q_s = \frac{\alpha_1\ W_b\ y_a\ u_s}{(1+e)} \tag{B.4}$$

where α_1 is a constant of proportionality. Substituting for y_a using Equations (B.2) and (B.3) and defining the volumetric sediment concentration as:

$$C_v = \frac{Q_s}{Q} \tag{B.5}$$

then leads to the result:

$$C_v = \alpha_1 \left(\frac{W_b}{D}\right)\left(\frac{D^2}{A}\right) \left[\frac{\lambda_s V^2}{8g(s-1)\ D \tan\phi}\right] \left\{\frac{u_s}{V}\left(1 - \frac{u_s}{V}\right)^2\right\} \qquad (B.6)$$

The terms in the { } brackets can be considered as a type of efficiency factor. Below the threshold of movement, u_s=0 and the transport efficiency is zero. Above the threshold, the efficiency increases until a maximum is reached when, according to Equation (B.6), u_s=V/3. The ratio u_s/V will be related to the mobility of the particles in the surface layer, and previous studies of sediment transport suggest that a useful measure of the mobility is the Shields parameter:

$$F_s^2 = \frac{\tau_s}{\rho g(s-1)\ d} = \frac{\lambda_s V^2}{8g(s-1)\ d_{50}} \qquad (B.7)$$

An alternative mobility number ($\tau_s/\rho w^2$) using the fall velocity w of the sediment particles was also tested but did not explain the experimental results as well as the Shields parameter above.

The above analysis therefore suggests that experimental data for pipes with deposited beds may be correlated by means of the transport parameter:

$$\eta = C_v\ (D/W_b)(A/D^2) \left[\frac{\lambda_s V^2}{8g(s-1)\ D}\right]^{-1} \qquad (B.8)$$

and the mobility parameter:

$$F_s = \left[\frac{\lambda_s V^2}{8g(s-1)\ d_{50}}\right]^{1/2} \qquad (B.9)$$

Such a plot should demonstrate a parabolic shape, with η equal to zero at some positive value of F_s and then increasing towards an asymptotic value at higher stages of bed-load movement. Beyond a certain point, the sediment will begin to be transported in suspension and η will increase above the asymptotic value. The friction angle ϕ is not included in Equation (B.8) because it can be considered as being constant for tests with deposited beds.

The above analysis can also be applied to conditions at the limit of deposition. It is assumed that the sediment is being transported as a stream of particles along the bottom of the pipe, and that deposition occurs when the shear stress exerted by the fluid on the surface layer of the sediment is no longer sufficient to overcome the frictional resistance at the pipe invert. For small proportional depths of sediment, it can be shown (see May, 1982) that the cross-sectional area A_a occupied by the sediment is given by:

$$\frac{A_a}{D^2} = \frac{4}{3}\left(\frac{y_a}{D}\right)^{3/2} \qquad (B.10)$$

The corresponding result to Equation (B.4) for the rate of sediment transport at the limit of deposition is therefore:

$$Q_s = \frac{4}{3}\alpha_2 \frac{y_a^{3/2} D^{1/2} u_s}{(1+e)} \tag{B.11}$$

Substituting for y_a using Equations (B.2) and (B.3) then leads to:

$$C_v = \frac{4}{3}(1+e)^{1/2} \alpha_2 \left(\frac{D^2}{A}\right) \left[\frac{\lambda_s V^2}{8g(s-1)\, D \tan \phi}\right]^{3/2} \left\{\frac{u_s}{V} \left(1 - \frac{u_s}{V}\right)^3\right\} \tag{B.12}$$

The terms in the { } brackets act as an efficiency factor whose value increases from zero at the threshold of movement to a maximum when u_s=V/4. As in the case of a deposited bed, the efficiency factor can be expected to depend on the mobility of the sediment particles in the surface layer.

This analysis therefore suggests that data for the limit of deposition may be correlated by means of a transport parameter:

$$\Omega = C_v\ (A/D^2) \left[\frac{\lambda_s V^2}{8gf\ (s-1)\ D}\right]^{-3/2} \tag{B.13}$$

and a mobility parameter:

$$G_s = \left[\frac{\lambda_s V^2}{8gf\ (s-1)\ d_{50}}\right]^{1/2} \tag{B.14}$$

A plot of Ω versus G_s can be expected to show a parabolic shape, with Ω tending towards an asymptotic value at higher stages of particle mobility. Both parameters contain a friction term f because, unlike the case of deposited beds, the friction angle ϕ is not a constant but will vary according to the surface texture of the pipe. For convenience, the value of f will be assumed to be unity for sediment particles travelling along smooth pipes such as those made of plastic or perspex. For rougher pipes, such as the concrete ones used in the later HR tests, f is likely to be greater than unity ; the effective value can be determined from an analysis of experimental data. Apart from the difference in friction coefficient, the mechanisms of sediment transport should be similar in smooth and rough pipes and described by the same relationship between the parameters Ω and G_s.